

# The Role of Emerin and Other Disease-Associated Genes in Myonuclear Movement and Muscle Development in *Drosophila*:

Author: Torrey Mandigo

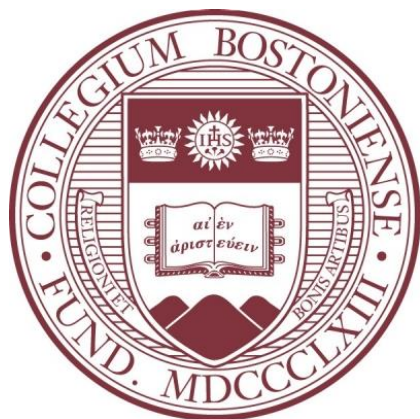
Persistent link: <http://hdl.handle.net/2345/bc-ir:108939>

This work is posted on [eScholarship@BC](#),  
Boston College University Libraries.

---

Boston College Electronic Thesis or Dissertation, 2020

Copyright is held by the author, with all rights reserved, unless otherwise noted.



# The Role of Emerin and Other Disease-Associated Genes in Myonuclear Movement and Muscle Development in *Drosophila*

Torrey Mandigo

A dissertation submitted to the Faculty of the Department of Biology

in partial fulfillment of the requirements for the degree of

Doctor of Philosophy

Boston College  
Morrissey College of Arts and Sciences  
Graduate School

April 2020



## **Abstract**

### **The Role of Emerin and Other Disease-Associated Genes in Myonuclear Movement and Muscle Development in *Drosophila***

Torrey Mandigo

Advisor: Eric S. Folker, Ph.D.

Skeletal muscle is a multinucleated cell type in which the many nuclei are precisely positioned to maximize the distance between adjacent nuclei. In order to reach this final positioning, nuclei undergo an elaborate set of movements during muscle development. The disruption of this process is evident throughout muscular dystrophies and myopathies. However, the contribution of aberrant nuclear positioning toward disease progression is unclear and the mechanisms regulating nuclear movement and positioning are poorly defined.

The goal of this thesis is to determine the contribution of disease-linked genes to the regulation of nuclear movement and positioning and how these mechanisms are coordinated in skeletal muscle. In this thesis, we utilize *Drosophila melanogaster* skeletal muscle as an *in vivo* model system to investigate nuclear positioning throughout muscle development and correlate aberrant nuclear positioning with a decrease in muscle function. We provide the first evidence of distinct mechanisms that are independently regulated by genes that are associated with two different muscle diseases, Emery-Dreifuss muscular dystrophy and Centronuclear myopathy (Chapter 2). We also provide evidence that Emerin-dependent regulation of the LINC complex is a critical determinant of nuclear

positioning and for the first time demonstrate a division of Emerin functions among the two *Drosophila emerin* homologs, *bocksbeutel* and *otefin* (Chapter 3). Finally, we conduct a proof-of-concept screen to identify novel regulators of muscle development and function (Chapter 4).

Together, the work presented in this thesis provides a framework to further our understanding of the mechanisms regulating nuclear movement and positioning as well as muscle development as a whole. Using the tools and techniques developed throughout this thesis, we provide novel insight into the mechanisms regulating nuclear movement and positioning and strengthen *Drosophila* as an *in vivo* model for investigating muscle development and function.

## Dedication

This dissertation is dedicated to Chanda “Bear” Torrey.



## **Acknowledgements**

Firstly to Eric Folker: I want to thank you for giving me the Research Technician job seven years ago and allowing me to continue pursuing my scientific career in your lab. I have learned a lot from you over the past seven years to the point that I can hear your comments in my head as I'm working on a presentation, planning experiments or writing. Your decision to choose someone with no fly or cell biology experience as the first person to join your lab was lucky for me because it set the path for my scientific career.

I would like to thank my dissertation committee, Dr. David Burgess, Dr. Sarah McMenamin and Dr. Vicki Losick, your guidance and questions over my time in graduate school have been invaluable. I enjoyed sharing my newest data with you and discussing the path of "what's next?".

To my lab mates, Dr. Alex Auld, Dr. Mary Ann Collins and Alexandra Burgess, it has been great to grow as scientists with all of you. Your friendship and adventures together have meant a lot throughout graduate school. You guys always made the work day more interesting and provided many necessary distractions from lab work.

To the undergraduates, Blake Turcich, Alyssa Anderson, Michael Hussey, Christine Hudson, Derek Sheen, Jaelyn Camuglia and Richard Moschella, that I had the

pleasure of working with. I enjoyed teaching you all and learned a lot from you all as well. Much of this thesis would not have been possible without your hard work.

To my partner-and-crime, Danny Beringer, although I didn't choose you as my one and only classmate, I'm not sure I would have been able to find anyone better. Thank you for your daily chats and insistence on keeping me up to date on everything Vine and Memes related. Our year was small but mighty.

To my squad and duo mates, Graham Thompson and Dave Monteiro, you are always there to pick me up and get me back into the action. Although our time spent together often comes at the expense of a couple hours of sleep, it was well worth it.

To my parents, Tina and Paul Mandigo, thank you for allowing your son to move to the big city of Boston to chase a career in science. I hope you are both proud of what I have been able to accomplish so far.

To my wife, Chelsea Mandigo, your support throughout graduate school has meant more than you will know. You have always encouraged and believed in me and I hope that I have made you proud. I can't wait to see what the rest of our lives have in store but I'm glad I'll be going through it with you.

# Table of Contents

<b>Dedication .....</b>	<b>i</b>
<b>Acknowledgements .....</b>	<b>ii</b>
<b>Table of Contents .....</b>	<b>iv</b>
<b>List of Abbreviations .....</b>	<b>ix</b>
<b>List of Figures and Tables.....</b>	<b>ix</b>
.....	
<b>1.0 Chapter 1: Introduction .....</b>	<b>1</b>
<b>1.1 Introduction to Muscular Dystrophies and Myopathies</b> <small>1Error! Bookmark not defined.</small>	
1.1.1 Emery-Dreifuss Muscular Dystrophy and the LINC complex.....	2
1.1.2 Centronuclear Myopathy and the MAD complex.....	4
<b>1.2 Introduction to Nuclear Movement and Positioning .....</b>	<b>7</b>
<b>1.3 Myoblast Fusion.....</b>	<b>10</b>
<b>1.4 Introduction to Myotendinous Junction Formation .....</b>	<b>12</b>
<b>1.5 Nuclear Movement and Positioning in Skeletal Muscle .....</b>	<b>14</b>
1.5.1 The LINC complex and nuclear positioning in skeletal muscle .....	16
1.5.2 The cytoskeleton and nuclear positioning in skeletal muscle .....	17
<b>1.6 Introduction to Emerin Functions.....</b>	<b>19</b>
1.6.1 Emerin's interactions with the LINC complex .....	21
1.6.2 Emerin's role in the regulation of transcription .....	22
<b>1.7 Remaining Questions.....</b>	<b>23</b>

<b>2.0 Chapter 2: Emery-Dreifuss Muscular Dystrophy-Linked Genes and Centronuclear Myopathy Linked Genes Regulate Myonuclear Movement by Distinct Mechanisms .....</b>	<b>26</b>
<b>2.1 Abstract .....</b>	<b>27</b>
<b>2.2 Introduction.....</b>	<b>27</b>
<b>2.3 Results.....</b>	<b>30</b>
2.3.1 Muscle function in <i>Drosophila</i> larvae requires genes mutated in patients with Emery-Dreifuss Muscular Dystrophy or Centronuclear Myopathy. ....	30
2.3.2 Genetic interactions between microtubule motors and EDMD- and CNM-linked genes in the <i>Drosophila</i> larva .....	38
2.3.3 Disruption of EDMD- and CNM-linked genes impact microtubule organization in the <i>Drosophila</i> larva .....	39
<b>2.4 Discussion.....</b>	<b>42</b>
<b>2.5 Materials and Methods .....</b>	<b>46</b>
2.5.1 <i>Drosophila</i> genetics .....	46
2.5.2 Larval Locomotion .....	47
2.5.3 Immunohistochemistry .....	48
2.5.4 Analysis of nuclear position in larvae .....	48
2.5.5 Analysis of microtubule organization in larvae .....	50
2.5.6 RNA isolation, construction of cDNA library and RT-PCR .....	51
<b>3.0 Chapter 3: <i>Drosophila</i> emerins control LINC complex localization and transcription to regulate myonuclear position .....</b>	<b>53</b>

<b>3.1</b>	<b>Abstract .....</b>	<b>54</b>
<b>3.2</b>	<b>Introduction.....</b>	<b>54</b>
<b>3.3</b>	<b>Results.....</b>	<b>57</b>
3.3.1	Disruption of EDMD-linked genes impact nuclear positioning in <i>Drosophila</i> embryo .....	57
3.3.2	Disruption of EDMD-linked genes impact nuclear positioning in <i>Drosophila</i> larvae .....	63
3.3.3	<i>Bocksbeutel</i> and <i>klarsicht</i> genetically interact to regulate nuclear positioning during muscle development .....	67
3.3.4	Disruption of EDMD-linked genes affect levels of nuclear localized <i>klarsicht</i> .....	72
3.3.5	Loss of <i>otefin</i> rescues nuclear positioning defects caused by disruption of <i>bocksbeutel</i> .....	75
<b>3.4</b>	<b>Discussion .....</b>	<b>77</b>
<b>3.5</b>	<b>Materials and Methods .....</b>	<b>80</b>
3.5.1	<i>Drosophila</i> genetics .....	80
3.5.2	Immunohistochemistry .....	81
3.5.3	Analysis of nuclear position in embryos .....	83
3.5.4	Analysis of nuclear position in larvae .....	84
3.5.5	Analysis of <i>klarsicht</i> localization in larvae .....	85
3.5.6	Analysis of nuclear area, Hoechst integrated density and fluorescence intensities .....	86
3.5.7	RT-qPCR .....	87

<b>4.0</b>	<b>Chapter 4: An RNAi based screen in <i>Drosophila</i> larvae identifies fascin as a regulator of myoblast fusion and myotendinous junction structure .....</b>	<b>89</b>
<b>4.1</b>	<b>Abstract .....</b>	<b>90</b>
<b>4.2</b>	<b>Introduction.....</b>	<b>91</b>
<b>4.3</b>	<b>Results.....</b>	<b>93</b>
4.3.1	Fascin is necessary for muscle function .....	93
4.3.2	Fascin is localized to the nucleus in <i>Drosophila</i> muscle.....	95
4.3.3	Fascin regulates myoblast fusion.....	97
4.3.4	Fascin-dependent fusion effects are evident in larvae .....	102
4.3.5	Fascin regulates muscle attachment .....	104
<b>4.4</b>	<b>Discussion .....</b>	<b>106</b>
<b>4.5</b>	<b>Materials and Methods .....</b>	<b>108</b>
4.5.1	<i>Drosophila</i> genetics .....	108
4.5.2	Larval locomotion assay .....	108
4.5.3	Immunohistochemistry .....	109
4.5.4	Image analysis .....	111
4.5.5	Analysis of general muscle architecture .....	112
<b>5.0</b>	<b>Chapter 5: Discussion .....</b>	<b>114</b>
<b>5.1</b>	<b>Summary and Significance.....</b>	<b>114</b>
5.1.1	Nuclear positioning is regulated by distinct mechanisms in different muscle diseases .....	114
5.1.2	<i>Drosophila emerlin</i> homologs regulates nuclear positioning by distinct mechanisms and impact nuclear positioning in contrasting manners.....	115

5.1.3	<i>Drosophila</i> larval mobility phenotypes are effective in screening for novel regulators of muscle development and function.....	116
<b>5.2</b>	<b>Broader Impact and Future Directions.....</b>	<b>117</b>
5.2.1	Distinct mechanisms underlie the nuclear positioning phenotypes present in EDMD and CNM.....	117
5.2.2	Distinct Emerin function's impact on disease-relevant phenotypes.....	118
5.2.3	A sensitive screening assay for novel regulators of muscle development and function .....	120
<b>5.3</b>	<b>Concluding Remarks .....</b>	<b>121</b>
<b>Appendix</b>	<b>.....</b>	<b>122</b>
<b>References</b>	<b>.....</b>	<b>129</b>

## List of Abbreviations

AEL, after egg lay; *Amph*, amphiphysin; *apRed*, apterous red; *bocks*, bocksbeutel; CNM, centronuclear myopathy; DO2, Dorsal muscle 2; *Dhc*, dynein heavy chain; EDMD, Emery–Dreifuss muscular dystrophy; *Khc*, kinesin heavy chain; *klar*, klarsicht; *koi*, klaroid; L1, 1st instar larval stage; L3, 3rd instar larval stage; LINC complex, linker of nucleoskeleton and cytoskeleton; LT, lateral transverse; MTJ, myotendinous junction; *mtm*, myotubularin; *Ote*, otefin; qPCR, quantitative PCR; RNAi, RNA interference; RT-PCR, reverse transcriptase PCR; Sn, singed; SUN, Sad1 and Unc84 homology domain; VL3, ventral longitudinal muscle 3.

## List of Figures and Tables

<b>Figure 1.1</b> – The Linker of Nucleoskeleton and Cytoskeleton complex -----	3
<b>Figure 1.2</b> – Canonical functions of CNM-linked genes -----	6
<b>Figure 1.3</b> – Model of myoblast fusion -----	11
<b>Figure 1.4</b> – Nuclear positioning in mammalian can <i>Drosophila</i> skeletal muscle -----	15
<b>Figure 1.5</b> – Cortical pathway of nuclear positioning -----	19
<b>Figure 2.1</b> – The EDMD-linked genes <i>bocksbeutel</i> and <i>klarsicht</i> , and the CNM-linked gene <i>amphiphysin</i> are necessary for proper locomotion and myonuclear position in <i>Drosophila</i> larvae -----	32
<b>Figure 2.2</b> – Analysis of nuclear position in <i>Drosophila</i> larvae-----	33
<b>Table 2.1</b> – Relative expression of EDMD- and CNM-linked genes when knockdown by RNAi -----	33

**Figure 2.3** – The effects of *bocksbeutel*, *klarsicht*, and *amphiphysin* on nuclear position in larval and embryonic muscles are muscle autonomous -----35

**Figure 2.4** – The effects of *bocksbeutel*, *klarsicht*, and *amphiphysin* on nuclear position in larval and embryonic muscles are muscle autonomous -----36

**Figure 2.5** – The effects of *bocksbeutel* and *amphiphysin* on nuclear position in larval muscle are muscle autonomous -----37

**Figure 2.6** – *bocksbeutel* genetically interacts with *dynein* and *kinesin* to affect nuclear positioning within larval muscles -----41

**Figure 2.7** – Both *bocksbeutel* and *amphiphysin* are necessary for proper microtubule organization -----42

**Figure 3.1** – The EDMD-linked genes *bocksbeutel*, *klarsicht*, *otefin* and *klaroid* are necessary for proper myonuclear positioning in *Drosophila* embryos and larvae -----60

**Figure 3.2** – Analysis of EDMD-linked gene alleles in combination with deficiencies are consistent with the alleles affecting muscle development -----62

**Figure 3.3** – The EDMD-linked genes *bocksbeutel*, *klarsicht*, *otefin* and *klaroid* affect the scaling of nuclear position relative to muscle edge -----65

**Figure 3.4** – *otefin* trans-heterozygote phenocopies the *ote<sup>DB</sup>* homozygote with respect to nuclear positioning relative to the muscle edge -----66

**Figure 3.5** – *bocksbeutel* genetically interacts with *klarsicht* to regulate nuclear positioning in embryonic and larval muscles -----68

**Figure 3.6** – *bocksbeutel* does not genetically interact with *otefin* or *klaroid* and *otefin* does not genetically interact with *klarsicht* or *klaroid*, to regulate nuclear positioning in embryonic muscles -----70

**Figure 3.7** – *bocksbeutel* does not genetically interact with *otefin* or *klaroid* and *otefin* does not genetically interact with *klarsicht* or *klaroid* to regulate nuclear positioning in larval muscles -----71

**Figure 3.8** – The EDMD-linked genes *bocksbeutel*, *otefin* and *klaroid* affect levels of nuclear localized Klarsicht -----74

**Figure 3.9** – Loss of the *otefin* rescues the nuclear positioning phenotype caused by disruption of *bocksbeutel* and restores nuclear localized Klarsicht to control levels -----76

**Figure 4.1** – An RNAi screen for larval locomotion identifies fascin as a regulator of muscle function -----94

**Figure 4.2** – Fascin is localized to actin and the nucleus in muscle -----96

**Figure 4.3** – Fascin is necessary for myoblast fusion -----98

**Figure 4.4** – Expression of RNAi against fascin late in embryonic development does not affect muscle development -----100

**Figure 4.5** – Fascin has muscle autonomous effects on myoblast fusion -----101

**Figure 4.6** – Genetic disruption of fascin did not affect larval muscle structure -----102

**Figure 4.7** – Muscle specific depletion of fascin results in smaller muscles with fewer nuclei -----103

**Figure 4.8** – Fascin is necessary for proper myotendinous junction organization -----105

**Table A1.1**– Muscle disease-linked mutants utilized-----122

**Table A1.2** – Data acquired during the limited RNAi-based screen for regulators of muscle function -----122-124

**Figure A2.1** – *Bocksbeutel* and *klarsicht* genetically interacts with components of the cortical pathway to regulate larval nuclear positioning -----126

**Figure A2.2** – *GM130* is necessary for proper myonuclear positioning in *Drosophila* larvae

-----127

# **Chapter 1:**

## **Introduction**

### **1.1 Introduction to Muscular Dystrophies and Myopathies**

Skeletal muscle is one of the three major muscle types and accounts for nearly half of an adult's body mass. Skeletal muscle provides us with the ability to produce mechanical force to move ourselves and objects in our external environment. However, until the early 1940s, the properties of skeletal muscle that allowed for force production were poorly understood. Force production by skeletal muscle is possible due to skeletal muscle's ability to contract. These contractions are generated by the unique, yet conserved, cellular organization of skeletal muscle and the organization of the myofibril network. The myofibril network consists of the repetitive sarcomere structures and its associated proteins that play a central role in muscle contraction in force generation (Ramsey and Street, 1940).

Muscular dystrophies and myopathies are a group of muscle diseases that are most notably characterized by impaired muscle function, progressive muscle weakness and muscle wasting. However, these symptoms are also shared by many neuromuscular diseases (Dubowitz et al., 2007a). Skeletal muscle is a somewhat unique tissue due to its multinucleated nature, which arises through cell-cell fusion events (Capers, 1960). In healthy individuals, the many nuclei in skeletal muscle are precisely positioned at the muscle periphery, while maximizing their distance between adjacent nuclei (Bruusgaard et al., 2003; Lei et al., 2009). Interestingly, a hallmark of muscular dystrophies and myopathies that separates them from neuromuscular disorders is the disrupted positioning of nuclei. This feature of muscular dystrophies and myopathies is so prevalent that

mispositioned nuclei has been used as a diagnostic tool to distinguish muscular dystrophies and myopathies from neuromuscular disorder for several decades (Dubowitz et al., 2007b). However, although muscular dystrophies and myopathies share many phenotypes, the genes and proteins affected in these diseases can range widely in the pathways and structures that they are canonically implicated in.

### **1.1.1 Emery-Dreifuss Muscular Dystrophy and the LINC complex**

Emery-Dreifuss muscular dystrophy (EDMD) was first characterized in the early 1960s by Emery and Dreifuss. EDMD is characterized by early contractures of the Achilles tendons and elbows, muscle weakness and wasting of the upper and lower limbs, and late onset cardiac conduction defects usually presenting after the age of twenty (Emery, 2000). As is common with muscular dystrophies, there is a higher occurrence of nuclei mispositioned in the center of the myofiber or clustered out at the periphery of the muscle cell when comparing muscle biopsies from patients and healthy individuals.

Multiple subtypes of EDMD have been identified that are phenotypically similar but are distinguished by their mode of inheritance. The most common form of EDMD, the X-linked form, is caused by mutations in the *STA (EMD)* gene, which encodes the nuclear membrane protein emerin (Bione et al., 1994). Emerin is primarily localized to the inner nuclear envelope (Fig. 1.1) and can interact with components of the nucleoskeleton, which is a filamentous meshwork lining the nucleoplasmic face of the inner nuclear membrane (Lee et al., 2001; Wilson and Foisner, 2010). One of the major components of the nucleoskeleton (Fig. 1.1), lamin A/C, has also been linked to EDMD, as the autosomal dominant and recessive forms of EDMD are caused by mutations in the *LMNA* gene, which

encodes lamin A/C (Bonne et al., 1999). However, in 2003, the European Neuromuscular Center published that mutational analysis in patients with EDMD found that mutations in the *STA* and *LMNA* gene only account for approximately 40% of EDMD cases, suggesting that other EDMD-linked genes existed (Bonne et al., 2003). Candidate studies began with known binding partners of emerin and lamin A/C that are highly expressed in muscle tissue.

From these candidate studies, additional EDMD-linked mutations were identified in the genes *SYNE1* and *SYNE2*, which encode the KASH-domain containing nesprin proteins, and in the genes *SUN1* and *SUN2*, which encode the SUN-domain containing SUN proteins (Meinke et al., 2014; Zhang et al., 2007). Both KASH- and SUN-domain containing proteins are localized to the nuclear membrane. However, KASH-domain containing proteins are primarily localized to and span the outer nuclear membrane, while SUN-domain containing proteins are primarily localized to and span the inner nuclear membrane (Fig 1.1).

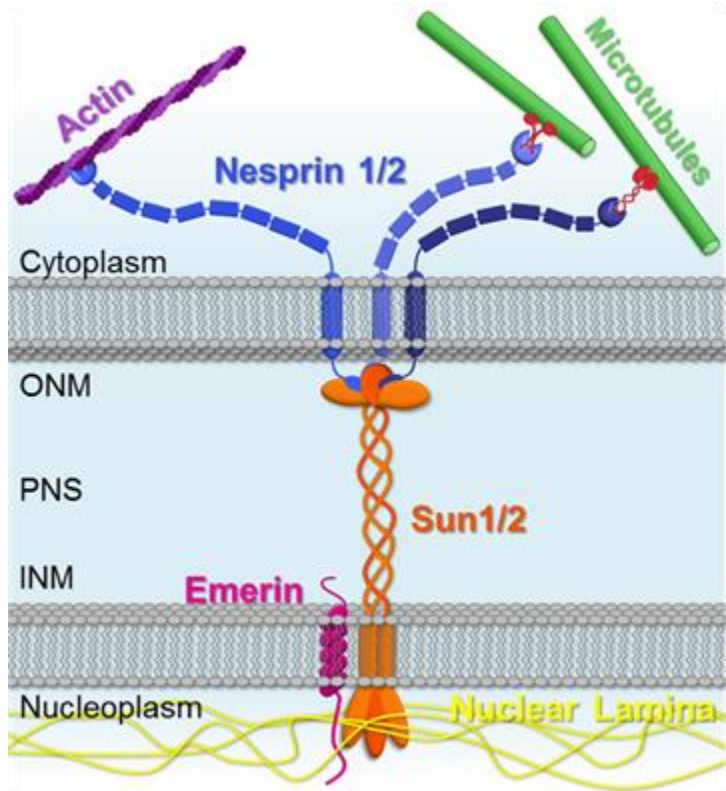


**Figure 1.1** The Linker of Nucleoskeleton and Cytoskeleton complex. The LINC complex is composed of Sun-domain proteins, SUN1/2 (orange) and KASH-domain proteins, nesprin 1/2 (blue). SUN-domain proteins span the inner nuclear membrane (INM) interacting with the nuclear lamina (yellow) within the nucleoplasm and KASH-domain proteins within the perinuclear space (PNS). KASH-domain proteins span the outer nuclear membrane (ONM) and interact with the actin cytoskeleton (purple) and microtubule cytoskeleton (green) within the cytoplasm.

These localizations lead to KASH-domain containing proteins projecting into both the cytoplasm and the lumen of the nuclear envelope and the SUN-domain containing proteins projecting into the nucleoplasm and the lumen of the nucleus envelope. Within the lumen of the nuclear envelope, KASH- and SUN-domain proteins interact, through their KASH- and SUN-domains, to form a protein complex known as the linker of nucleoskeleton and cytoskeleton (LINC Complex) (Sosa et al., 2012).

As the name suggest, KASH-domain containing proteins can also interact with components of the cytoskeleton within the cytoplasm, while SUN-domain containing proteins can interact with components of the nucleoskeleton in the nucleoplasm (Fig 1.1). This linkage through the LINC complex facilitates the transduction of force from the cytoskeleton to the nucleus (Crisp et al., 2006; Starr and Fischer, 2005; Zhang et al., 2001). All together lamin A/C, the KASH-domain proteins and SUN-domain proteins share a clear and important function through the LINC complex. However, it is unclear if and how emerin, the genetic basis of the most common form of EDMD, fits within this apparent shared function of the EDMD-linked proteins. Furthermore, how these genes and protein products lead to the symptoms experienced by patients with EDMD also remains unclear and the mechanisms that are disrupted in mutations from patients with EDMD are poorly understood.

### **1.1.2 Centronuclear Myopathy and the MAD complex**

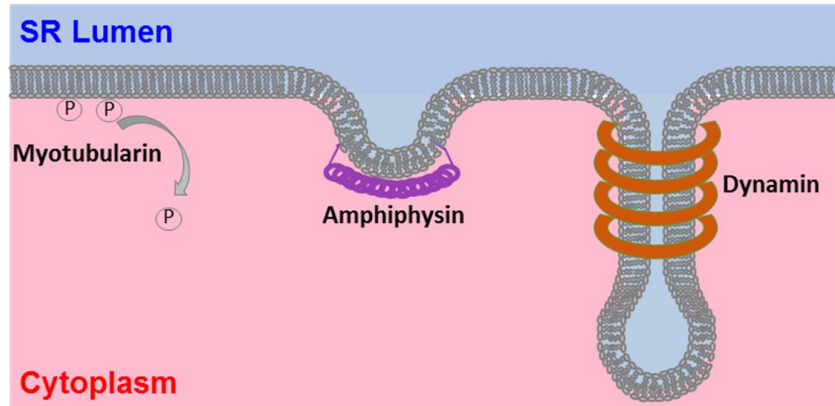
Centronuclear Myopathies (CNM) are a group of congenital myopathies that were also first described in the 1960s, by Spiro *et al.* and by Sher *et al.* (Sher et al., 1967; Spiro et al., 1966). As the name suggest, CNMs are characterized by the increased number of

nuclei located within the center of the myofiber. Clinically, the presentation of CNM can vary, however generally patients experience muscle weakness and hypotonia, which can either be present from birth or present progressively with both often leading to delayed motor milestones. Some forms of CNM can also lead to facial weakness, respiratory insufficiency or difficulty swallowing (Romero, 2010). These differences in the clinical presentation of CNM initially lead to the sub-classification of three main types of CNM, based on the severity of symptoms and age at onset. These CNM sub-classifications were later grouped by their mode of inheritance and classified as the X-linked recessive form, the autosomal dominant form and the autosomal recessive form.

The X-linked recessive form, which is the most lethal form, has been linked to mutations in the *MTM1* gene, which encodes the phosphatase myotubularin 1 (Laporte et al., 1996). The autosomal dominant form, which accounts for nearly 50% of all CNM, cases has been linked to mutations in the *DNM2* gene, which encodes the large GTPase dynamin 2 (Bitoun et al., 2005). Finally, the autosomal recessive form, which is the rarest form of CNM, has been linked to mutations in the *BINI* gene, which encodes the adaptor protein amphiphysin 2 (Nicot et al., 2007).

Canonically, the protein products of these CNM-linked genes function in the development and structure of the transverse tubule (T-tubule) in skeletal muscle, which plays an important role in excitation-contraction coupling and regulating calcium levels (Jungbluth et al., 2007). For example, amphiphysin-dependent activation of N-WASP is

necessary for the proper formation of the junction between the T-tubules and the sarcoplasmic reticulum by



regulating membrane shape in cultured myofiber systems (Fig 1.2) (Falcone et al.,

**Figure 1.2** Canonical functions of CNM-linked genes. Diagram of the canonical functions of the Centronuclear myopathy-linked proteins. Myotubularin, amphiphysin and dynamin function in the development, shaping and function of the T-tubules through their ability to regulate phosphorylation state of membrane lipids (myotubularin), to regulate membrane curvature and tubulation (amphiphysin and dynamin).

2014). Dynamin 2 has been largely studied for its role in membrane trafficking pathways, where dynamin 2 assembles around the neck of budding vesicles and conformational changes induced by GTP hydrolysis lead to the fission of the vesicle membrane (Fig. 1.2) (Ferguson and Camilli, 2012). However, dynamin 2 has been shown to have an increase in GTPase activity and less GTP-induced disassembly compared to wild type in all the CNM-linked dynamin 2 mutations biochemically characterized (Chin et al., 2015; James et al., 2014; Kenniston and Lemmon, 2010; Wang et al., 2010). Furthermore, hyperactivation of dynamin 2 causes disorganization and fragmentation of T-tubules (Chin et al., 2015; Cowling et al., 2011; Gibbs et al., 2014). Finally, myotubularin 1 is known to regulate membrane lipid composition of the membrane by regulating the phosphorylation state of phosphatidylinositol thus controlling phosphatidylinositol turnover (Fig. 1.2) (Blondeau et al., 2000; Taylor et al., 2000). The phosphorylation state of phosphatidylinositol can also impact membrane trafficking and endocytosis thereby affecting excitation-contraction

coupling and calcium regulation by T-tubules (Al-Qusairi et al., 2009; Nicot and Laporte, 2008).

Although CNM-linked proteins all share a function in the development and structure of the T-tubule, these proteins also have functions related to the regulation of the cytoskeleton. For instance, Amphiphysin contributes to the attachment between the nucleus and the microtubule and actin cytoskeleton, through direct binding to actin and the microtubule associated protein CLIP170 (D'Alessandro et al., 2015). Dynamin 2 was originally identified as a microtubule associated protein (Shpetner and Vallee, 1989) and dynamin 2 GTPase activity is stimulated by dynamin 2 polymerization around microtubules (Maeda et al., 1992; Warnock et al., 1997). Additionally, dynamin 2 regulates dynamic instability of microtubules, independent of GTPase activity (Tanabe and Takei, 2009). Finally, a structural role for MTM1 as a scaffolding protein for proteins such as the intermediate filament desmin, has also been suggested, independent of MTM1's enzymatic activity, and may play a role in the maintenance of organelle positioning in skeletal muscle (Amoasii et al., 2012). All together these shared cytoskeletal regulatory functions of CNM-linked proteins suggest that CNM may not only be a disease of the T-tubules and instead may involve dysregulation of the cytoskeleton as a potential contributor to CNM pathologies.

## **1.2 Introduction to Nuclear Movement and Positioning**

Although classically depicted as a static organelle positioned within the center of the cell, the nucleus is actually a highly dynamic and actively positioned organelle. In fact, nuclear movement is a highly conserved process and the precise position of the nucleus is

often necessary for specialized cellular processes (Gundersen and Worman, 2013). Cell division is one cellular process in which precise positioning of the nucleus is required in order to produce proper formation of daughter cells. During cell division in budding yeast and fission yeast, the nucleus is actively moved and positioned either into the bud neck of budding yeast or to the site of the division plane in fission yeast to ensure the proper separation of genetic material in each daughter cell (Almonacid and Paoletti, 2010; Shaw et al., 1998; Ten Hoopen et al., 2012; Tran et al., 2001; Yeh et al., 1995). Similarly, after fertilization of mammalian or invertebrate eggs, the male and female pronuclei are moved toward the center of the egg, where they fuse. This movement and positioning of the pronuclei into the center of the cell ensure that the first division creates two equal blastomeres (Minc et al., 2011).

Nuclear movement and positioning also serves important functions in non-dividing cells. For example, in the developing *Drosophila* optic epithelium, nuclear movement helps to establish the characteristic arrangement of cells in the ommatidium through the movement of the nucleus basally and then apically (Patterson et al., 2004). A similar set of movements, known as interkinetic nuclear migration, occurs in the vertebrate neuroepithelium as the nuclei undergo a series of basal and apical movements throughout the cell cycle in order to clear room for neighboring epithelial cells to divide, increasing the number of cells within the available space (Baye and Link, 2008; Del Bene, 2011). The nucleus is also often actively moved and positioned during cell migration as the nucleus is moved rearward in the cell, away from the leading edge. This rearward movement of the nucleus is accompanied by a reorientation of the centrosome toward the leading edge, further facilitating the polarization of the migrating cell (Gomes et al., 2005). Nuclear

movement is also important in the addition of newly formed neurons into preexisting circuits. As newly formed neurons migrate and incorporate into neural circuits, the nucleus is actively moved and squeezed through tight spaces to allow the neuron to reach its desired target (Vallee et al., 2009).

Nuclear movement and positioning is also critical in multinucleated cells. Multinucleated cells can form either through the fusion of multiple mononucleated cells or by multiple rounds of nuclear division without cytokinesis. In these multinucleated cells, the movement and position of the many nuclei are precisely regulated and are often important to proper cellular function. In the multinucleated osteoclasts, the many nuclei cluster toward the center of the syncytium. In osteoclasts, the number of nuclei present is linearly related to bone resorption efficiency. Furthermore, it has been demonstrated that all nuclei within a single osteoclast exhibit a similar global transcriptional activity, suggesting that the clustering of these nuclei may act as an efficient way of tightly regulating gene expression of the up to 200 nuclei that can be present within a single osteoclast (Boissy et al., 2002). In the syncytial filamentous fungi *Ashbya gossypii*, nuclei position themselves evenly throughout the hyphae. In developing hyphae, nuclei can asynchronously undergo nuclear division without cytokinesis and move nuclei into the new cytoplasm of the growing hyphae to provide nourishment (Dundon et al., 2016; Gibeaux et al., 2017). Finally, one of the most well-characterized syncytial tissue in which nuclear movement and positioning is highly regulated is skeletal muscle. In skeletal muscle, nuclei go through a series of movements to eventually maximize the distance between one another. However, some locations along the muscle maintain a unique positioning of nuclei such as the neuromuscular junction. At the neuromuscular junction 3 to 6 nuclei cluster

and are anchored under the postsynaptic membrane, where these nuclei display distinct expression profiles compared to other non-neuromuscular junction-associated nuclei (Grady et al., 2005; Rossi et al., 2000).

The above examples demonstrate the high conservation of nuclear movement and positioning in a range of cell types and cellular functions. Although the functions of some of these nuclear movements are understood, in unique cell types, such as multinucleated cells, the functions of nuclear movements and position are less clear. Additionally, the mechanisms that regulate nuclear movement and positioning are only beginning to be elucidated. In some tissues such as skeletal muscle there is a high correlation between mispositioned nuclei and human disease. However, the direct contribution of nuclear positioning to normal tissue function is poorly understood.

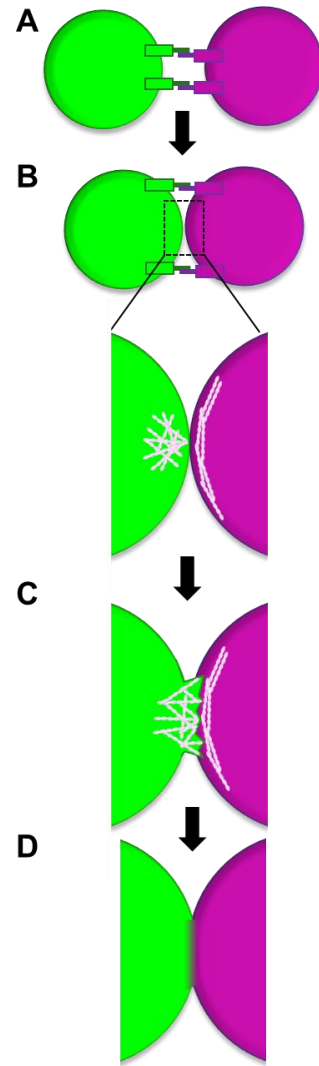
### **1.3 Myoblast Fusion**

In order to better understand nuclear movements and positioning, it is crucial to understand how the skeletal muscle achieves its multinucleated state. The first step in skeletal muscle development is initiated by the differentiation of progenitor cells into myoblasts, which become specified as either founder cells or fusion-competent myoblasts. This specification, along with the identity of each founder cell, is determined by the unique combination of transcription factors expressed within each myoblast (Dobi et al., 2015). Next, the fusion between these two cell types, founder cells and fusion-competent myoblasts, must occur to generate syncytial muscle cells. The stages of myoblast fusion begin with cell-cell recognition, followed by membrane juxtaposition and actin

**Figure 1.3 Model of myoblast fusion** (A) Myoblast fusion is initiated by the recognition of founder cells (FC, Purple) by fusion-competent myoblast (FCM, Green) (B) Membrane juxtaposition and actin polymerization leads to actin structures to form in both the FCM and FC. (C) Formation and invasion of finger-like membrane protrusions into the FC (D) Next, a fusion pore is formed. Followed by pore expansion and cytoplasmic continuity. Figure adapted from (Abmayr and Pavlath, 2012).

rearrangement. Once the membranes are in close proximity and the actin cytoskeleton has been organized for cell fusion, pore formation begins and allows for cytoplasmic continuity between the fused cells (Fig. 1.3).

In *Drosophila* and vertebrates, myoblast fusion occurs in two phases. The first is the fusion of individual myoblasts, such as the fusion between founder cells and fusion-competent myoblasts. While the second phase is the fusion of more myoblasts to the developing myotube (Abmayr and Pavlath, 2012; Beckett and Baylies, 2007; Harris et al., 1989; Richardson et al., 2008). Independent of which phase of myoblast fusion is occurring, the fusion event begins with the recognition and adhesion of the fusing cells (Fig 1.3A). This is mediated by members of the cell-specific immunoglobulin super family, which ensure that fusion is a highly specific process (Artero et al., 2001; Bour et al., 2000; Ruiz-Gómez et al., 2000; Strünkelnberg et al., 2001). In founder cells and fusion-competent myoblasts, recognition and adhesion lead to a signaling cascade that induces the remodeling of the actin cytoskeleton in both the founder cell and fusion competent myoblast. As a result, the F-actin within the fusion competent myoblast forms a focus structure, while the F-actin within the founder cell or,



in later rounds of fusion, the developing myotube forms a thin sheath (Fig 1.3B) (Sens et al., 2010). The F-actin focus that is formed in the fusion competent myoblast is regulated by the ARP2/3 complex and thought to provide mechanical force to push the membranes of fusing cells into close proximity through the formation of invasive finger-like membrane protrusions (Kim et al., 2015a). The invasive membrane protrusions of the fusion competent myoblast begin to invade the founder cell, inducing an inward curvature on the founder cell's plasma membrane, which goes on to form the single-channel fusion pore between the two fusing cells (Fig 1.3C,D) (Sens et al., 2010). Interestingly, experiments have demonstrated that prior to the completion of fusion, proteins associated with the actin focus, including the actin focus itself, must be removed from the fusion site before the fusion is complete and cytoplasmic continuity is achieved (Richardson et al., 2007). Although the steps of myoblast fusion are fairly well understood, only a few proteins have had their role in myoblast fusion characterized and it is still unclear if novel regulators of myoblast fusion exist.

## **1.4 Introduction to Myotendinous Junction Formation**

In order for the developing myotube to mature into a fully functional muscle, a specialized junction that connects the muscle to the tendon cell must be formed. This junction, known as the myotendinous junction (MTJ), is essential for allowing muscles to maintain their shape and force transmission without muscle detachment during muscle contraction (Valdivia et al., 2017). In *Drosophila*, the formation of the MTJ is initiated by the secretion of a chemoattractant from the tendon cell called Slit, which interacts with the muscle membrane receptors Robo1 and Robo3 (Kramer et al., 2001; Ordan and Volk,

2015). Upon the recognition of the tendon cell by the muscle cell, the two cells begin to form cell-cell contact. This contact is strengthened by folding of the muscle cell membrane to form protrusions and invaginations, which increase the surface area between the muscle and tendon cell, allowing the membrane to resist the forces of muscle contraction (Tidball and Lin, 1989).

After the initial attachment is made, both cells secrete extracellular matrix proteins that can help to strengthen the muscle attachment (Brown, 2000). However, in *Drosophila* larvae, two types of muscle-tendon attachments have been identified. The first are direct muscle attachments where one muscle cell attaches to a tendon cell with little extracellular matrix protein being secreted. The second are indirect muscle attachments where multiple muscle cells initially contact the same tendon cell, then substantial amounts of extracellular matrix protein is secreted (Prokop et al., 1998). The MTJ involves several proteins, however within the extracellular matrix Collagen I and Tenascin-care are enriched near the tendon and Laminins and Collagen IV are enriched near the muscle (Aumailley and Smyth, 1998; Chiquet and Fambrough, 1984). Within the protrusions and invaginations of the muscle cell, actin filaments extend from the last Z-line and interact with subsarcolemmal proteins, thereby indirectly interacting with the extracellular matrix (Kojima et al., 2008). The interactions between the cell membrane and the extracellular matrix are mediated by integrins which are expressed in both the muscle and tendon cells (Cheresh and Mecham, 1994). However, the initial cell-cell contact, after the recognition of the tendon cell by the muscle cell, is able to occur normally in the absence of integrins, suggesting that integrins may play an important role in strengthening the MTJ rather than facilitating the initial formation of the attachment (Prokop et al., 1998).

Although some mechanisms for the development of the MTJ have been identified, much of the work stems from *Drosophila* research. Mechanistically, very little is known about the formation and maturation of the MTJ in mammals. What is known is that the MTJ serves a similar role in forming a stable attachment between the muscle and tendon cell in mammals. Furthermore, the importance of integrins in strengthening the MTJ has also been demonstrated (Bao et al., 1993; Schweitzer et al., 2010). However, the mechanisms involved are only beginning to become elucidated and a more complete understanding of the proteins involved would facilitate our understanding of this important cell-cell interaction.

## **1.5 Nuclear Movement and Positioning in Skeletal Muscle**

Nuclear positioning in skeletal muscle is extremely precise and requires an elaborate set of movements throughout muscle development. The importance of nuclear movement in skeletal muscle is highlighted by the conservation of similar movements from Humans to *Drosophila*. First, upon the fusion of free myoblasts, the nucleus is deposited into the growing myotube. The nucleus is then actively moved to the center of the myotube, in mammalian cells, where it aligns with previously deposited nuclei (Fig. 1.4A) (Cadot et al., 2012; Kelly and Zacks, 1969). Similarly, nuclei are deposited into a single cluster

within the ventral end of the later transverse muscles of *Drosophila*, where nuclear movements in *Drosophila* have been best characterized (Folker et al., 2012; Folker et al., 2014; Metzger et al., 2012).

As the myotube matures, nuclei are moved from the center of the myofiber in mammalian cells. These nuclei are moved to the periphery of the myofiber where they space out to maximize the distance between each other and become anchored in place (Fig. 1.4A) (Bruusgaard et al., 2003; Capers, 1960).

Similarly, nuclei separate from the ventral cluster to form a dorsal and ventral cluster in *Drosophila*. These clusters then migrate directionally to their respective muscle poles. After the nuclear clusters reach their respective muscle poles, they begin to move back into the center of the muscle, periodically leaving nuclei behind, becoming evenly spaced and maximizing the distance between adjacent nuclei (Fig. 1.4B) (Folker et al., 2012; Folker et

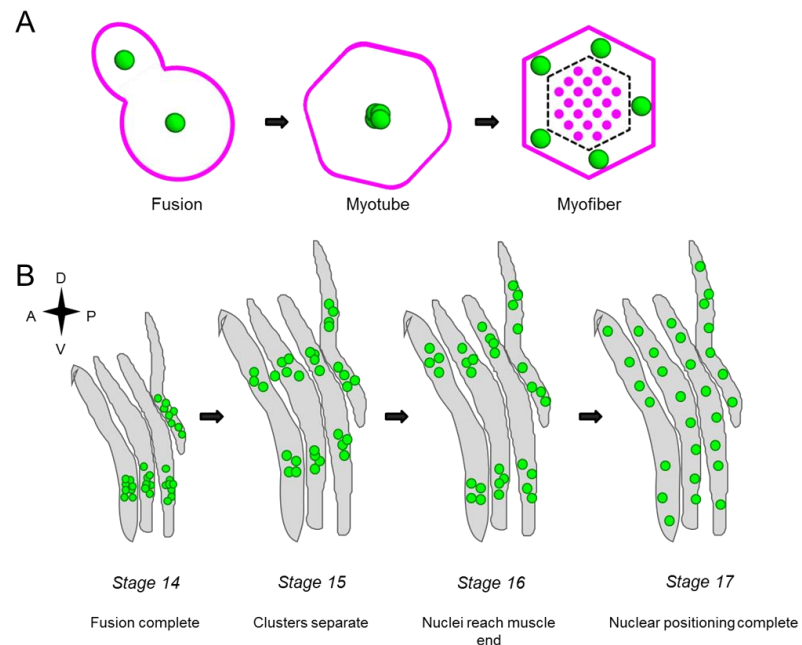


**Figure 1.4 Nuclear positioning in mammalian and *Drosophila* skeletal muscle**

(A) Cross-section illustrations of nuclear movements during muscle development and muscle repair. Upon fusion nuclei (green) are moved to the center of the myotube. As the myotubes matures into a myofiber, nuclei are moved to the periphery of the myofiber. (B) Nuclear movements in the lateral transverse muscles of *Drosophila melanogaster*. Upon the completion of fusion, nuclei are positioned within a single cluster within the ventral end of the muscle. This cluster then separates into two clusters with each traveling directionally to their respective poles. Once the clusters reach the muscle poles, they move back in to the muscle and position themselves evenly throughout the muscle fiber. Adapted from (Folker and Baylies, 2013).

al., 2014; Metzger et al., 2012). This highly conserved cellular process of nuclear movement in skeletal muscle suggest the importance of proper nuclear movement and positioning in skeletal muscle. However, the reason for these movements and the mechanisms that regulate the process are only starting to be elucidated.

### **1.5.1 The LINC complex and nuclear positioning in skeletal muscle**

One aspect of nuclear movement and positioning that has become clear is the contribution of the LINC complex. The importance of both the KASH-domain and the SUN-domain proteins in nuclear positioning has been extensively demonstrated. For example, by displacing endogenous KASH-domain containing protein, nesprin 1, from the nucleus by expression of a dominant negative nesprin 1, that lacks the ability to interact with the cytoskeleton, nuclei became mispositioned and moved less dynamically in C2C12 myotubes (Grady et al., 2005; Wilson and Holzbaur, 2012). Mechanistically, nesprin 1 also has a role in the recruitment of the centrosomal proteins PCM-1 and Akap450 to the nuclear envelope, where they function in microtubule nucleation. Nesprin 1 can also recruit the microtubule motor kinesin to the nuclear surface in mammalian cell culture. However, the ability of nesprin 1 to recruit PCM-1 and Akap450 was independent of kinesin recruitment to the nuclear surface. Nonetheless, proper nuclear positioning was only possible if nesprin 1 was able to recruit both centrosomal proteins and kinesin (Espigat-Georger et al., 2016; Gimpel et al., 2017; Wilson and Holzbaur, 2015). KASH-domain containing proteins interaction with SUN-domain containing proteins in the lumen of the nuclear envelope is also essential for proper nuclear positioning. Removal of the KASH-domain leads to anchorage defects and mispositioned nuclei in mammalian cells (Chapman et al., 2014;

Zhang et al., 2009) while removal of the KASH-domain from either KASH-domain containing protein in *Drosophila* caused clustering of nuclei in the larval muscles (Elhanany-Tamir et al., 2012). Similarly, deletion of both SUN-domain containing proteins, SUN-1 and SUN-2, resulted in clustered nuclei throughout the muscle (Lei et al., 2009) and deletion of the SUN domain protein, Klaroid, caused mispositioned nuclei in *Drosophila* embryonic musculature (Elhanany-Tamir et al., 2012). Interestingly, overexpression of Klaroid also leads to mispositioning and clustering of nuclei in *Drosophila* (Tan et al., 2018). Together these data suggest the LINC complex plays a crucial role regulating nuclear positioning yet this function must itself be regulated for proper nuclear positioning to be reached, as both too much and too little of some LINC complex components impact nuclear positioning. Furthermore in systems with multiple KASH-domain containing or SUN-domain containing proteins, how the functions of each are balanced against each other are only beginning to be elucidated.

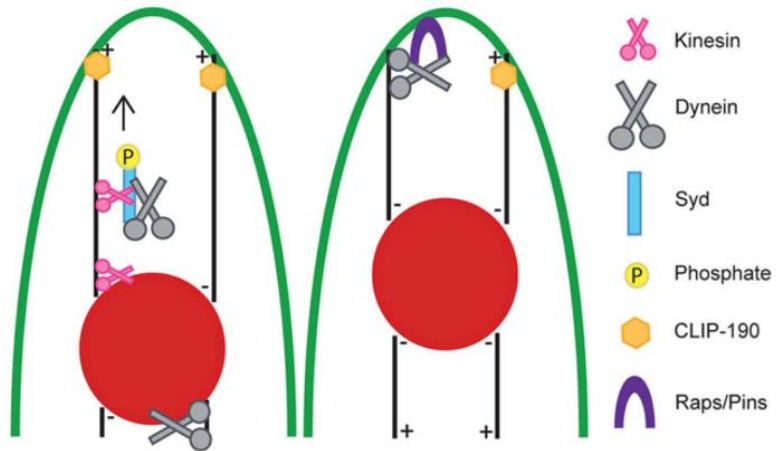
### **1.5.2 The cytoskeleton and nuclear positioning in skeletal muscle**

The cytoskeleton has also been demonstrated to provide the force necessary for nuclear movement and positioning (Gundersen and Worman, 2013). However, due to the uniqueness of skeletal muscle, our understanding of mechanisms regulating nuclear movement and positioning in other cell types are difficult to translate to skeletal muscle. For example, the microtubule cytoskeleton drives nuclear positioning in many tissues. However, in muscle, the organization of the microtubule cytoskeleton is different from most other cell types. Instead of anchoring the minus-ends of microtubules at a single microtubule organizing center (MTOC), muscle cells have many MTOCs. Upon the fusion

of myoblasts in culture, the single MTOC, known as the centrosome, is disassembled and the material is redistributed to the nuclear envelope and to a lesser extent the Golgi apparatus (Ralston et al., 2001; Tassin et al., 1985). This organization of MTOCs was found to produce a network of microtubules at the end of the myotubes with their plus-ends generally oriented toward the cortex, while in the center of the myotubes microtubules produce an antiparallel microtubule network in C2C12 cells. These networks of microtubules are essential for nuclear movement, as disrupting or severing these networks leads to a dramatic reduction in nuclear movement and positioning (Gache et al., 2017; Wilson and Holzbaur, 2012). However, whether unique mechanisms utilizing these networks of microtubules are used to regulate nuclear positioning in skeletal muscle is unclear.

Although there are differences in microtubule organization, many cytoskeletal-interacting proteins implicated in nuclear movement and positioning within various cell types, also play a role in skeletal muscle. For example, the microtubule motors, kinesin and dynein, which drive nuclear positioning in nearly every system where nuclear movement has been studied, also regulate nuclear movement and positioning in skeletal muscle (Tapley and Starr, 2013). Both kinesin-1 and cytoplasmic dynein localize to the nuclear envelope in myotubes and their depletion leads to a decrease in nuclear dynamics (Wilson and Holzbaur, 2012). In *Drosophila* skeletal muscle, Kinesin and Dynein have been demonstrated to drive nuclear movement through multiple pathways. One such pathway is known as the cortical pathway. Similar to mechanisms detailed in other systems, the

cortical pathway works through cortical-anchored Dynein pulling on microtubules linked to the nucleus (Folker et al., 2012; Kotak and Gönczy, 2013). However, this cortical



localization of Dynein arises by Kinesin-mediated transport of Dynein (Fig. 1.5) (Folker et al., 2012).

**Figure 1.5 Cortical pathway of nuclear positioning.** Suggested functions of microtubule-associated proteins in nuclear positioning. Phosphorylation of Sunday driver (Syd) regulates kinesin-dependent cortical localization of dynein. At the cortex, CLIP-190 stabilizes cortex-microtubule interactions. Raps stabilizes cortical dynein localization allowing dynein to pull on microtubules that are attached to the nucleus. Adapted from (Schulman et. al., 2014).

Kinesin also interacts with the microtubule associated protein Enscosin/MAP7 which is essential for the separation of nuclei in developing *Drosophila* embryonic musculature and mammalian cell culture, respectively (Metzger et al., 2012; Sung et al., 2008). Although multiple mechanisms for regulating myonuclear movement and positioning involving Kinesin and Dynein have been suggested, how these mechanisms are coordinated and interact with other known mechanisms remains unclear.

## 1.6 Introduction to Emerin Functions

As previously mentioned, emerin was first identified by genetic mapping of samples from patients with the most common form of EDMD, X-linked EDMD (Bione et al., 1994; Emery and Dreifuss, 1966). However, it was not until two years later that emerin was identified as a nuclear envelope membrane protein (Manilal et al., 1996; Nagano et al.,

1996). Since that time much more has been elucidated about emerin localization and its function in the cell. For example, the mechanism through which emerin reaches its inner nuclear membrane localization is predominately by the guided entry of tail-anchored proteins pathway. Since emerin is synthesized in the cytoplasm, it is incorporated into the membrane of the ER and targeted to the inner nuclear membrane through TRC40-mediated targeting. Interestingly, patient-derived mutants of emerin have been found to impair TRC40-mediated targeting and the guided entry of tail-anchored proteins pathway, suggesting reduced levels of functional emerin, in the inner nuclear membrane, may contribute to the molecular pathogenesis of EDMD (Pfaff et al., 2016). However, some non-canonically localized populations of emerin have also been identified. In human dermal fibroblasts, emerin was detected at the outer nuclear membrane as well as on ER-Golgi intermediate compartments. These findings open the possibility of alternative emerin functions, at these locations, impacting disease pathogenesis (Salpingidou et al., 2007).

Emerin's more canonical functions mainly utilize the LEM domain of emerin, which is named after the proteins it was first identified in (LAP2, emerin and MAN1). The LEM domain is an approximately 40 residue domain that is best characterized for its ability to interact with the DNA-binding protein Barrier-to-autointegration factor (BAF) (Lin et al., 2000; Mansharamani and Wilson, 2005; Wagner and Krohne, 2007). BAF specifically binds to double-stranded DNA and histones, which allows the LEM domain and BAF interaction to regulate global nuclear organization by connecting interphase chromosomes to the nuclear lamina (Cai et al., 2001; Furukawa et al., 2003; Laguri et al., 2001; Montes De Oca et al., 2005; Zheng et al., 2002). Emerin itself is an integral part of the nuclear lamina and downregulation of both LEM domain containing proteins disrupts co-assembly

of the nuclear lamina in *C. elegans* (Liu et al., 2000; Liu et al., 2003; Margalit et al., 2005). Furthermore, the importance of emerin's role in the nuclear lamina is highlighted by the fact that emerin mutations found in EDMD patients altered nuclear envelope elasticity and increased nuclear fragility (Rowat et al., 2006). However, the known functions of emerin function in regulating nuclear movement and other EDMD-linked pathologies is only beginning to be understood.

### **1.6.1 Emerin's interactions with the LINC complex**

The network of interacting partners of emerin has continued to grow since emerin was first identified. One interesting group of proteins that interact with emerin are the SUN- and KASH-domain containing proteins. However, not all isoforms of these proteins interact with emerin in the same manner. For instance, emerin and the SUN-domain proteins are both localized to the inner nuclear membrane and contain luminal and nucleoplasmic domains. However, the direct interaction between emerin and SUN-domain proteins is mediated by the nucleoplasmic domain of both proteins (Haque et al., 2010). Interestingly, there are two SUN-domain containing proteins, SUN1 and SUN2, which contain divergent N-termini in mammals (Crisp et al., 2006; Haque et al., 2006). Sequence alignment of both SUN-domain containing proteins found the emerin-binding domain to be absent from the shorter SUN2 N-terminal domain and only a weak interaction was detected between SUN2 and emerin. Although both SUN1 and SUN2 interact with emerin, the difference in binding affinity suggest that SUN1 and SUN2 may have different modes of interacting with emerin (Haque et al., 2010). Immunoprecipitation assays have also identified emerin as a binding partner of small isoforms of the KASH-domain containing

proteins nesprin 1 and nesprin 2 (Mislow et al., 2002; Zhang et al., 2005). However, the luminal domains of nesprin and emerin are not long enough to span the luminal space to interact (Wang et al., 2012; Wolff et al., 2001). Interestingly, although larger forms of the KASH-domain containing proteins, nesprin 1 and 2, localize to the outer nuclear membrane, immunolocalization studies showed C-termini of nesprin colocalization with emerin suggesting an inner nuclear membrane localization for some smaller isoforms of nesprin 1 and nesprin 2 (Mislow et al., 2002; Zhang et al., 2005). In cells where emerin is mislocalized to the ER, smaller nesprin 2 isoforms colocalized with emerin in aggregates within the ER (Zhang et al., 2005). Although emerin interacts with components of the LINC complex, different isoforms of LINC complex components interact differently with emerin. However, in systems where there are multiple isoforms or homologs of emerin, such as *Drosophila*, where both Bocksbeutel and Otefin share similar homology to emerin, little is known about their overlap in binding partners or even their functions.

### **1.6.2 Emerin's role in the regulation of transcription**

Emerin also has a fairly well characterized role in the regulation of transcription. In particular, emerin plays an important role in the global chromatin organization of the nucleus. Mapping of chromatin interactions found that approximately 40% of the *Drosophila* and Human genome contact the nuclear envelope and components of the nuclear lamina. These regions of chromatin that interact with components of the nuclear lamina were termed lamin-associated domains (LADs) and emerin-associated domains (EADs) depending on whether they interacted with lamin or emerin (Guelen et al., 2008; Pickersgill et al., 2006). LADs and EADs are largely made up of heterochromatic regions

and are often characterized by low gene density and repressive chromatin marks due to their peripheral localization (Finlan et al., 2008; Peric-Hupkes et al., 2010; Reddy et al., 2008). The repressive nature of the nuclear periphery arises partially due to a regulatory complex composed of emerin, BAF, HDAC1 and HDAC3 (Holaska and Wilson, 2007). In fact, binding of emerin to HDAC3 recruits HDAC3 to the nuclear periphery where emerin stimulates the catalytic activity of HDAC3. The importance of this interaction is highlighted by some unique emerin mutations that disrupt HDAC3 binding and lead to EDMD (Demmerle et al., 2012). Emerin also regulates transcription through direct interactions with multiple transcription factors. For some of these interactions, such as the transcription factors germ cell-less (GCL) and LIM-domain-only 7 (LMO7), binding to emerin is required for proper nuclear localization and therefore transcription of its target genes (Holaska et al., 2003; Holaska et al., 2006). Emerin also binds and regulates the nuclear localization of the WNT signaling transcription factor  $\beta$ -catenin (Markiewicz et al., 2006; Tilgner et al., 2009). However, knockdown of  $\beta$ -catenin also leads to a decrease in mRNA expression and nuclear accumulation of emerin, suggesting emerin and  $\beta$ -catenin regulate each other's expression and localization (Tilgner et al., 2009). Although, emerin's role in regulating transcription is fairly well understood, little is known about how the transcriptional regulatory function of emerin factors into EDMD pathologies.

## **1.7 Remaining Questions**

The work in this thesis is a culmination of two goals: 1. Understanding how EDMD- and CNM-linked genes coordinate nuclear movement and positioning and 2. Developing an assay to expand the candidates of genes that regulate muscle development and function.

Which together further our understanding of the connection between skeletal muscle development and disease.

Toward the first goal of this thesis, the mechanisms that drive nuclear movement and positioning are only beginning to become elucidated. In particular, how is the movement and positioning of the many nuclei within a syncytium regulated and coordinated? Although some mechanisms have been uncovered for specific steps of myonuclear movement and positioning, how these mechanisms function together or in isolation to regulate nuclear positioning remains uncertain. Furthermore, as mispositioned nuclei are a hallmark of many different muscular dystrophies, it remains unclear if mispositioned nuclei in distinct muscle disease arise from defects in a common mechanism.

While the LINC complex-dependent mechanisms regulating nuclear movement and positioning is one of the best characterized, how emerin fits within these mechanisms is poorly understood. Additionally, in *Drosophila* there are two homologs of *emerin*, *bocksbeutel* and *otefin*. This raises questions about the redundancy of these homologues or whether various functions of emerin have been split between Bocksbeutel and Otefin.

Toward the second goal of this thesis, due to the short life span and relative ease of handling, *Drosophila* has proved invaluable as a scientific screening tool. However, very few screens have been performed to identify regulators of skeletal muscle development and function. Therefore, it is unclear whether unidentified regulators remain. Furthermore, are there adaptations to pre-existing assays that can be made to better harness the screening power of *Drosophila* and better understand the mechanisms regulating muscle development and function?

This work aims to contribute toward both goals mentioned previously. This thesis begins by investigating the mechanisms regulating nuclear movement and positioning that are disrupted in EDMD and CNM. In particular, whether mispositioned nuclei present in both diseases arise from common or distinct mechanisms (Chapter 2). Next, this thesis investigates the role that emerin plays in regulating nuclear movement and positioning, with a focus on the two *Drosophila emerin* homologs, *bocksbeutel* and *otefin* (Chapter 3). Finally, this thesis concludes with the development and implementation of a high throughput screening assay to identify and characterize novel regulators of muscle development and function (Chapter 4).

## **Chapter 2:**

# **Emery-Dreifuss Muscular Dystrophy-linked genes and Centronuclear myopathy-linked genes regulate myonuclear movement by distinct mechanisms**

*The content in this chapter was adapted from:*

**Collins, M.A., Mandigo, T.R., Camuglia, J.M., Vazquez, G.A., Anderson, A.J., Hudson, C.H., Hanron, J.L., and Folker, E.S.** (2017) Emery-Dreifuss muscular dystrophy-linked genes and Centronuclear myopathy-linked genes regulate myonuclear movement by distinct mechanisms. *Molecular Biology of the Cell*. **28**: 2303-2317.

## 2.1 Abstract

Muscle cells are a syncytium in which the many nuclei are positioned to maximize the distance between adjacent nuclei. Although mispositioned nuclei are correlated with many muscle disorders, it is not known whether this common phenotype is the result of a common mechanism. To answer this question, the expression of genes linked to Emery-Dreifuss muscular dystrophy (EDMD) and Centronuclear myopathy (CNM) was disrupted in *Drosophila*, and the position of the nuclei was evaluated. We found that the genes linked to EDMD and CNM were each necessary to properly position nuclei. However, the specific phenotypes were different. EDMD-linked genes were necessary for the initial separation of nuclei into distinct clusters, suggesting that these factors relieve interactions between nuclei. CNM-linked genes were necessary to maintain the nuclei within clusters as they moved toward the muscle ends, suggesting that these factors were necessary to maintain interactions between nuclei. Together these data suggest that nuclear position is disrupted by distinct mechanisms in EDMD and CNM.

## 2.2 Introduction

Based on their abundance and their repetitive structure, myofibers, the cellular units of skeletal muscle, have long been a model system to identify cell biological mechanisms that underlie development. Yet, many features of myofiber structure, such as their syncytial nature, are specialized for muscle cells. During the development of an individual muscle cell, many mononucleated myoblasts fuse to form a syncytial myofiber that can contain up to thousands of nuclei (Kim et al., 2015b), each of which is precisely positioned. Most

nuclei are distributed evenly throughout the muscle, with a small cluster of nuclei associated with the neuromuscular junction (Bruusgaard et al., 2003; Bruusgaard et al., 2006). Disruptions in the distribution of nuclei have been correlated with muscle disease for several decades (Dubowitz et al., 2007b). Two muscle diseases in which mispositioned nuclei are abundant are Emery-Dreifuss muscular dystrophy (EDMD) (Sewry et al., 2001) and Centronuclear Myopathy (CNM) (Spiro et al., 1966). Yet it is not clear whether the position of the nuclei is a consequence of ongoing muscle repair or if mispositioned nuclei contribute to muscle weakness and muscle deterioration. More fundamentally, it is not known whether mispositioned nuclei in disparate muscle diseases arise from common or distinct mechanisms.

To determine whether mispositioned nuclei are the result of a common cellular disruption, or are due to disease-specific cellular defects, the position of nuclei was evaluated in *Drosophila* that had disruptions in genes linked to EDMD or CNM. Each of the genes mutated in patients with EDMD encodes for a protein that is localized to the nucleoskeleton or the nuclear envelope (Meinke et al., 2011). Based on this localization, the function of some EDMD-linked genes with respect to nuclear position has been tested in muscle (Dialynas et al., 2010; Elhanany-Tamir et al., 2012; Zhang et al., 2009), in cultures of myoblast-derived cells (Cadot et al., 2012; Wilson and Holzbaur, 2015), and in other cell types (Gundersen and Worman, 2013).

In mammals, *SYNE1* and *SYNE2* are necessary for the clustering of nuclei at the postsynaptic side of the neuromuscular junction (Zhang et al., 2007; Zhang et al., 2009). Furthermore, Nesprin proteins and SUN proteins regulate the distribution of nuclei throughout the muscle in *Drosophila* embryos and larvae (Elhanany-Tamir et al., 2012),

and in mammalian cell culture systems (Wilson and Holzbaaur, 2015). Additionally, Emerin is essential for nuclear movement during cell migration (Chang et al., 2013). However, these experiments were all completed in different systems making it difficult to compare the functions of each factor with respect to nuclear movement during muscle development *in vivo*.

Despite the name Centronuclear myopathy, there has been little investigation of the causes or consequences of mispositioned nuclei with respect to CNM. The genes mutated in patients with CNM encode for proteins that regulate the development and structure of the T-tubule in skeletal muscle, or the release of calcium in skeletal muscle (Jungbluth et al., 2007). Therefore, it is thought that defects in  $\text{Ca}^{2+}$  signaling and T-tubule structure underlie CNM. However, we have recently demonstrated that the movement of nuclei in muscle is an early event in muscle development that precedes myofibril assembly (Auld and Folker, 2016), and therefore prior to a fully developed T-tubule network (Flucher et al., 1993).

Furthermore, it has recently been demonstrated that the proteins linked to CNM have additional cellular functions. Specifically, Amphiphysin-dependent activation of N-WASP was demonstrated to be a prerequisite for triad formation (the junction between the T-tubules and the sarcoplasmic reticulum) and was necessary for proper movement of nuclei to the periphery of a cultured myofiber system (Falcone et al., 2014). Additionally, Amphiphysin contributed to the attachment between the nucleus and the cytoskeleton and nuclear movement in culture (D'Alessandro et al., 2015). This latter function suggests that nuclear position may be regulated by the concerted actions of Amphiphysin (and perhaps other CNM-linked genes) and the proteins linked to EDMD that localize to the nucleus.

We have compared the effects of genes linked to CNM and EDMD during muscle development in *Drosophila* larvae. This system combines a short developmental timeline with optical clarity and rich genetic resources which made it possible to measure the precise distribution of nuclei in vivo and correlate mispositioned nuclei with a decrease in muscle function. Consistent with previous reports (Elhanany-Tamir et al., 2012), the LINC complex, which has been linked to EDMD, contributed to larval myonuclear positioning. Additionally, the CNM-linked genes *amphiphysin* (*amph*) and *myotubularin* (*mtm*) are also necessary for positioning myonuclei in both the larva. However, the effects of the CNM-linked genes were milder and are mechanistically distinct. CNM-linked genes and EDMD-linked genes exhibit different interactions with the microtubule motors dynein and kinesin. Thus, nuclear position is likely disrupted by distinct mechanisms in different muscle disorders.

## 2.3 Results

### 2.3.1 Muscle function in *Drosophila* larvae requires genes mutated in patients with Emery-Dreifuss Muscular Dystrophy or Centronuclear Myopathy

To determine whether EDMD- and CNM-linked genes affect muscle function, larval locomotion was tested in larvae from which *otefin* (*Drosophila* *emerin*), *bocksbeutel* (*Drosophila* *emerin*), *klaroid* (*Drosophila* *SUN*), *klarsicht* (*Drosophila* *nesprin*) or *amphiphysin* was zygotically removed with the respective *ote*<sup>B279</sup>, *bocks*<sup>DP01391</sup>, *koi*<sup>HRKO80.w</sup>, *klar*<sup>l</sup> or *amph*<sup>26</sup> alleles (Table A1.1). *bocks*<sup>DP01391</sup>, *klar*<sup>l</sup>, and *amph*<sup>26</sup> homozygotes moved more slowly than their respective heterozygous and control larvae (Fig. 2.1A). These data indicate that *bocksbeutel*, *klarsicht*, and *Amphiphysin* are all necessary for proper muscle

function. Both *ote*<sup>B279</sup> and *koi*<sup>HRK080.w</sup> were homozygous lethal and thus the impact of these alleles on animal movement could not be determined.

To determine whether the impact on muscle function was correlated with mispositioned nuclei, the spacing of nuclei in *Drosophila* larvae was measured. The distance between nuclei in *Drosophila* larvae has been measured in many studies (Elhanany-Tamir et al., 2012; Folker et al., 2012; Metzger et al., 2012; Schulman et al., 2014), but only rarely has the effect of muscle size been considered (Folker et al., 2012; Schulman et al., 2014), and never has the number of nuclei been considered. We measured the internuclear distance as a function of muscle size and the number of nuclei to determine how evenly nuclei were distributed (Fig. 2.1 and Fig. 2.2). In control larvae, the distribution of nuclei was consistent. In most muscles, nuclei were arranged in two lines, parallel to the long axis of the muscle. Both control genotypes, *twist-GAL4*, *apRed* and *DMef2-GAL4*, *apRed* had nearly identical internuclear distance ratios of 78% of maximal. In *bocks*<sup>DP01391</sup> and *klar*<sup>l</sup> larvae nuclei were in a single line, positioned centrally within the muscle, and parallel to the long axis of the muscle (Fig. 2.1B). Quantitatively, the internuclear distance was 55% of maximal for both *bocks*<sup>DP01391</sup> and *klar*<sup>l</sup> larvae (Fig. 2.1C). In *amph*<sup>26</sup> larvae, there were regions of single file nuclei and regions with clusters of nuclei (Fig. 2.1B). Quantitatively, in *amph*<sup>26</sup> larvae the internuclear distance

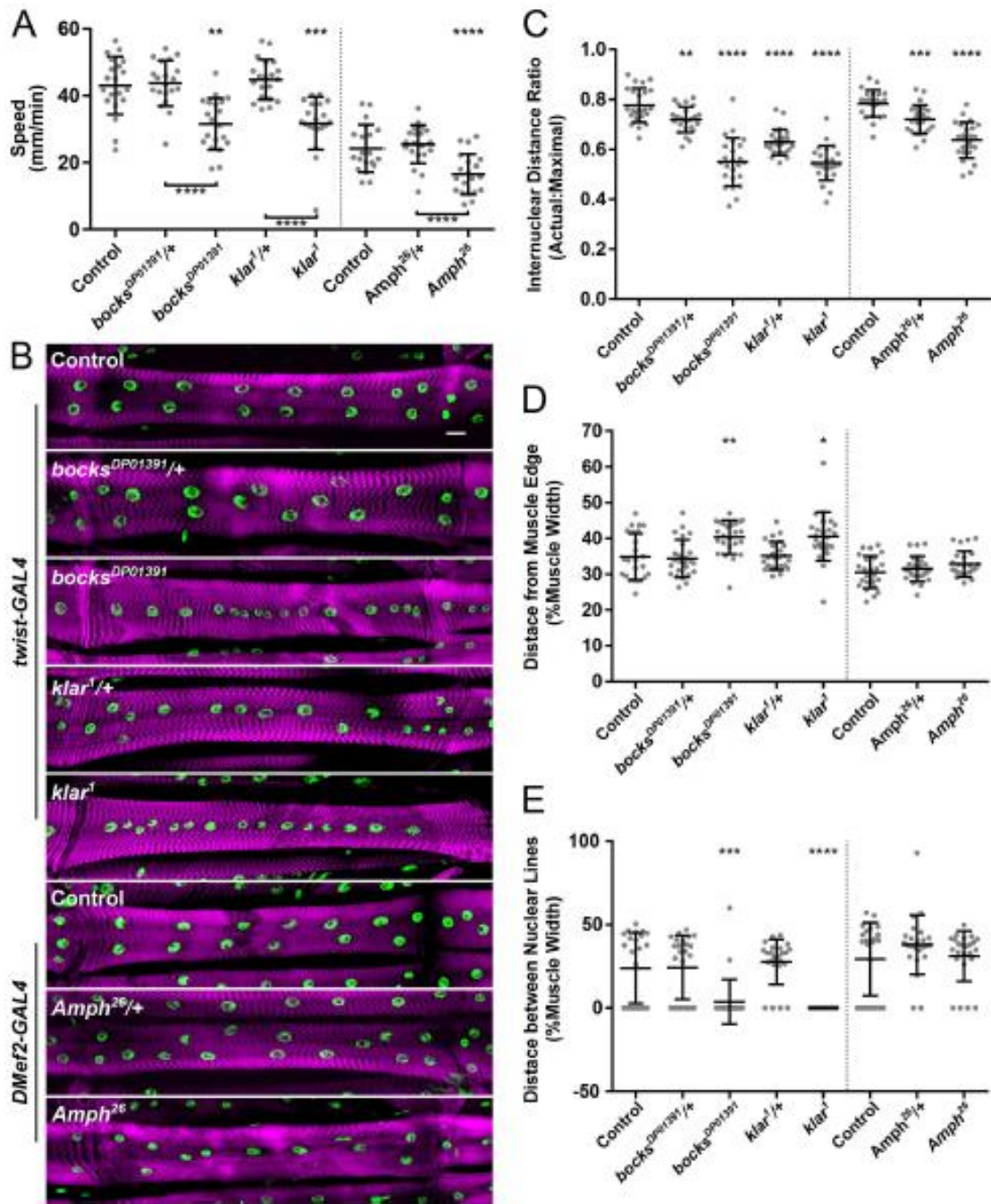


**Figure 2.1** The EDMD-linked genes *bocksbeutel* and *klarsicht*, and the CNM-linked gene *Amphiphysin* are necessary for proper locomotion and myonuclear position in *Drosophila* larvae. (A) The average speed of *Drosophila* larvae as they crawl toward an odorant stimulus. Error bars indicate s.d. from 20 larvae. (B) Immunofluorescence images of VL3 muscles from dissected stage L3 larvae. The sarcomeres were stained with phalloidin (magenta) and the nuclei were stained with Hoechst (green). Scale bar, 25 $\mu$ m. (C) The ratio of actual internuclear distance to maximal internuclear distance in larval muscles from the indicated genotypes. (D) The distance between nuclei and the nearest muscle edge in larval muscles from the indicated genotypes. (E) The distance between nuclear lines in larval muscles from the indicated genotypes. (C-E) Data points indicate the average values of nuclei within a single VL3 muscle. Error bars indicate s.d. from 24 VL3 muscles. Student's t-test was used for comparison to controls. \* $P$ <0.05, \*\* $P$ <0.005, \*\*\* $P$ <0.0005, \*\*\*\* $P$ <0.00005.

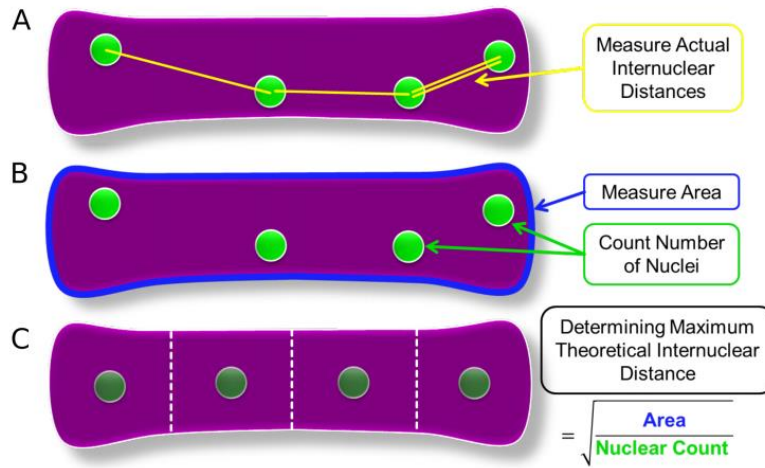


**Figure 2.2** Analysis of nuclear position in *Drosophila* larvae. (A-C) Muscle is in magenta, nuclei are green. (A) The distance between the center of each nucleus and the center of its nearest neighbor was measured. (B) The area of the muscle was measured and the number of nuclei were counted. (C) The square root of the area divided by the number of nuclei was calculated to determine the theoretical maximum internuclear distance for each muscle.

was 64% of maximal (Fig. 2.1C). Nuclear position was also measured relative to the muscle edge in each genotype. In *bocks*<sup>DP01391</sup> and *klar*<sup>1</sup> larvae, nuclei were further from the muscle edge compared to control (Fig. 2.1D). However, nuclear position relative to the muscle edge was not affected in *amph*<sup>26</sup> larvae. Finally, the distance between the two parallel lines was similar in *amph*<sup>26</sup> and control larvae. However, this value was nearly zero in most *bocks*<sup>DP01391</sup> and *klar*<sup>1</sup> larvae (Fig. 2.1E). These data indicate that all three of *bocks*, *klar*, and *amph* are necessary for proper nuclear positioning in larval muscle, but that the specific phenotype caused by the loss of *bocksbeutel* or *klarsicht* is different from the phenotype caused by the loss of *amphiphysin*.

To determine whether the impact of each gene on nuclear position was muscle autonomous, the GAL4/UAS system was used to deplete each protein specifically from muscle. UAS-RNAi

Genes	WT	RNAi
<i>Ote</i>	1.00	0.25
<i>bocks</i>	1.00	0.35
<i>koi</i>	1.00	0.20
<i>klar</i>	1.00	0.40
<i>mtm</i>	1.00	0.62
<i>Amph</i>	1.00	0.30

**Table 2.1** Relative expression of EDMD- and CNM-linked genes when knockdown by RNAi. Relative expression of transcripts from single embryos for EDMD- and CNM-linked proteins. Values are shown for the most efficient knockdown driven ubiquitously by *Tubulin-GAL4*. Values are normalized to RP49 transcript and displayed with control expression levels normalized to a value of 1.

expression, using RNAi lines that were validated by RT-PCR (Table 2.1), was driven from embryonic stage 12 through larval development under the control of *DMef2-GAL4*. RNAi experiments included another CNM-linked gene *Myotubularin1* (*mtm*), which is mutated in some patients with a severe form of CNM (Liechti-Gallati et al., 1991). Muscle-specific depletion of either *bocks* or *klar* phenocopied the null larvae (*bocks*<sup>DP01931</sup> and *klar*<sup>l</sup>) as large regions of muscle had nuclei arranged in a single line rather than two parallel lines (Fig. 2.3A) and the average internuclear distance was 63% of maximal (Fig. 2.3B). Muscle-specific depletion of *koi* resembled *bocks*- and *klar*-depleted larvae in that nuclei formed a single line with an internuclear distance ratio of 68% of maximal (Fig. 2.3A and B). Muscle-specific depletion of *Ote* led to larvae with nuclei forming several clusters and an internuclear distance ratio of 68% of maximal (Fig. 2.3A and B). Expression of *amph* RNAi or *mtm* RNAi caused a milder phenotype (Fig. 2.3A) with the evenness of nuclear position being 70% and 74% of maximal (Fig. 2.3B). Additionally, *DMef2-GAL4* mediated depletion of each gene product, except for *mtm*, resulted in nuclei that were positioned further from the muscle edge compared to control Fig. 2.3C). The effects on the distance between lines of nuclei were more complicated. Lines of nuclei were closer together when *koi* or *klar* was depleted, while lines of nuclei were further apart when *mtm* was depleted compared to controls (Fig. 2.3D).

Because *DMef2-GAL4* mediated expression of an RNAi in muscle begins at stage 12 of embryonic development and continues throughout larval development, *twist-GAL4*, was used to acutely drive the expression of the RNAi earlier in development from stage 8 through stage 13 in the mesoderm. Thus, with this manipulation, the expression of each gene is disrupted only during a short, and defined time period early in muscle development.

*twist-GAL4* mediated depletion of each gene phenocopied the *DMef2-GAL4* mediated depletion with respect to the evenness of nuclear spacing (Fig. 2.4A and B). However *twist-*

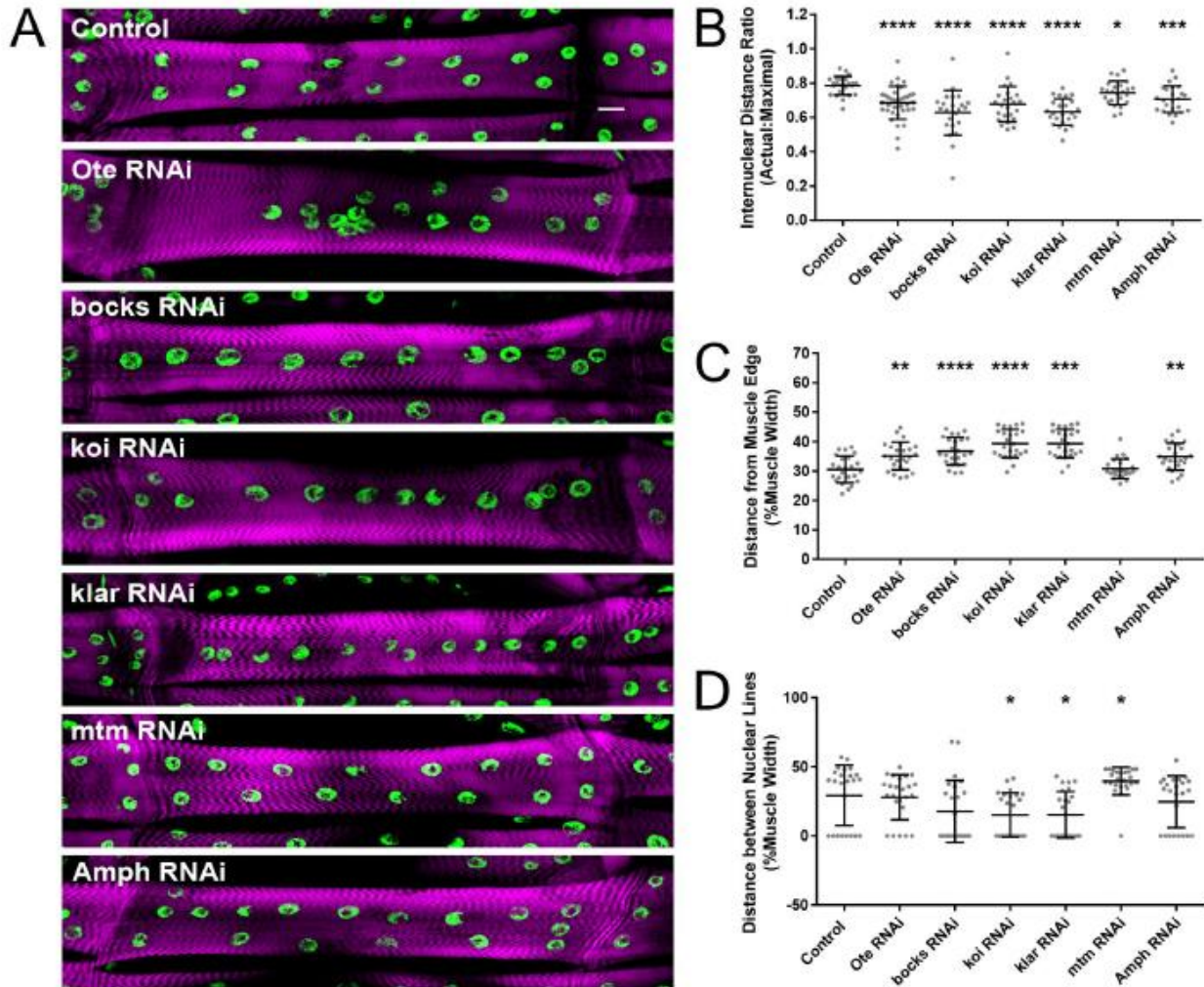


**Figure 2.3** The effects of *bocksbeutel*, *klarsicht*, and *Amphiphysin* on nuclear position in larval muscles are muscle autonomous. (A) Immunofluorescence images of VL3 muscles from stage L3 larvae that expressed RNAi against the indicated gene under the control of the muscle specific driver, *DMef2-GAL4*. The sarcomeres were stained with phalloidin (magenta) and the nuclei were stained with Hoechst (green). Scale bar, 25 $\mu$ m. (B) The ratio of actual internuclear distance to maximal internuclear distance in larval muscles that expressed the indicated UAS-RNAi constructs under the control of the muscle specific driver, *DMef2-GAL4*. Data points indicate the average value for all nuclei within a single VL3 muscle. (C) The distance between nuclei and the nearest muscle edge in larvae that expressed the indicated UAS-RNAi constructs under the control of *DMef2-GAL4*. Data points indicate the average distance from the muscle edge of all nuclei within a single VL3 muscle. (D) The distance between nuclear lines in larval muscles from larvae that expressed the indicated UAS-RNAi constructs under the control of *DMef2-GAL4*. Data points indicate the average distance between nuclear lines within a single VL3 muscle. (B-D) Error bars indicate s.d. from 24 VL3 muscles. Student's t-test was used for comparison to controls. \* $P < 0.05$ , \*\* $P < 0.005$ , \*\*\* $P < 0.0005$ , \*\*\*\* $P < 0.00005$ .

*GAL4* mediated expression of RNAi against each gene did not impact the position of nuclei relative to the muscle edge (Fig. 2.4C) or the distance between lines of nuclei (Fig. 2.4D).

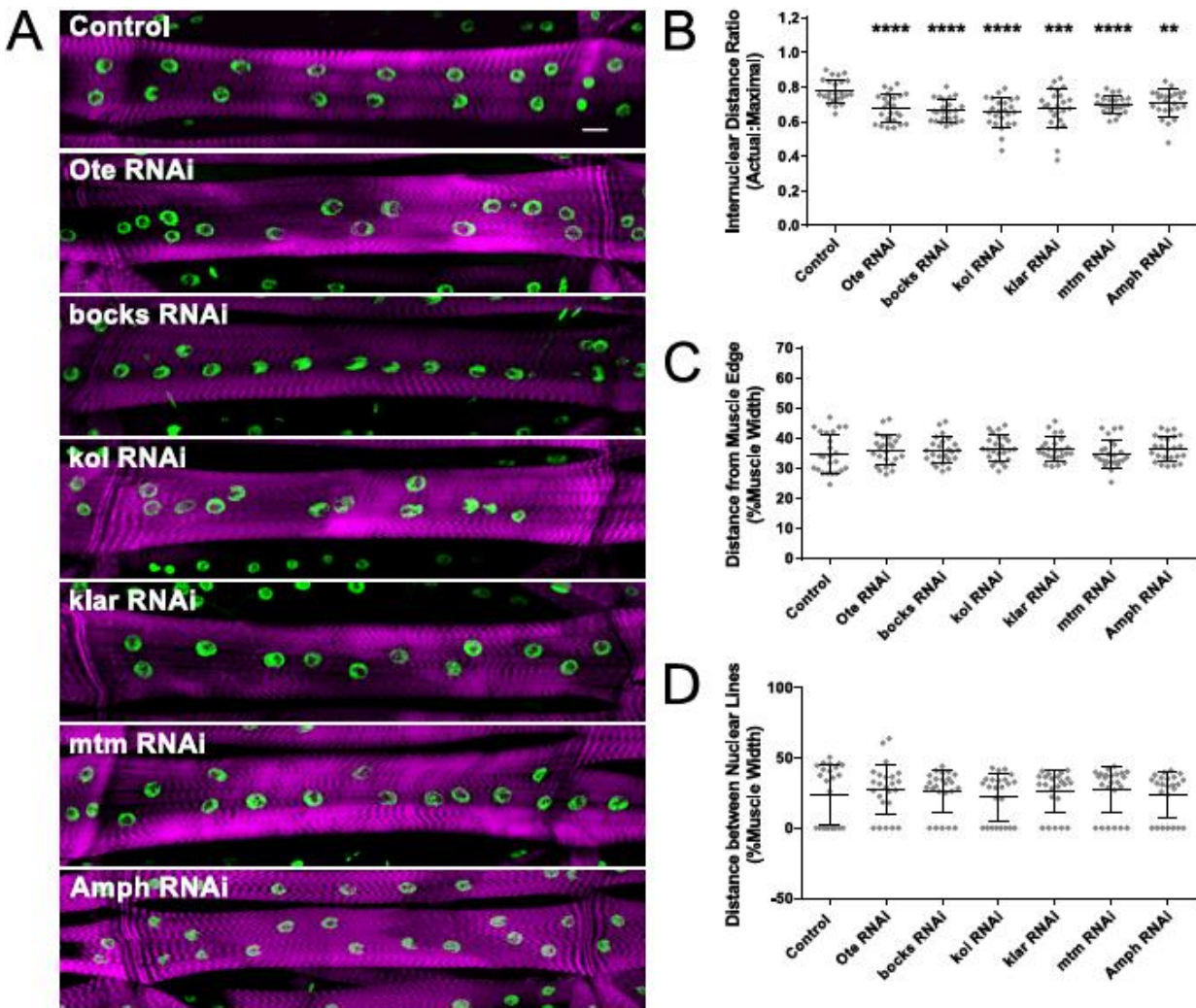


**Figure 2.4** The effects of *bocksbeutel*, *klarsicht*, and *Amphiphysin* on nuclear position in larval muscles are mesoderm autonomous. (A) Immunofluorescence images of VL3 muscles from stage L3 larvae that expressed RNAi against the indicated gene under the control of the muscle specific driver, *Twist-GAL4*. The sarcomeres were stained with phalloidin (magenta) and the nuclei were stained with Hoechst (green). Scale bar, 25 $\mu$ m. (B) The ratio of actual internuclear distance to maximal internuclear distance in larval muscles that expressed the indicated UAS-RNAi constructs under the control of the muscle specific driver, *Twist-GAL4*. Data points indicate the average value for all nuclei within a single VL3 muscle. (C) The distance between nuclei and the nearest muscle edge in larvae that expressed the indicated UAS-RNAi constructs under the control of *DMef2-GAL4*. Data points indicate the average distance from the muscle edge of all nuclei within a single VL3 muscle. (D) The distance between nuclear lines in larval muscles from larvae that expressed the indicated UAS-RNAi constructs under the control of *Twist-GAL4*. Data points indicate the average distance between nuclear lines within a single VL3 muscle. (B-D) Error bars indicate s.d. from 24 VL3 muscles. Student's t-test was used for comparison to controls. \* $P < 0.05$ , \*\* $P < 0.005$ , \*\*\* $P < 0.0005$ , \*\*\*\* $P < 0.00005$ .

These data suggest that the general distribution of nuclei throughout the muscle is regulated early in development but that additional regulation of the position of nuclei relative to the muscle edge occurs later.

To determine whether *bocksbeutel* and *amphiphysin* are only required for the initial positioning of nuclei, or are also required to maintain nuclear positioning during larval development, expression of the *bocksbeutel* and *amphiphysin* RNAi was driven under the control of *MHC-GAL4*, which drives expression of the RNAi later in development from the L1 larval stage throughout adulthood. *MHC-GAL4* mediated depletion of *bocksbeutel* or *amphiphysin* resulted in a disruption of nuclear positioning throughout the muscle (Fig 2.5A and B). Additionally depletion of either *bocksbeutel* or *amphiphysin* impacted the distance between lines of nuclei either producing nuclear lines that were closer together or

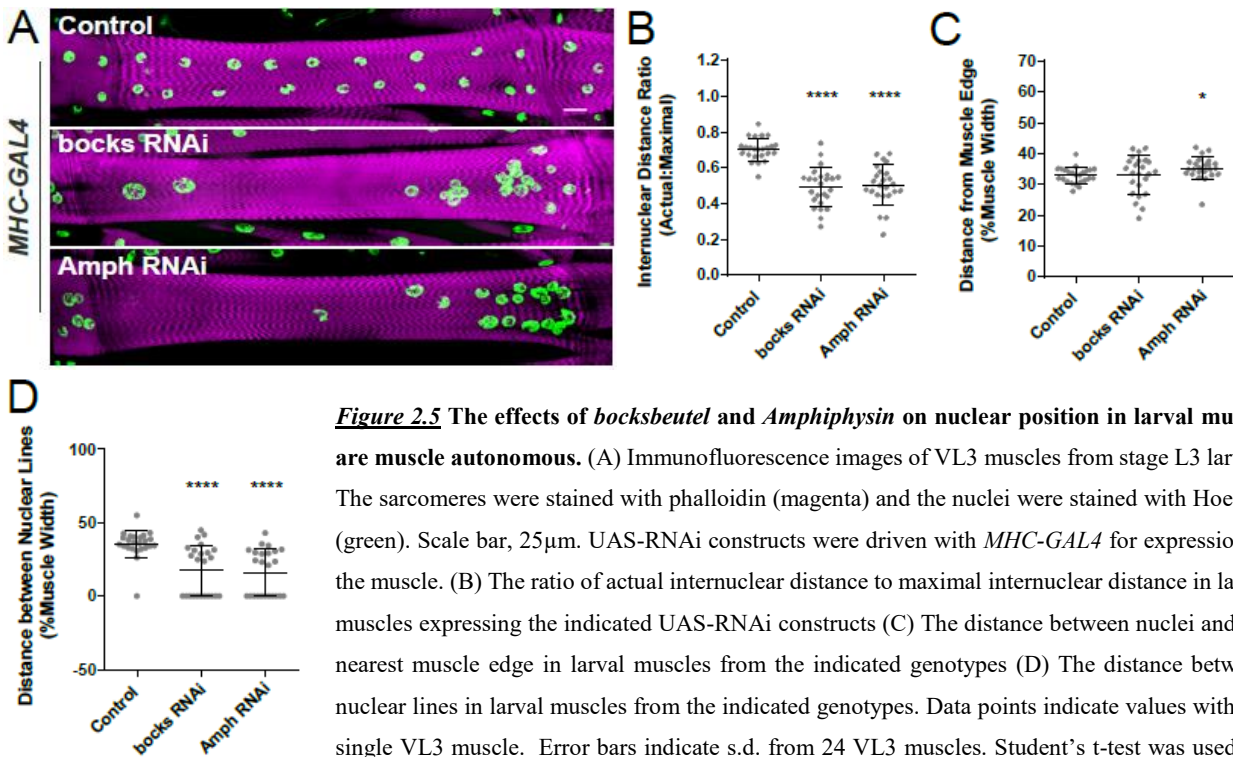


**Figure 2.5** The effects of *bocksbeutel* and *Amphiphysin* on nuclear position in larval muscle are muscle autonomous. (A) Immunofluorescence images of VL3 muscles from stage L3 larvae. The sarcomeres were stained with phalloidin (magenta) and the nuclei were stained with Hoechst (green). Scale bar, 25 $\mu$ m. UAS-RNAi constructs were driven with *MHC-GAL4* for expression in the muscle. (B) The ratio of actual internuclear distance to maximal internuclear distance in larval muscles expressing the indicated UAS-RNAi constructs (C) The distance between nuclei and the nearest muscle edge in larval muscles from the indicated genotypes (D) The distance between nuclear lines in larval muscles from the indicated genotypes. Data points indicate values within a single VL3 muscle. Error bars indicate s.d. from 24 VL3 muscles. Student's t-test was used for comparison to controls. \* $P < 0.05$ , \*\*\*\* $P < 0.00005$ .

no discernable nuclear lines (Fig 2.5D). However only depletion of *amphiphysin* disrupted the position of nuclei relative to the muscle edge (Fig 2.5C). This data suggests that both *bocksbeutel* and *amphiphysin* are both required during larval development to maintain nuclear positioning within larval muscles.

### 2.3.2 Genetic interactions between microtubule motors and EDMD- and CNM-linked genes in the *Drosophila* larva

To determine whether there are distinct genetic interactions between the EDMD-linked and CNM-linked genes and established pathways known to affect nuclear positioning, genetic interactions between microtubule motors and *bocksbeutel* and *amphiphysin* were tested with respect to nuclear positioning in larvae (Fig. 2.6). The average internuclear distance was 69% of maximal for *dhc64C<sup>4-19</sup>/+*, *bocks<sup>DP01391</sup>/+* larvae compared to 76% and 72% of maximal for *dhc64C<sup>4-19</sup>/+* and *bocks<sup>DP01391</sup>/+* individual heterozygotes respectively (Fig 2.6B). Similarly, the average internuclear distance was 68% of maximal for *khc<sup>8</sup>/+*; *bocks<sup>DP01331</sup>/+* larvae compared to 72 % of maximal for both *khc<sup>8</sup>/+* and *bocks<sup>DP01391</sup>/+* individual heterozygotes (Fig 2.6B). However in *dhc64C<sup>4-19</sup>/+*, *bocks<sup>DP01391</sup>/+* and *khc<sup>8</sup>/+*; *bocks<sup>DP01331</sup>/+* nuclei were properly positioned relative to the muscle edge (Fig 2.6C). Furthermore, in those regions of the muscle where nuclei do form two lines, the two lines are properly spaced relative to one another (Fig 2.6D). Conversely, *dhc64C<sup>4-19</sup>* and *khc<sup>8</sup>* do not genetically interact with *amph<sup>26</sup>* to regulate the distribution of nuclei throughout the muscle (Fig 2.6E-H). Together, these data indicate that *bocksbeutel* regulates nuclear positioning in larvae through a microtubule motor dependent mechanism

while *amphiphysin* regulate nuclear positioning through a microtubule motor independent mechanism.

### **2.3.3 Disruption of EDMD- and CNM-linked genes impacts microtubule organization in the *Drosophila* larva.**

Since the nuclear membrane is one of the sites of the MTOC in muscle (Espigat-Georger et al., 2016; Tassin et al., 1985; Zaal et al., 2011), we investigated whether the depletion of *bocksbeutel* or *amphiphysin* alter the organization of the microtubule cytoskeleton. The microtubule network appeared normal in embryos, but the small cell size and the clustering of nuclei prohibited careful analysis. Therefore, microtubule organization was evaluated in larvae (Fig 2.7A and C). First we investigated whether nuclei were able nucleate microtubules by counting the number of nuclei that had a ring of microtubule staining around them (Fig 2.7A). In control and *bocks*<sup>DP01391</sup> larvae 100% of nuclei had a ring of microtubules, however in *amph*<sup>26</sup> larvae only 69% of nuclei had associated microtubule rings (Fig 2.7B). Microtubule distribution around nuclei with microtubule rings was also measured (Fig 2.7C and D). The distribution of microtubules was measured as the ratio of intensity of tubulin staining oriented dorsally and ventrally from the nucleus versus the intensity of tubulin staining oriented anteriorly and posteriorly from the nucleus. In *bocks*<sup>DP01391</sup> larvae the distribution of microtubules around the nucleus was altered with more microtubules emanating in the dorsal/ventral direction versus the anterior/posterior direction as demonstrated by the microtubule distribution ratio of 0.77 compared to 1.17 in controls (Fig 2.7D). The distribution of microtubules around nuclei with associated microtubule rings in *amph*<sup>26</sup> larvae microtubules were evenly distributed

with a distribution ratio of 1.04 (Fig 2.7B). These data indicate that both *bocksbeutel* and *amphiphysin* are necessary for proper microtubule organization in larvae, however *bocksbeutel* and *amphiphysin* affect different aspects of microtubule organization.

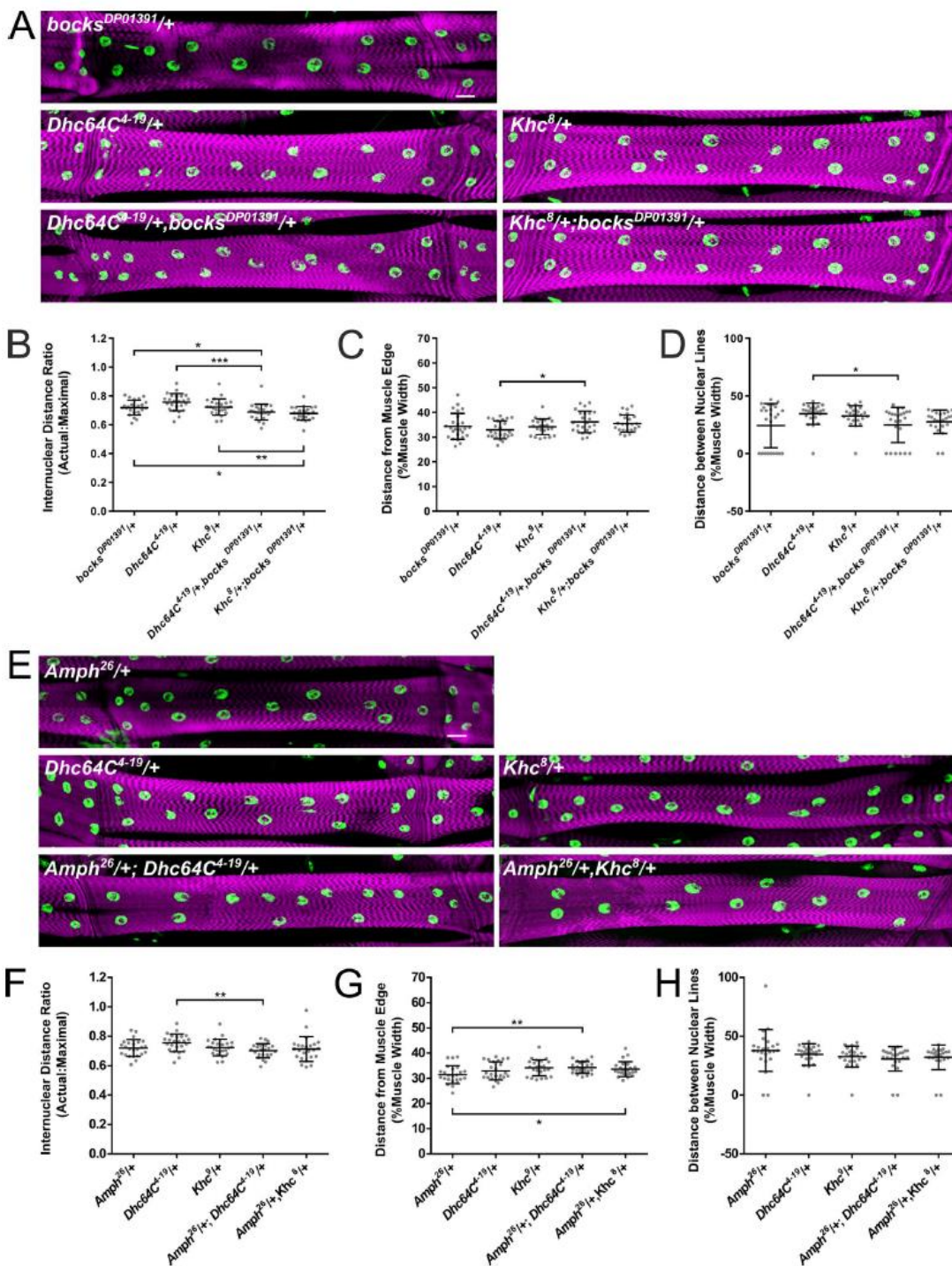


**Figure 2.6** *bocksbeutel* genetically interacts with *dynein* and *kinesin* to affect nuclear positioning within larval muscles. (A,E) Immunofluorescence images of VL3 muscles from stage L3 larvae of indicated genotypes. The sarcomeres were stained with phalloidin (magenta) and the nuclei were stained with Hoechst (green). Scale bar: 25 $\mu$ m. (A) *bocks*<sup>DP01391</sup> mutants were crossed with *dhc64C*<sup>4-19</sup> or *khc*<sup>8</sup> to create double heterozygotes. (E) *amph*<sup>26</sup> mutants were crossed with *dhc64C*<sup>4-19</sup> or *khc*<sup>8</sup> to create double heterozygotes. (B,F) The ratio of actual internuclear distance to maximal internuclear distance in larval muscles from the indicated genotypes. (C,G) The distance between nuclei and the nearest muscle edge in larval muscles from the indicated genotypes. (D,H) The distance between nuclear lines in larval muscles from the indicated genotypes. Data points indicate the average values within a single VL3 muscle. Error bars indicate s.d. from 24 VL3 muscles. Student's t-test was used for comparison to controls. \**P*<0.05, \*\**P*<0.005, \*\*\**P*<0.0005.

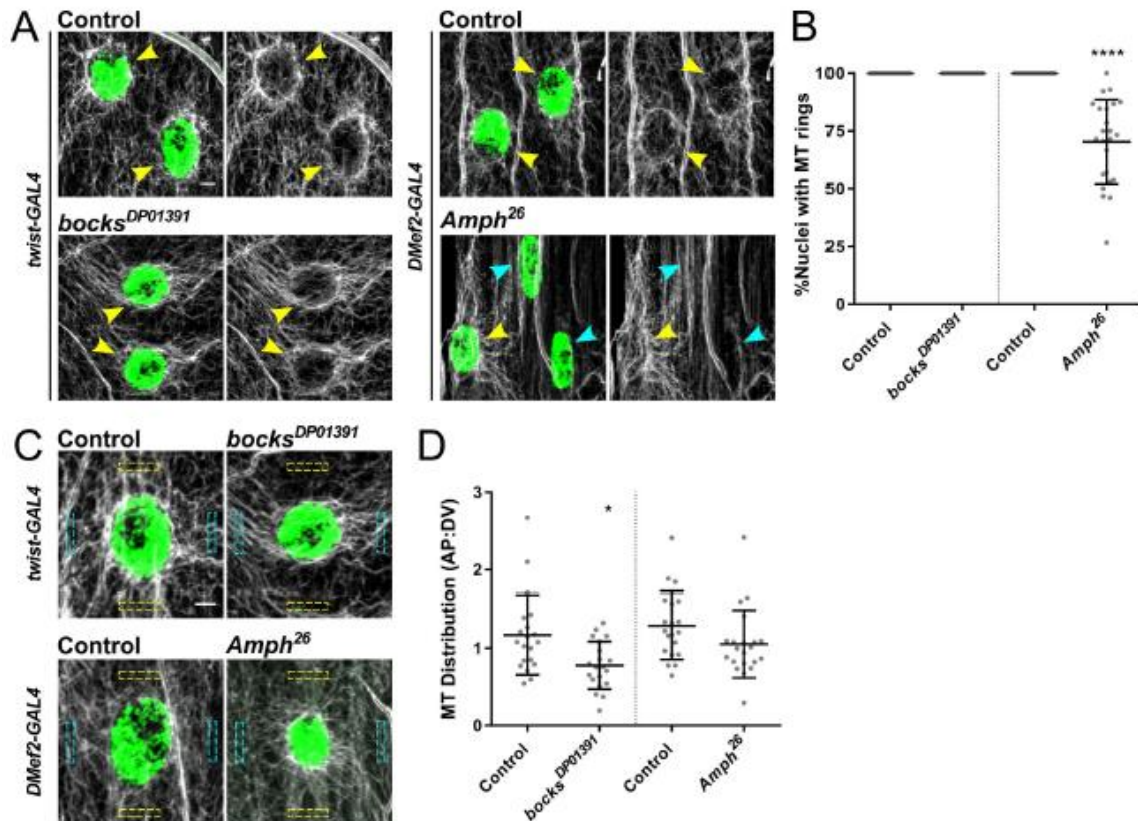


**Figure 2.7** Both Bocksbeutel and Amphiphysin are necessary for proper microtubule organization. (A) Immunofluorescence images of nuclei from VL3 muscles from stage L3 larvae. Microtubules were identified by immunostaining for  $\alpha$ -tubulin (gray) and the nuclei were stained with Hoechst (green). Yellow boxes indicate location of anterior and posterior measurements for microtubule intensity. Cyan boxes indicate location of dorsal and ventral measurements of microtubule intensity. Scale bar, 5 $\mu$ m. (B) The polarity of microtubules around the nucleus in larval muscles. Data points indicate the ratio of the average integrated density from the anterior and posterior positions to the average integrated density of microtubule staining from the dorsal and ventral positions of a single nucleus. (C) Immunofluorescence images of nuclei from VL3 muscles from stage L3 larvae. Microtubules were identified by immunostaining for  $\alpha$ -tubulin (gray) and the nuclei were stained with Hoechst (green). Yellow arrowheads indicate nuclei with associated microtubule rings. Cyan arrowheads indicate nuclei lacking associated microtubule rings. Scale bar, 5 $\mu$ m. (D) Counts of nuclei with associated microtubule rings. Data points indicate percent of nuclei within a single VL3 muscle of an L3 larva that have an associated microtubule ring. Student's t-test was used for comparison to controls. \* $P < 0.05$ , \*\*\*\* $P < 0.00005$ .

## 2.4 Discussion

We have used *Drosophila* musculature to investigate whether aberrant nuclear position that is related to EDMD and CNM results from a common mechanism. We find that disruption of EDMD- and CNM-linked genes in *Drosophila* recapitulate the phenotype

of mispositioned nuclei that are evident in the human diseases. Moreover, we find that the mechanism by which nuclear position is disrupted is muscle autonomous. However, these data also indicate that the specific phenotype is different dependent on whether EDMD- or CNM-linked genes are disrupted.

In interpreting these data it is important to note that each of the alleles used is a null. However, only the *emerin* mutation leading to EDMD is thought to be a complete loss of function. The *amph* mutations that have been linked to CNM and the *SYNE1* and *SYNE2* mutations that have been linked to EDMD are missense mutations. The impact of these specific mutations that cause disease is a critical next step. Nevertheless, that the functions of these genes with respect to nuclear position are disrupted by null mutations indicates that this is one function to explore in disease models.

The distinction in phenotype that is caused by disruptions in EDMD-linked genes versus disruptions in CNM-linked genes is apparent in the larval stage of *Drosophila* development. The inability to resolve the single chain of nuclei in the larvae with disrupted EDMD-linked genes suggests that EDMD-linked genes are necessary to resolve nucleus-nucleus interactions. Similarly, the few number of mispositioned nuclei in larvae with disrupted CNM-linked genes is consistent with nuclei being disengaged from other nuclei and therefore occupying a space too near another nucleus. Together these data suggest that the two sets of genes have opposing functions with respects to nucleus-nucleus interactions and nuclear movement. It is important to note that the interactions between nuclei are likely indirect. The proteins encoded for by *klarsicht* and *bocksbeutel* are nesprin proteins and emerin proteins respectively. Each of these proteins can localize to the outer nuclear envelope and regulate interactions between the nucleus and the cytoskeleton (Chang et al.,

2013; Salpingidou et al., 2007; Starr and Han, 2002). Additionally, in muscle, the nuclear envelope is crucial for the organization of the microtubule cytoskeleton (Espigat-Georger et al., 2016; Tassin et al., 1985). Therefore it is likely that nucleus-nucleus interactions are mediated by the cytoskeleton. Consistent with this, loss of either *bocks* or *amph* disrupts microtubule organization (Fig. 2.7). In *bocks*<sup>DP01391</sup> larvae, the distribution of microtubules around each nucleus was polarized along the dorsal/ventral axis of the muscle compared to control larvae in which the microtubules were evenly distributed around the each nucleus. In *amph*<sup>26</sup> larvae, when microtubules emanate from each nucleus, they are distributed evenly as in controls. However not all nuclei have associated microtubules. Together these data suggests a role for the microtubule cytoskeleton in mediating the balance between nucleus-nucleus interactions.

RNAi experiments were used to demonstrate that the effects of these genes on nuclear position in muscle were muscle autonomous and suggested that some functions are temporally restricted. With respect to each RNAi, continued depletion of the protein by expression of the RNAi under the control of the *DMef2-Gal4* driver did not exaggerate the general evenness of nuclear distribution compared to the more acute depletion driven by *twist-Gal4* (compare Fig 2.3 to Fig 2.4). In fact, with regards to one factor, *mtm*, the phenotype was less dramatic suggesting it primarily functions early in development. Furthermore, the position of nuclei relative to the edge of the muscle was significantly affected only when specific proteins were depleted throughout muscle development with the *DMef2-Gal4* driver. The importance of nuclear position relative to the muscle edge is not clear. However, these data suggest that each of these genes contributes to nuclear position by several mechanisms that may be separated by developmental time.

Despite the general disruption of nuclear positioning across all genotypes analyzed, there were some notable differences in the severity of phenotypes produced between proteins associated with EDMD. Although *bocks* and *Ote* are both considered *Drosophila* homologs of emerin, depletion of *bocksbeutel* more strongly disrupted nuclear positioning than depletion of *Otefin*. These differences may suggest that *bocksbeutel* and *Otefin* may have distinct functions and regulatory roles in the process of nuclear positioning. This would not be the first indication that *bocksbeutel* and *Otefin*, the two *Drosophila* homologs of emerin have distinct functions. With respect to fertility, *Drosophila* are more sensitive to the loss of *Otefin* than they are to the loss of *bocksbeutel* (Barton et al., 2014). Because we find the opposite effect with respect to nuclear position in muscle, these data together suggest that *bocksbeutel* and *Otefin* may have specific roles in different tissues.

Our conclusion that EDMD- and CNM-linked genes disrupt nuclear position by distinct mechanisms is supported by the differences in their genetic interactions. *bocks* genetically interacts with the microtubule motors dynein and kinesin while *amph* does not. These data suggest that *bocks* regulates nuclear movement via the described microtubule-dependent pathways (Folker et al., 2012; Folker et al., 2014; Metzger et al., 2012). The mechanism by which *amph* regulates nuclear movement and nucleus-nucleus interactions is not clear. Recent data from cell culture suggests that this may be an actin-dependent process (D'Alessandro et al., 2015; Falcone et al., 2014). However, we have shown that *amph* is necessary for proper microtubule organization at the nucleus, suggesting that nucleus-nucleus interactions may be microtubule-dependent.

In all, these data suggest that although mispositioned nuclei are a phenotype common to both CNM and EDMD, the underlying mechanism is different in each disease.

That genes linked to distinct muscle diseases impact nuclear position by different mechanisms is critical to understanding the impact of nuclear position on muscle health. These conclusions dictate that the mechanisms that underlie mispositioned nuclei in each muscle disease must be individually identified, and not considered collectively. However, these data also suggest that there may be a web of genetic pathways that have counteracting, and balancing effects. Thus, there may be viable methods to improve nuclear distribution either genetically or pharmacologically.

## 2.5 Materials and Methods

### 2.5.1 *Drosophila* genetics

All stocks were grown under standard conditions at 25°C. Stocks used were apRed (Richardson et al., 2007), *bocks*<sup>DP01391</sup> (Bloomington *Drosophila* Stock Center, 21846), *klar*<sup>l</sup> (Bloomington *Drosophila* Stock Center, 3256), *amph*<sup>26</sup> (Bloomington *Drosophila* Stock Center, 6498), UAS-*bocks* RNAi (Bloomington *Drosophila* Stock Center, 38349), UAS-*klar* RNAi (Bloomington *Drosophila* Stock Center, 36721), UAS-*koi* RNAi (Bloomington *Drosophila* Stock Center, 40924), UAS-*Ote* RNAi (Bloomington *Drosophila* Stock Center, 39009), UAS-*mtm* RNAi (Bloomington *Drosophila* Stock Center, 31552), and UAS-*amph* RNAi (Bloomington *Drosophila* Stock Center, 53971), *Dhc64C*<sup>4-19</sup> (Gepner et al., 1996), and *Khc*<sup>δ</sup> (Brendza et al., 1999). Mutants were balanced and identified using *CyO*, *DGY* and *TM6b*, *DGY*. UAS-RNAi constructs were driven specifically in the mesoderm using *twist-GAL4*, *apRed*, specifically in the muscle using *DMef2-GAL4*, *apRed*, or specifically in larval muscles using *MHC-GAL4*. Regarding apRed specifically, this fly expresses a nuclear localization signal (NLS) fused to the

fluorescent protein DsRed downstream of the *apterous* mesodermal enhancer. This results in the specific labeling of the nuclei within the lateral transverse muscles of the *Drosophila* embryo (Richardson et al., 2007). The *twist-GAL4*, *apRed*, *DMef2-GAL4*, *apRed* *Drosophila* lines were made by recombining the *apRed* promoter and the specific GAL4 driver. In the case of *twist-GAL4*, *apRed*, both elements are on the second chromosome. In the case of *DMef2-GAL4*, *apRed*, both elements are on the third chromosome. There are slight variations between the two genotypes so each has been used as a control in all experiments.

### **2.5.2 Larval Locomotion**

Larval speed was measured as previously described (Louis et al., 2008; Metzger et al., 2012) with minor modifications. Stage 16 and 17 embryos were selected for the presence or absence of fluorescent balancers and placed on yeast-coated molasses agar plates at 21°C overnight. L1 larvae were selected and placed into a vial containing standard fly food. After 4 days L3 larvae were picked from the vial and tracked on a 3% agarose gel as they crawled toward an odor source of ethyl butyrate (32.5%; Sigma, 15701) diluted in paraffin oil (Sigma, 18512). Larvae were tracked with an Iphone (Apple) using OSnap! Pro (Justin Cegnar) for 3 minutes with images taken every 5 seconds. Tracks were processed using the Manual Tracking plugin on ImageJ software (NIH). At least 20 larvae were tracked for each genotype.

### **2.5.3 Immunohistochemistry**

Larvae were dissected as previously described (Louis et al., 2008; Metzger et al., 2012) with minor modifications. Larvae were dissected in ice-cold PIPES dissection buffer containing 100 mM PIPES (Sigma-Aldrich, P6757), 115 mM D-Sucrose (Fisher Scientific, BP220-1), 5 mM Trehalose (Acros Organics, 182550250), 10 mM Sodium Bicarbonate (Fisher Scientific, BP328-500), 75 mM Potassium Chloride (Fisher Scientific, P333-500), 4 mM Magnesium Chloride (Sigma-Aldrich, M1028) and 1 mM EGTA (Fisher Scientific, 28-071-G), then fixed with 10% formalin (Sigma-Aldrich, HT501128).

Mouse anti- $\alpha$ Tubulin (1:200, Sigma-Aldrich T6199) was used in larvae. Conjugated fluorescent secondary antibodies used were Alexa Fluor 488 donkey-anti-mouse (1:200, Life Technologies), Acti-stain 555 phalloidin (1:400, Cytoskeleton PHDH1-A) and Hoechst 33342 (1  $\mu$ g/ml) were used in larvae. Larvae were mounted in ProLong Gold (Life Technologies, P36930) and imaged with an APOCHROMAT 40X, 1.4 NA objective with a 0.5-X optical zoom for nuclear positioning analysis and at a 2.0-X optical zoom for microtubule analysis.

### **2.5.4 Analysis of nuclear position in larvae**

We have developed a means to measure internuclear distance that takes into account nuclear count and muscle size in order to determine how evenly nuclei are positioned, as opposed to how close together nuclei are. This measurement represents how ideally nuclei are positioned. In this method, the actual internuclear distance is determined by measuring the distance from the center of each nucleus to the center of its nearest nuclear neighbor. The nearest nucleus could be in any direction relative to the nucleus in question.

Thus, sometimes the nearest nucleus was positioned adjacently on the long axis of the muscle whereas the nearest neighbor for another nucleus might be adjacent on the short axis of the muscle. Next, the area of the muscle is measured and the number of nuclei are counted. The maximal internuclear distance is determined by taking the square root of the muscle area divided by the nuclear count. This value represents the distance between nuclei, if internuclear distance was fully maximized. The ratio between the actual internuclear distance and the maximal internuclear distance ratio was then used to determine how even nuclei were distributed. This method allows as to essentially normalize the internuclear distance to both nuclear count and muscle area which leads to a more representative means of comparison between muscles, larvae and genotypes.

Additionally, the distance of each nucleus from the lengthwise edge of the muscle was determined by measuring the shortest distance from the center of the nucleus to the nearest long edge of the muscle. Similarly the distance between the parallel lines of nuclei in each muscle was measured. To be considered a line of nuclei, it was necessary for at least four nuclei that covered at least 25% of the muscle length to be included. Nuclei were considered to be in the same nuclear line if the nuclei were present in the same dorsal or ventral half of the muscle. The distance between nuclear lines was measured by using the segmented line tool on ImageJ software (NIH) to trace the nuclear lines then the average distance between each line was determined. When only 1 nuclear line was present the distance between nuclear lines was considered to be zero.

### 2.5.5 Analysis of microtubule organization in larvae

The number of nuclei within a muscle that had microtubules nucleating from them was counted in VL3 muscles from L3 larvae. Nuclei were counted as nucleating microtubules if a ring of microtubules around the nucleus was present. A nuclear ring was classified as an increase in  $\alpha$ -tubulin staining around the periphery of the nucleus and microtubules radiating from the nucleus. The percent of nuclei with nuclear rings relative to all nuclei within the muscle was recorded.

Microtubule distribution around the nucleus was measured from VL3 muscles from L3 larvae by measuring the integrated density of the  $\alpha$ -tubulin staining. The integrated density was measured from a 10  $\mu\text{m}$  by 2  $\mu\text{m}$  region positioned 15  $\mu\text{m}$  anteriorly and 15  $\mu\text{m}$  posteriorly from the center of the nucleus. Similarly, the integrated density was also measured from a 2  $\mu\text{m}$  by 10  $\mu\text{m}$  region positioned 15  $\mu\text{m}$  dorsally and 15  $\mu\text{m}$  ventrally from the center of the nucleus. Integrated densities from the anterior and posterior positions were averaged, as were the integrated densities from the dorsal and ventral positions. A ratio between the average anterior/posterior and dorsal/ventral integrated densities was used to determine the microtubule distribution ratio with a value of 1 correlating to an even distribution of microtubules around the nucleus, a value of  $>1$  correlating to more microtubules distributed in the anterior/posterior regions relative to the nucleus and a value of  $<1$  correlating to more microtubules distributed in the dorsal/ventral regions relative to the nucleus.

### 2.5.6 RNA isolation, construction of cDNA library, and RT-PCR

RNAi knockdown efficiency was measured in single embryos. Because muscle composes a small portion of the total mass of the embryo, RNAi was expressed ubiquitously to test efficiency using the *Tubulin-GAL4* driver. Embryos were washed in 50% bleach to remove the outer membrane and then washed with water. Single embryos of each genotype (*Tubulin-GAL4*, *UAS-ote* RNAi, *UAS-bocks* RNAi, *UAS-koi* RNAi, *UAS-klar* RNAi, *UAS-mtm* RNAi, *UAS-amph* RNAi) were selected at stage 17 of embryo development using the morphology of the gut and appearance of the trachea as previously described (Beckett and Baylies, 2007). To extract and isolate RNA, individual embryos were then crushed in an Eppendorf tube in 1 mL of TRIzol according to manufacturer's instructions (Invitrogen, 15596026). RNA integrity and concentration were determined using NanoDrop2000 system (Thermo Fisher Scientific Inc). The cDNA library was established by performing reverse transcription using the SuperScript VILO cDNA Synthesis Kit (Invitrogen, 11-754-050), according to manufacturer's protocol. Purified RNA was incubated with SuperScript III reverse transcriptase at 42° C for 2 h and then reactions were terminated at 85° C for 5 min. RT-PCR was set up after inactivation of reverse transcription using the GoTaq Flexi DNA Polymerase (Promega, M8291). Primers were designed to amplify a ~120–base pair sequence within each targeted mRNA and a 315–base pair sequence within *RP49* as a control. The denaturing temperature was 95° C, the annealing temperature was 49° C, and the extension temperature was 72° C, and 40 amplification cycles were run. The primers used were *RP49* forward 5'-TACAGGCCCAAGATCGTGAA-3', *RP49* reverse 5'-GACAATCTCCTTGCGCTTCT-3', *ote* forward 5'-AGCCCAAGGCTATGTGACTG-3', *ote* reverse 5'-

GATTCCTGGCAAATGTGCTT-3', *bocks* forward 5'-TTACACACGCGAAGTTGACC-3', *bocks* reverse 5'-GTGGCTCGTATGTGGGAAGT-3', *koi* forward 5'-CTCAGAAGTGTCCCCTCACC-3', *koi* reverse 5'-GTGGCTCGTATGTGGGAAGT-3', *klar* forward 5'-CCCTCCATATCAACCAGGAC-3', *klar* reverse 5'-GGCAAGACTTTCGTCGAACT-3', *mtm* forward 5'-CAAAGTGGCAGACGGCTATT-3', *mtm* reverse 5'-GAACTACGACGGAGGTGCTC-3', *amph* forward 5'-GGAAGGCAAAGTGCATCTC-3', and *amph* reverse 5'-GAACAGATTTGGCCAGCATT-3'. PCR products were run on a 2% agarose gel and visualized with ethidium bromide. Gels were imaged using Typhoon FLA 9500 (GE Healthcare Life Sciences). Band intensities were quantified using ImageQuant. Values were normalized to expression of RP49 and displayed with control expression normalized to 1.

## **Chapter 3:**

### ***Drosophila* emerins control LINC complex localization and transcription to regulate myonuclear position**

*The content in this chapter was adapted from:*

**Mandigo, T.R., Turcich, B.D., Anderson, A.J., Hussey, M.R., and Folker, E.S. (2019)**  
*Drosophila* emerins control LINC complex localization and transcription to regulate myonuclear position. *Journal of Cell Science*. **132**: jcs235580.

### **3.1 Abstract**

Mispositioned nuclei are a hallmark of skeletal muscle disease. Many of the genes that are linked to Emery-Dreifuss muscular dystrophy (EDMD) encode proteins that are critical for nuclear movement in various cells, suggesting that disruptions in nuclear movement and position may contribute to disease progression. Yet how these genes are coordinated to move nuclei is not known. Here we focused on two different emerin proteins, Bocksbeutel and Otefin and their effects on nuclear movement. Although nuclear position was dependent on both, elimination of either Bocksbeutel or Otefin produced distinct phenotypes that were based in differential effects on the KASH-domain protein Klarsicht. Specifically, loss of Bocksbeutel reduced Klarsicht localization to the nucleus and resulted in a disruption in nuclear separation. Loss of Otefin increased the transcription of Klarsicht and led to premature separation of nuclei and their positioning closer to the edge of the muscle. Consistent with opposing functions, nuclear position is normal in *otefin; bocksbeutel* double mutants. These data indicate emerin-dependent regulation of Klarsicht levels in the nuclear envelope are a critical determinant of nuclear position.

### **3.2 Introduction**

Skeletal muscle cells are characterized in part by the many nuclei that share a common cytoplasm. After the many nuclei are incorporated by iterative rounds of fusion, nuclei undergo a complex set of movements that leave them evenly spaced at the periphery of the cell. These movements are conserved throughout evolution (Folker and Baylies, 2013) and nuclei are mispositioned in the muscle cells of individuals with various muscle

disorders (Dubowitz et al., 2007b), suggesting that they are fundamental to muscle development.

One particular disease, Emery-Dreifuss muscular dystrophy (EDMD), is caused by mutations in a set of genes that encode proteins that mechanically link the nucleus to the cytoskeleton (Crisp et al., 2006; Folker and Baylies, 2013; Lombardi et al., 2011; Starr and Han, 2002). Many of the genes that are mutated in patients with EDMD encode for proteins that localize to the nucleus, including the inner nuclear membrane protein emerin, the structural nuclear protein lamin A/C, and the linker of nucleoskeleton and cytoskeleton complex (LINC complex). The LINC complex is composed of SUN-domain proteins and KASH-domain proteins. SUN-domain proteins span the inner nuclear membrane and interact with the nucleoskeleton within the nucleus and with KASH-domain proteins in the lumen of the nuclear envelope. KASH-domain proteins span the outer nuclear membrane and interact with the cytoskeleton in the cytoplasm. Functionally, these proteins are critical for nuclear positioning in muscle cells (Roman and Gomes, 2018). Additionally, each gene is critical for nuclear movement in non-muscle cell types (Gundersen and Worman, 2013) indicating that regulation of nuclear movement is a fundamental function of EDMD-linked genes. Yet, how these individual components are coordinated to move nuclei is not known.

Emerin, the first identified cause of EDMD, is a LEM domain containing protein that is primarily localized to the inner nuclear membrane (Bione et al., 1994; Manilal et al., 1996; Nagano et al., 1996). LEM domain proteins interact with lamin and barrier-to-autointegration factor, and through these interactions can localize chromosomes to the nuclear periphery (Cai et al., 2001; Laguri et al., 2001; Zheng et al., 2002). Emerin also interacts with SUN1 and SUN2 (Haque et al., 2010) as well as short isoforms of KASH-

domain proteins that localize to the inner nuclear envelope (Mislow et al., 2002; Wheeler et al., 2007). How each of these functions contributes to muscle development in general, or nuclear positioning during muscle development specifically, is not known. *Drosophila* provide an interesting system in which to study this mechanism as the *Drosophila* genome encodes only three LEM domain containing proteins, dMAN1, Bocksbeutel and Otefin (Ashery-Padan et al., 1997; Ashery-Padan et al., 2015; Pinto et al., 2008; Wagner et al., 2004; Wagner et al., 2006). dMAN1 is the homolog of LEM2 and MAN1 but both Bocksbeutel and Otefin are homologs of emerin (Wagner et al., 2006). Within the LEM domains Bocksbeutel and Otefin are 70% similar, however outside the LEM domain the similarity drops to 28% (Barton et al., 2014). Additionally, the expression patterns of these two emerin homologs differ, with uniform expression of Bocksbeutel throughout development, while Otefin is more highly expressed in embryos and 1<sup>st</sup> instar larvae compared to later developmental stages (Wagner et al., 2006). The existence of two emerin-like proteins makes it possible that emerin functions are distributed between two separate proteins in *Drosophila* and therefore might simplify the process of understanding how each emerin function is coordinated and the contribution of each to muscle development. Currently little is known about the functions of Bocksbeutel as no overt phenotypes have been identified, although investigations have been primarily focused on adult stages of development (Barton et al., 2014). However, some functions have been identified for Otefin. For example, Otefin has been shown to influence the cell cycle. As loss of Otefin leads to nuclear lamina dysfunction triggering disrupted maintenance of the cell cycle in germ stem cells (Barton et al., 2018). Additionally, Otefin has been demonstrated to interact with the SMAD complex to tether gene loci to the nuclear

periphery as a possible method of gene silencing (Jiang et al., 2008). Although some functions of Otefin have been uncovered, previous research investigating the origin of the tissue restricted affects caused by loss of specific LEM domain proteins suggest that LEM domain proteins may possess cell type specific functions that do not overlap with other LEM domain proteins (Barton et al., 2014).

We investigated the effects of emerin and other genes linked to EDMD during muscle development in *Drosophila* embryos and larvae (Collins et al., 2017). Consistent with previous reports, several EDMD-linked genes are critical for proper nuclear positioning (Collins et al., 2017; Elhanany-Tamir et al., 2012). Additionally, the *Drosophila emerin* homologs, *bocksbeutel* and *otefin*, both regulate nuclear position in embryonic and larval stages. However, the precise nuclear positioning phenotypes that arise upon disruption of these genes differ. These differences are based on their distinct effects on the nuclear localization of the *Drosophila* KASH-domain protein, Klarsicht. Thus, nuclear level of Klarsicht is a critical regulator of nuclear positioning, which is differentially regulated by *bocksbeutel* and *otefin*.

### **3.3 Results**

#### **3.3.1 Disruption of EDMD-linked genes impacts nuclear positioning in the *Drosophila* embryo**

Like mammalian skeletal muscles, *Drosophila* body wall muscles contain many nuclei that are precisely positioned to maximize the distance between nuclei. Two EDMD-linked genes, *bocksbeutel* (*bocks*, *Drosophila emerin*) and *klarsicht* (*klar*, *Drosophila* KASH-domain protein) (Table A1.1), are known regulators of nuclear positioning in both

embryonic and larval muscle (Collins et al., 2017; Elhanany-Tamir et al., 2012). Whether the effect on nuclear position in muscle is a conserved consequence of disrupting EDMD-linked genes or specific to those two genes is not clear. Furthermore, the genetic mechanism(s) by which these genes regulate nuclear position is not known. As a first step toward answering both questions, we measured nuclear position in animals with mutations, which had previously not been characterized, in *otefin* (*ote*, *Drosophila* emerin) and *klaroid* (*koi*, *Drosophila* SUN) (Table A1.1).

In stage 16 control embryos, nuclei were positioned in two equal-sized clusters with one near the dorsal end of the muscle and the other near the ventral end of the muscle (separated; equal distribution) (Fig 3.1A,B). In *bocks*<sup>DP01391</sup> homozygous mutants and *klar*<sup>l</sup> homozygous mutants, nuclei remained as a single cluster near the ventral end of the muscle (clustered phenotype), spread through the center of the muscle with no distinct dorsal or ventral cluster (spread phenotype), or separated into two clusters of unequal size (separated; unequal distribution) as previously described (Fig. 3.1A,B) (Collins et al., 2017). In animals with the *ote*<sup>DB</sup> mutation, an amorphic allele caused by a nonsense mutation (Barton et al., 2013) that had not previously been investigated with respect to nuclear positioning, nuclei separated into two clusters. However there was an increase in the frequency of nuclei found in the center of the muscle (central phenotype) (Fig 3.1A,B). In animals with the *koi*<sup>EY03560</sup> mutation, an allele with a p-element insertion in an early intron of *koi* (Technau and Roth, 2008) previously uninvestigated with respect to nuclear positioning, nuclei remained as a single cluster or separated into two clusters of unequal size as was seen in *bocks*<sup>DP01391</sup> and *klar*<sup>l</sup> mutants (Fig 3.1A,B).

We also measured the distance from the dorsal and ventral ends of muscles to the nearest nucleus. Compared to controls, nuclei were positioned 63%, 59% and 48% further from the dorsal muscle end in *bocks*<sup>DP01391</sup>, *klar*<sup>l</sup> and *koi*<sup>EY03560</sup> embryos respectively. Additionally, compared to controls, nuclei were positioned 11%, 12% and 15% closer to the ventral end of the muscle. Conversely, compared to controls, nuclei were positioned 11% closer to the dorsal muscle end in *ote*<sup>DB</sup> embryos (Fig 3.1C,D). Crossing each mutant allele to a deficiency replicated the nuclear positioning defects observed in homozygous mutants (Fig 3.2A-D), except for *bocks*<sup>DP01391/Df</sup>, which had a high frequency of fusion defects and missing muscles (Fig 3.2A). Due to the muscles defects in *bocks*<sup>DP01391/Df</sup> embryos, only embryos with properly formed muscles were analyzed for nuclear positioning, leading to a bias in analysis of healthier embryos. Together these data indicate that *bocksbeutel*, *klarsicht* and *klaroid* have a similar effect on nuclear positioning but that *otefin* has unique effects on nuclear position.

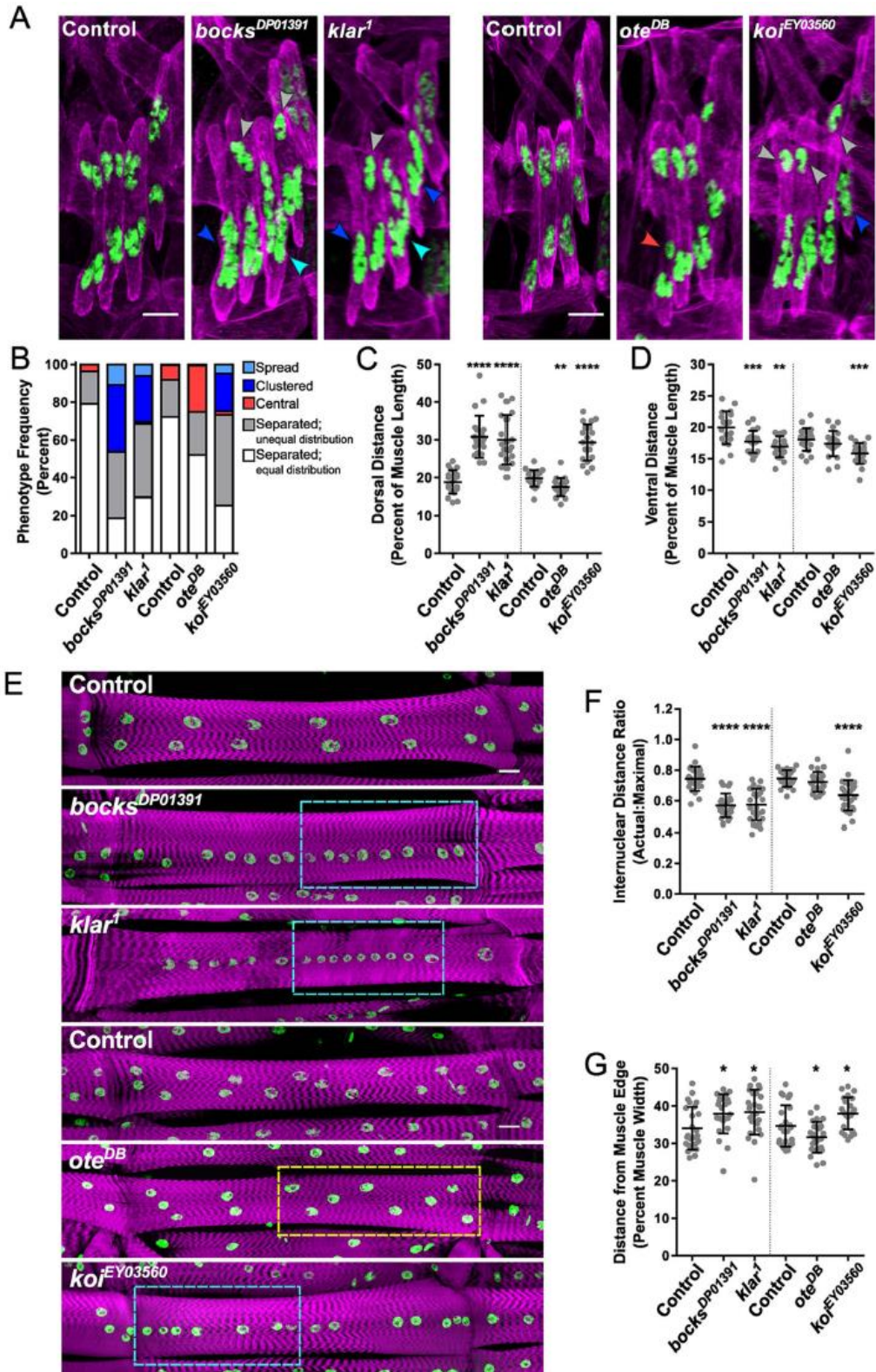


**Figure 3.1** The EDMD-linked genes *bocksbeutel*, *klarsicht*, *otefin* and *klaroid* are necessary for proper myonuclear positioning in *Drosophila* embryos and larvae. (A) Immunofluorescence projection images of lateral transverse (LT) muscles in one hemisegment from stage 16 (16h AEL) embryos of indicated genotypes. Magenta, Tropomyosin/muscles; green, dsRed/nuclei. Arrowheads indicate disrupted nuclear positioning phenotypes. Dark Blue, clustered nuclear positioning; Gray, unequal separation of nuclear clusters; Light Blue, spread nuclear positioning; Red, central nuclei. Scale bar, 10  $\mu$ m. Separate controls (*Twist-GAL4, apRed* (first control) and *DMef2-GAL4, apRed* (second control)) were used to control for variations caused by differences in genetic background. (B) Qualitative analysis of the frequency at which nuclear positioning phenotypes occur in the indicated genotypes. (C,D) Distance between the dorsal end of the muscle and the nearest nucleus (C) and between the ventral end of the muscle and the nearest nucleus (D) for the indicated genotypes normalized to muscle length. Each data point represents the average distances from all measured muscles within a single embryo. Error bars indicate the SD from 20 embryos. (E) Immunofluorescence projection images of Ventral Longitudinal 3 (VL3) muscles from dissected L3 larvae of the indicated genotype. Magenta, Phalloidin/muscles; green, Hoechst/nuclei. Dashed boxes indicate disrupted nuclear positioning phenotypes; Light Blue, single file nuclei; Yellow, three lines of offset nuclei with nuclei closer to the muscle edge. Scale bar, 25  $\mu$ m. Separate controls (*Twist-GAL4, apRed* (first control) and *DMef2-GAL4, apRed* (second control)) were used to control for variations caused by differences in genetic background. (F) The ratio of actual internuclear distance to maximal internuclear distance in larval muscles from the indicated genotypes. Data points indicate the average value for the internuclear distance ratio for all nuclei within a single VL3 muscle. Error bars indicate the SD from 24 VL3 muscles. (G) The distance between nuclei and the nearest muscle edge in larval muscles from the indicated genotypes. Data points indicate the average distance from the muscle edge for all nuclei within a single VL3 muscle. Error bars indicate the SD from 24 VL3 muscles. Student's *t-test* were used for comparison to controls. \* $p < 0.05$ , \*\* $p < 0.01$ , \*\*\* $p < 0.001$ , \*\*\*\* $p < 0.0001$ .

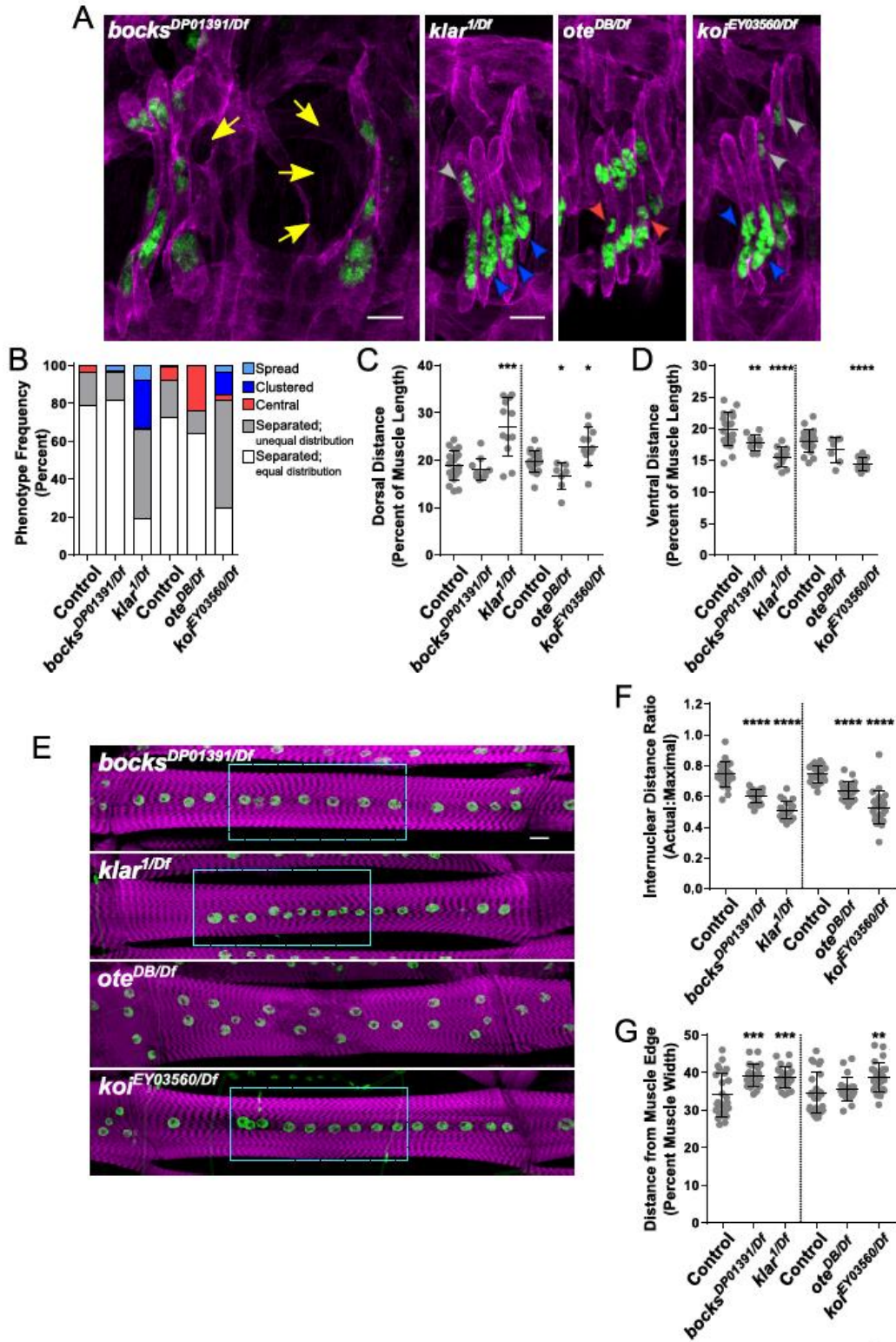


**Figure 3.2 Analysis of EDMD-linked gene alleles in combination with deficiencies are consistent with the alleles affecting muscle development.** (A) Immunofluorescence projection images of lateral transverse (LT) muscles in one hemisegment from stage 16 (16h AEL) embryos of indicated genotypes. Magenta, Tropomyosin/muscles; green, dsRed/nuclei. Yellow arrows indicate missing muscles. Arrowheads indicate disrupted nuclear positioning phenotypes. Dark Blue, clustered nuclear positioning; Gray, unequal separation of nuclear clusters; Red, central nuclei. Scale bar, 10  $\mu$ m. (B) Qualitative analysis of the frequency at which nuclear positioning phenotypes occur in the indicated genotypes. (C,D) Distance between the dorsal end of the muscle and the nearest nucleus (C) and between the ventral end of the muscle and the nearest nucleus (D) for the indicated genotypes normalized to muscle length. Each data point represents the average distances from all measured muscles within a single embryo. Error bars indicate the SD from at least 7 embryos. (E) Immunofluorescence projection images of Ventral Longitudinal 3 (VL3) muscles from dissected L3 larvae of the indicated genotype. Magenta, Phalloidon/muscles; green, Hoechst/nuclei. Dashed boxes indicate disrupted nuclear positioning phenotypes; Light Blue, single file nuclei. Scale bar, 25  $\mu$ m. (F) The ratio of actual internuclear distance to maximal internuclear distance in larval muscles from the indicated genotypes. Data points indicate the average value for the internuclear distance ratio for all nuclei within a single VL3 muscle. Error bars indicate the SD from 24 VL3 muscles. (G) The distance between nuclei and the nearest muscle edge in larval muscles from the indicated genotypes. Data points indicate the average distance from the muscle edge for all nuclei within a single VL3 muscle. Error bars indicate the SD from 24 VL3 muscles. Student's *t-test* were used for comparison to controls. \* $p < 0.05$ , \*\* $p < 0.01$ , \*\*\* $p < 0.001$ , \*\*\*\* $p < 0.0001$ .

### 3.3.2 Disruption of EDMD-linked genes impacts nuclear positioning in the *Drosophila* larvae

To test whether the disruptions in nuclear positioning persist through larval development, we measured nuclear distribution in *bocks*<sup>DP01391</sup>, *klar*<sup>l</sup>, *ote*<sup>DB</sup> and *koi*<sup>EY03560</sup> mutant L3 larvae as previously described (Collins et al., 2017). In controls, nuclei were typically positioned in two parallel lines on the long axis of the muscle (Fig 3.1E) with an internuclear distance ratio of 75% of maximal (Fig 3.1F). In *bocks*<sup>DP01391</sup> and *klar*<sup>l</sup> larvae, nuclei formed a single line in the center of the muscle as previously described (Fig 3.1E) (Collins et al., 2017), which phenocopied *klar* null larvae (Ding et al., 2017). The internuclear distance ratio was 57% and 58% of maximal for *bocks*<sup>DP01391</sup> and *klar*<sup>l</sup> larvae respectively (Fig 3.1F). Nuclear positioning in *koi*<sup>EY03560</sup> larvae phenocopied *bocks*<sup>DP01391</sup>

and *klar<sup>l</sup>* larvae with a single line of nuclei positioned in the center of the muscle (Fig 3.1E) with an internuclear distance ratio of 60% of maximal (Fig 3.1F). Additionally, nuclei in *bocks<sup>DP01391</sup>*, *klar<sup>l</sup>* and *koi<sup>EY03560</sup>* larvae were all positioned further from the muscle edge compared to controls (Fig 1G). It has been previously demonstrated that nuclear positioning relative to the muscle edge scales with cell width (Windner et al., 2019). Therefore we measured the average width of VL3 muscles and found that there was no significant difference between the average width of control, *bocks<sup>DP01391</sup>*, *klar<sup>l</sup>* and *koi<sup>EY03560</sup>* muscles (Fig 3.3A) suggesting that the observed nuclear positioning defects are not a consequence of thinner muscles and instead are bona fide disruptions in nuclear positioning.

To further investigate these nuclear positioning disruptions, we analyzed the relationship between the average distance of nuclei from the muscle edge as a function of muscle width. The slope of the line fit to the control data was nearly zero (Fig 3.3B,C,F) indicating that the nuclei maintain a relatively constant distance from the edge of the muscle independent of the muscle size. In *bocks<sup>DP01391</sup>*, *klar<sup>l</sup>* and *koi<sup>EY03560</sup>* animals, nuclei were positioned further from the muscle edge as the muscle widened indicating that nuclei had lost the ability to separate into two lines and maintain the proper distance from the muscle edge (Fig 3.3C,D,E,F,H). The similarities in all measurements of nuclear position between *bocksbeutel*, *klarsicht* and *klaroid* mutants suggest that these genes regulate nuclear positioning through a common mechanism.

In contrast, the spacing between nuclei in *ote<sup>DB</sup>* larvae was similar to controls. However, in some regions of the muscle there were three lines of offset nuclei (Fig 3.1E, yellow box). This resulted in disrupted nuclear positioning relative to the muscle edge (Fig

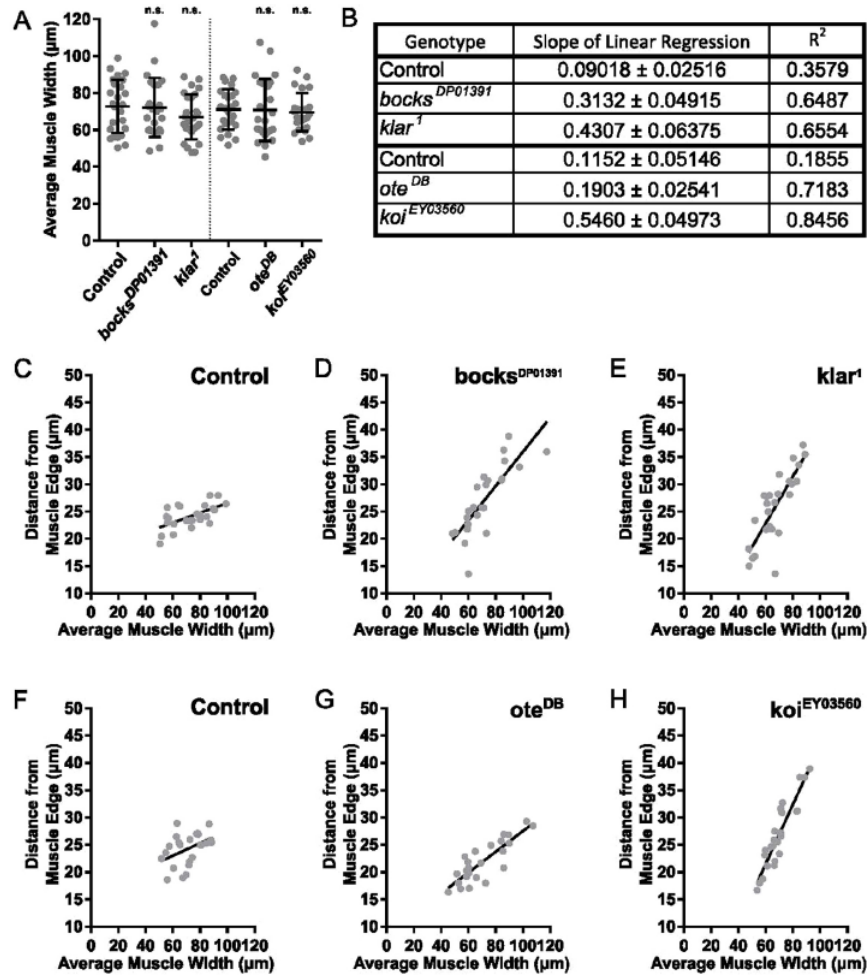


**Figure 3.3** The EDMD-linked genes *bocksbeutel*, *klarsicht*, *otefin* and *klaroid* affect the scaling of nuclear position relative to muscle edge. (A) Average muscle width of VL3 muscles from dissected L3 larvae in the indicated genotypes. n.s.  $p > 0.5$ . (B) Slope and R<sup>2</sup> values of the linear regressions for each dataset. (C-H) Distance from the muscle edge as a function of average muscle width of VL3 muscles from dissected L3 larvae in the indicated genotypes. Solid black line represents linear regression of the dataset. Separate controls (*Twist-GAL4*, *apRed* (C, *first control*) and *DMef2-GAL4*, *apRed* (F, *second control*)) were used to control for variations caused by differences in genetic background.

3.1G), but proper spacing of nuclei relative to other nuclei (Fig 3.1F). Additionally, as muscle width increased, the distance between the muscle edge and the nuclei scaled similarly to controls (Fig 2G). This indicated that although nuclei were closer to the muscle edge in *ote*<sup>DB</sup> mutants, the effect was not caused by a difference in muscle width.

Crossing each mutant allele to a deficiency replicated the nuclear positioning defects observed in homozygous mutants (Fig 3.2E-G), with the exception of *ote*<sup>DB/Df</sup>. *ote*<sup>DB/Df</sup> had more severe nuclear positioning defects compared to homozygous mutant

larvae, possibly due to the additional genes affected by the deficiency. Therefore, to confirm that the *ote* mutation caused the nuclear positioning defects, we examined trans-heterozygotes of two distinct *ote* alleles. Similar to *ote*<sup>DB</sup> homozygote larvae, the internuclear distance in *ote*<sup>DB/B279</sup> larvae was similar to controls, but nuclei were significantly closer to the edge of the muscle than in controls (Fig 3.4A-C). That the disruption of *otefin* expression caused a distinct phenotype in homozygous and trans-heterozygous mutants further indicated that *otefin* regulates nuclear positioning differently than *bocksbeutel*, *klarsicht* and *klaroid*.

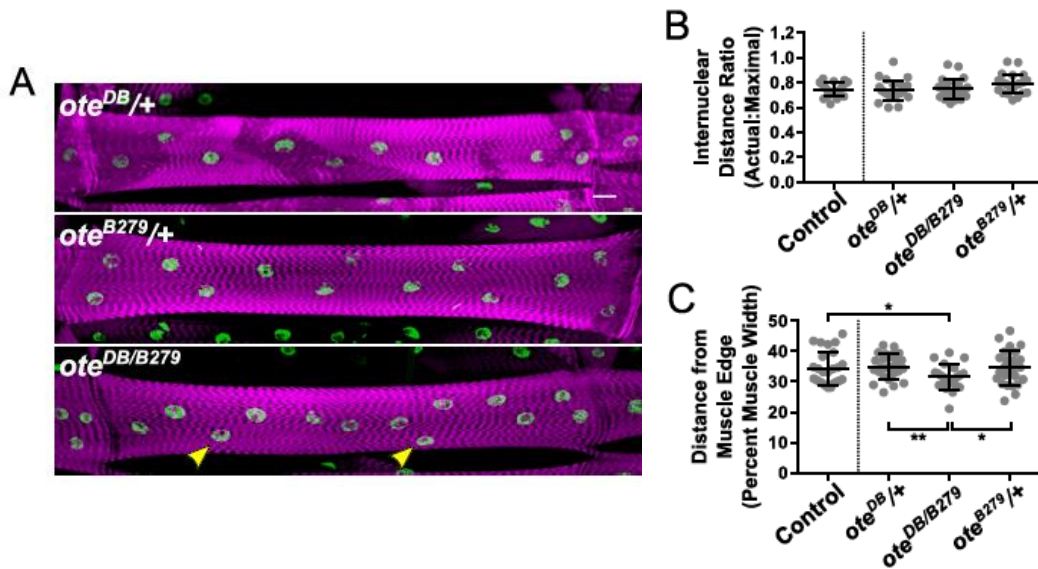


**Figure 3.4** *otefin* trans-heterozygote phenocopies the *ote*<sup>DB</sup> homozygote with respect to nuclear positioning relative to the muscle edge. (A) Immunofluorescence projection images of VL3 muscles from dissected L3 larvae of the indicated genotype. Magenta, Phalloidin/muscles; green, Hoechst/nuclei. Yellow arrowheads indicate nuclei that are closer to the muscle edge. Scale bar, 25  $\mu$ m. (B) The ratio of actual internuclear distance to maximal internuclear distance in larval muscles from the indicated genotypes. Data points indicate the average value for the internuclear distance ratio for all nuclei within a single VL3 muscle. Error bars indicate the SD from 24 VL3 muscles. (C) The distance between nuclei and the nearest muscle edge in larval muscles from the indicated genotypes. Data points indicate the average distance from the muscle edge for all nuclei within a single VL3 muscle. Error bars indicate SD from 24 VL3 muscles. \*p < 0.05, \*\*p < 0.01.

### 3.3.3 *Bocksbeutel* and *klarsicht* genetically interact to regulate nuclear positioning during muscle development

Since *bocks*<sup>DP01391</sup> mutants share nuclear positioning phenotypes with *klar*<sup>l</sup> and *koi*<sup>EY03560</sup> mutants, we investigated whether *bocksbeutel* and the other *Drosophila* emerlin homolog, *otefin*, genetically interact with other EDMD-linked genes to regulate nuclear positioning during embryonic and larval muscle development. In *bocks*<sup>DP01391/+</sup>, *klar*<sup>l/+</sup> doubly-heterozygous embryos, the frequencies of clustered nuclei, spread nuclei and two separate clusters of unequal size were increased compared to either individual heterozygote (Fig 3.5A,B). Additionally, the distance between the dorsal muscle end and the nearest nucleus was increased relative to each individual heterozygote (Fig 3.5C), and the distance between the ventral end of the muscle and the nearest nucleus was decreased compared to each individual heterozygote (Fig 3.5D). In *bocks*<sup>DP01391/+</sup>, *klar*<sup>l/+</sup> doubly-heterozygous larvae, nuclei formed a single line positioned in the center of the muscle, parallel to the long axis of the muscle. This phenotype was absent from each of the individual heterozygotes, although some regions of *bock*<sup>DP01391/+</sup> and *klar*<sup>l/+</sup> single heterozygote larval muscles contained single file nuclei (Fig 3.5E). Quantitatively the internuclear distance ratio was significantly reduced in *bocks*<sup>DP01391/+</sup>, *klar*<sup>l/+</sup> doubly-heterozygous larval muscles compared to either individual heterozygote (Fig 3.5F). Nuclei were also further from the muscle edge in *bocks*<sup>DP01391/+</sup>, *klar*<sup>l/+</sup> double heterozygotes compared to each individual heterozygote (Fig 3.5G). No genetic interactions were found between *bocks*<sup>DP01391</sup> and either *ote*<sup>DB</sup> or *koi*<sup>EY03560</sup> in embryonic (Fig 3.6A-F) or larval (Fig 3.7A-E) muscles. Additionally, no genetic interactions were found between *ote*<sup>DB</sup> and *klar*<sup>l</sup> and

*kol<sup>EY03560</sup>* in embryonic (Fig 3.6G-L) or larval (Fig 3.7F-J) muscles. The genetic interaction between *bocksbeutel* and *klarsicht* suggest that Klarsicht may be a differentiating factor between the distinct mechanisms used to regulate nuclear positioning by Bocksbeutel and Otefin.

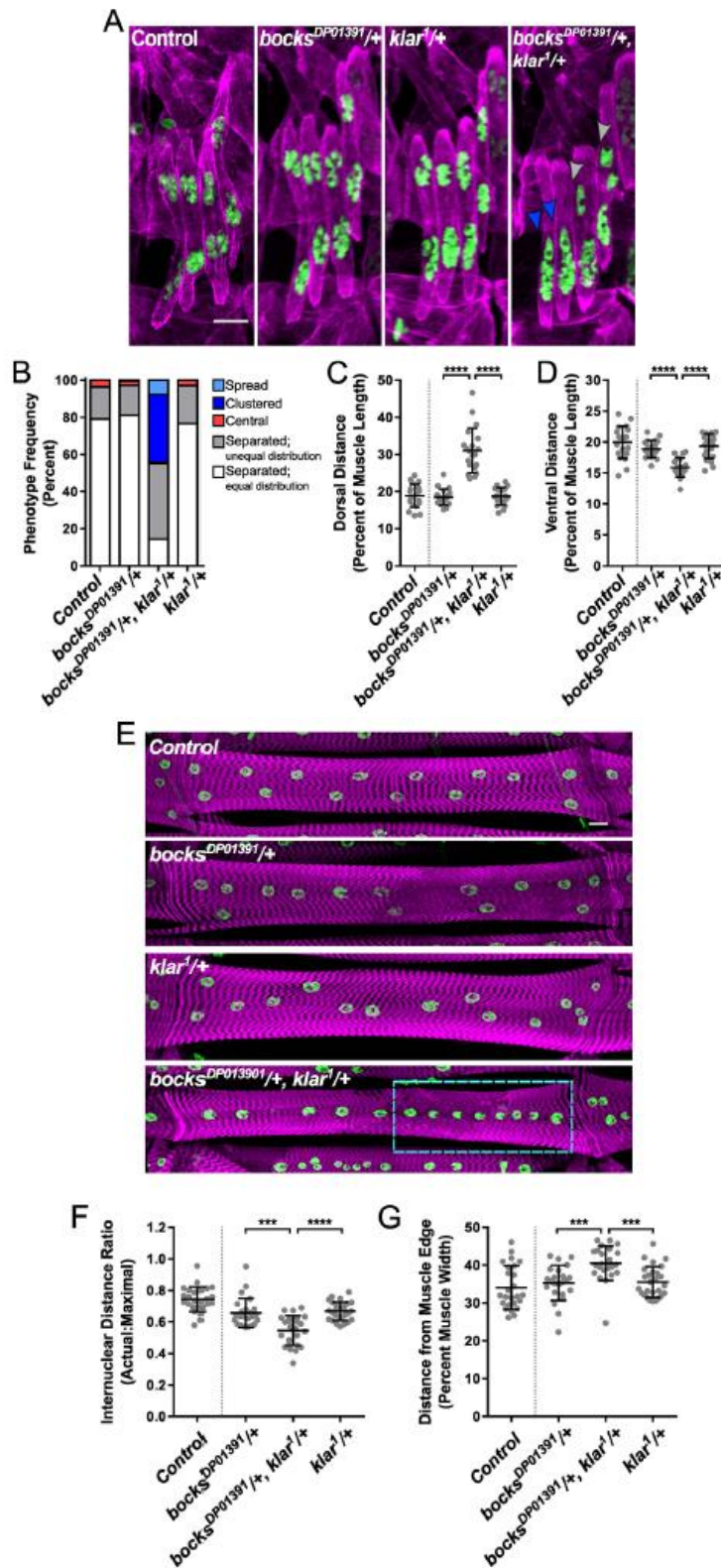


**Figure 3.5 *bocksbeutel* genetically interacts with *klarsicht* to regulate nuclear positioning in embryonic and larval muscles.** (A) Immunofluorescence projection images of LT muscles in one hemisegment from stage 16 (16h AEL) embryos with the indicated genotypes. Magenta, Tropomyosin/muscles; green, dsRed/nuclei. Arrowheads indicate disrupted nuclear positioning phenotypes. Dark Blue, clustered nuclear positioning; Gray, unequal separation of nuclear clusters. Scale bar, 10  $\mu$ m. Twist-GAL4, apRed was used as a control. (B) Qualitative analysis of the frequency at which nuclear positioning phenotypes occur in the indicated genotypes. (C,D) Distance between the dorsal end of the muscle and the nearest nucleus (C) and between the ventral end of the muscle and the nearest nucleus (D) for the indicated genotypes normalized to muscle length. Each data point represents the average distance for all muscles measured within a single embryo. Error bars indicate the SD from 20 embryos. (E) Immunofluorescence projection images of VL3 muscles from dissected L3 larvae of the indicated genotype. Magenta, Phalloidon/muscles; green, Hoechst/nuclei. Dashed boxes indicate disrupted nuclear positioning phenotypes; Light Blue, single file nuclei. Scale bar, 25  $\mu$ m. Twist-GAL4, apRed was used as a control. (F) The ratio of actual internuclear distance to maximal internuclear distance in larval muscles from the indicated genotypes. Data points indicate the average value for the internuclear distance ratio for all nuclei within a single VL3 muscle. Error bars indicate the SD from 24 VL3 muscles. (G) The distance between nuclei and the nearest muscle edge in larval muscles from the indicated genotypes. Data points indicate the average distance from the muscle edge for all nuclei within a single VL3 muscle. Error bars indicate SD from 24 VL3 muscles. Student's t-test were used for comparison to controls. \*\*\*p < 0.001, \*\*\*\*p < 0.0001.

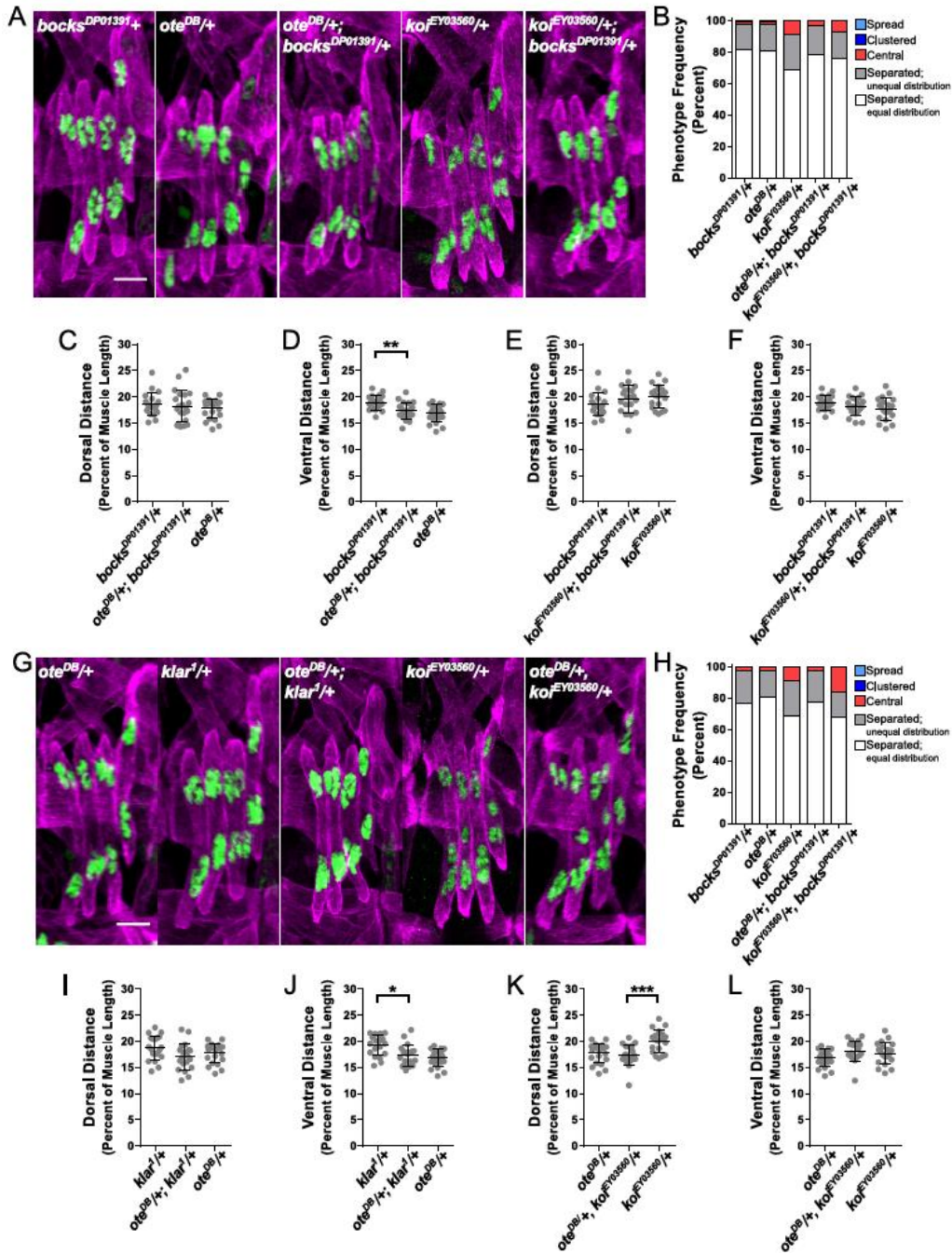


**Figure 3.6** *bocksbeutel* does not genetically interact with *otefin* or *klaroid* and *otefin* does not genetically interact with *klarsicht* or *klaroid*, to regulate nuclear positioning in embryonic muscles. (A,G) Immunofluorescence projection images of LT muscles in one hemisegment from stage 16 (16h AEL) embryos with the indicated genotypes. Magenta, Tropomyosin/muscles; green, dsRed/nuclei. Scale bar, 10  $\mu$ m. (B,H) Qualitative analysis of the frequency at which nuclear positioning phenotypes occur in the indicated genotypes. (C-F, I-L) Distance between the dorsal end of the muscle and the nearest nucleus (C,E,I,K) and between the ventral end of the muscle and the nearest nucleus (D,F,J,L) for the indicated genotypes normalized to muscle length. Each data point represents the average distance for all muscles measured within a single embryo. Error bars indicate the SD from 20 embryos. Student's t-test were used for comparison to controls. \*p < 0.05, \*\*p < 0.01, \*\*\*p < 0.001.

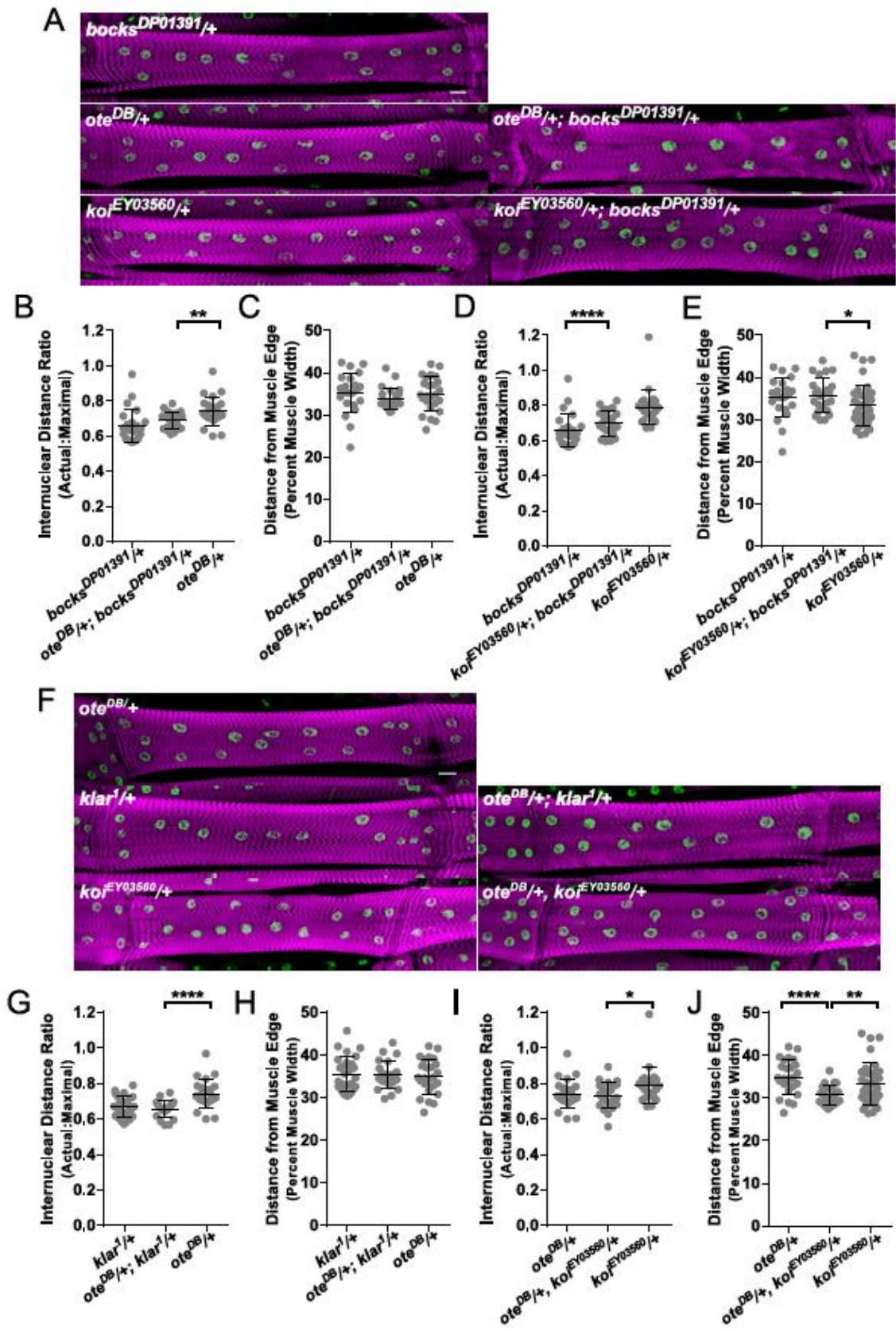


**Figure 3.7** *bocksbeutel* does not genetically interact with *otefin* or *klaroid* and *otefin* does not genetically interact with *klarsicht* or *klaroid* to regulate nuclear positioning in larval muscles. (A,F) Immunofluorescence projection images of VL3 muscles from dissected L3 larvae of the indicated genotype. Magenta, Phalloidon/muscles; green, Hoechst/nuclei. Scale bar, 25  $\mu$ m. (B,D,G,I) The ratio of actual internuclear distance to maximal internuclear distance in larval muscles from the indicated genotypes. Data points indicate the average value for the internuclear distance ratio for all nuclei within a single VL3 muscle. Error bars indicate the SD from 24 VL3 muscles. (C,E,H,J) The distance between nuclei and the nearest muscle edge in larval muscles from the indicated genotypes. Data points indicate the average distance from the muscle edge for all nuclei within a single VL3 muscle. Error bars indicate SD from 24 VL3 muscles. Student's t-test were used for comparison to controls. \*p < 0.05, \*\*p < 0.01, \*\*\*\*p < 0.0001.

### 3.3.4 Disruption of EDMD-linked genes affect levels of nuclear localized klarsicht

In order to better understand the genetic interaction between *bocksbeutel* and *klarsicht*, we examined Klarsicht localization in *bocks*<sup>DP01391</sup> and *klar*<sup>l</sup> mutants. In both *bocks*<sup>DP01391</sup> and *klar*<sup>l</sup> mutants, nuclear Klarsicht levels were reduced compared to controls (Fig 3.8A,B). Combined with the similar nuclear positioning phenotype in both *bocksbeutel* and *klarsicht* mutants, these data suggest that Bocksbeutel contributes to nuclear position by regulating the levels of Klarsicht in the nuclear envelope. Similarly, in *koi*<sup>EY03560</sup> mutants, which exhibit nuclear positioning defects similar to *bocks*<sup>DP01391</sup> and *klar*<sup>l</sup> (Fig 3.1A-G), nuclear Klarsicht levels were also reduced compared to controls (Fig 3.8A,B). Conversely, in *ote*<sup>DB</sup> mutants, which are phenotypically distinct from *bocks*<sup>DP01391</sup>, *klar*<sup>l</sup> and *koi*<sup>EY03560</sup> (Fig 3.1A-G), nuclear Klarsicht levels were increased compared to controls (Fig 3.8A,B). These data combined with the clustering phenotype in embryonic muscles and the single file nuclear positioning phenotype in larval muscles being phenocopied by our *klar*<sup>l/Df</sup> mutant (Fig 3.2E-G) and muscle specific knockdown of *klar* by RNAi (Collins et al., 2017) suggest that these nuclear positioning phenotypes result from a reduction in Klarsicht in the nuclear envelope, while the central nucleus phenotype in embryonic muscles and nuclei positioning closer to the edge in larval muscles results from an increase in Klarsicht in the nuclear envelope. To test the latter hypothesis, we

overexpressed Klarsicht. Overexpressed Myc-tagged Klarsicht localized to the nuclear envelope and, similar to *ote*<sup>DB</sup> mutation, caused nuclei to be positioned closer to the edge of the muscle compared to controls (Fig 3.9A-D). These data further suggest that reduced Otefin levels disrupt nuclear position by an increase in Klarsicht in the nuclear envelope.

Because the LINC complex and emerin can either directly or indirectly regulate transcriptional activity (Holaska and Wilson, 2007; Lee et al., 2001; Navarro et al., 2016; Wilkinson et al., 2003), we investigated the transcript levels of EDMD-linked genes in each mutant to determine whether nuclear Klarsicht levels changed due to altered transcription or altered protein localization. All transcript levels were the same in *bocks*<sup>DP01391</sup> mutants and controls. In particular, there was no change in *klar* transcript levels (Fig 3.8C), suggesting that the decreased Klarsicht immunofluorescence represented a change in its localization. Additionally, no changes in EDMD-linked genes were observed at the transcript level in *klar*<sup>l</sup> mutants compared to controls (Fig 3.8D). However, in *ote*<sup>DB</sup> mutants there was an increase in *klar* transcript levels compared to controls (Fig 3.8E) suggesting that the increase in nuclear Klarsicht levels is caused by an increase in transcription of the *klar* gene. Additionally, in *koi*<sup>EY03560</sup> mutants, there was a significant increase in *bocks* transcript levels compared to controls (Fig 3.8F) suggesting that SUN protein levels contribute to the regulation of emerin gene transcription.

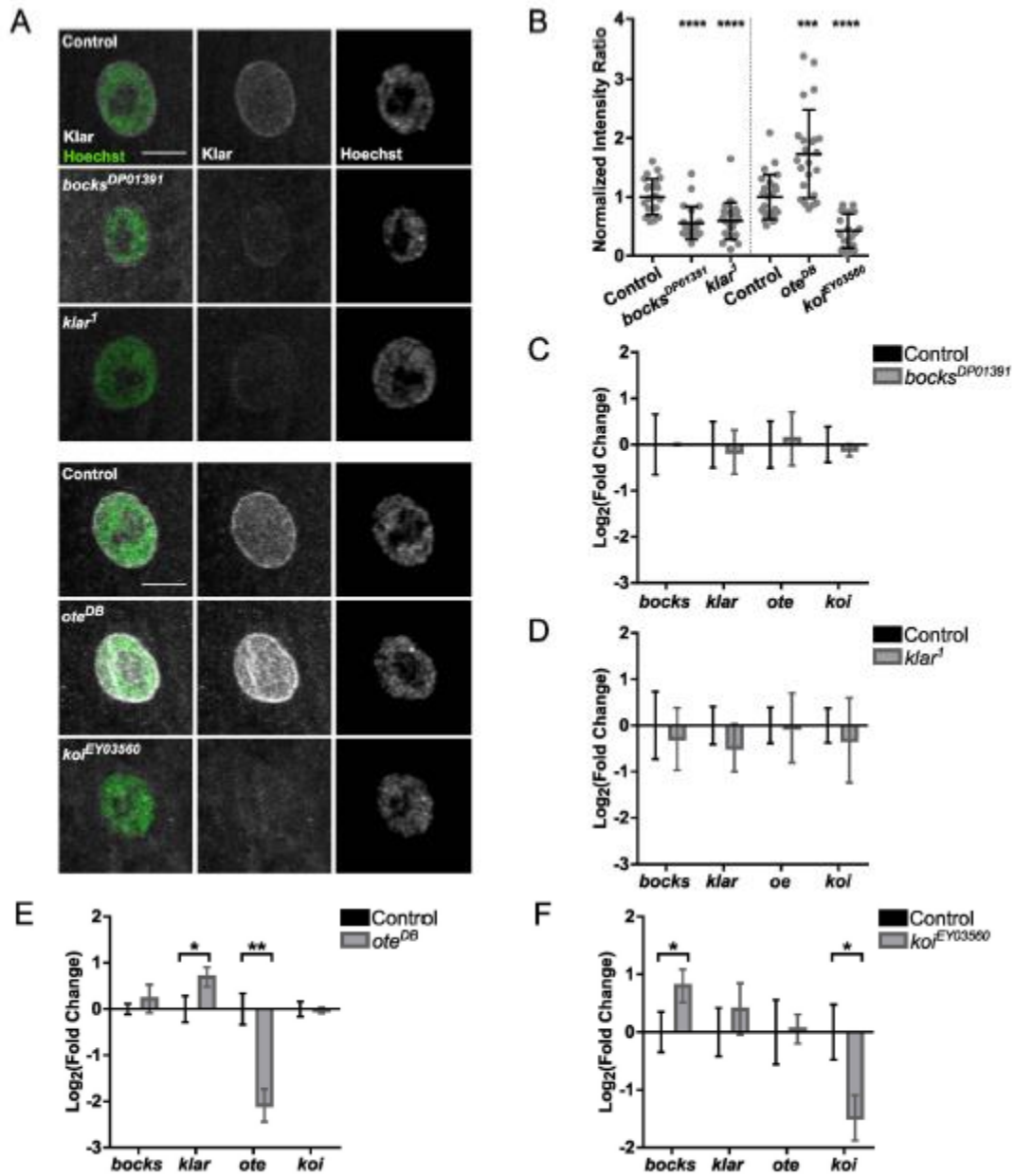


**Figure 3.8** The EDMD-linked genes *bocksbeutel*, *otefin* and *klaroid* affect levels of nuclear localized Klarsicht. (A) (Left) Overlaid immunofluorescence images of nuclei in VL3 muscles from dissected L3 larvae of the indicated genotype. Gray, Klarsicht; Green, Hoechst/nuclei. Scale bar, 10  $\mu$ m. (Middle, Right) Grayscale, Klarsicht (middle); Grayscale, Hoechst/nuclei (right). Separate controls (Twist-GAL4, apRed (first control) and DMef2-GAL4, apRed (second control)) were used to control for variations caused by differences in genetic background. (B) Intensity ratio for average Klarsicht immunofluorescence, with background fluorescence subtracted, normalized to the maximum Hoechst immunofluorescence and nuclear size. Error bars indicate SD from at least 20 nuclei. (C,D,E,F) Gene expression by qRT-PCR of EDMD-linked genes in *bocks*<sup>DP01391</sup> (C), *klar*<sup>1</sup> (D), *ote*<sup>DB</sup> (E) and *koi*<sup>EY03560</sup> (F) normalized to levels of RP49, GAPDH and  $\alpha$ Tub84b. Gene expression is represented as fold change relative to twist-GAL4, apRed (C,D) or DMef2-GAL4, apRed (E,F) controls. Error bars indicate SD from three biological replicates. Student's t-test of  $\Delta$ Ct values were used for comparison to controls. \* $p < 0.05$ , \*\* $p < 0.01$ , \*\*\* $p < 0.001$ , \*\*\*\* $p < 0.0001$ .

### 3.3.5 Loss of *Otefin* rescues nuclear positioning defects caused by disruption of *bocksbeutel*

Since *bocks*<sup>DP01391</sup> homozygous mutants and *ote*<sup>DB</sup> homozygous mutants have different effects on nuclear Klarsicht levels, we investigated whether the functions of Bocksbeutel and Otefin counterbalance each other to regulate nuclear positioning. In *bocks*<sup>DP01391</sup> larvae (Fig 3.1E, 3.9E), nuclei formed a single line positioned in the center of the muscle, parallel to the long axis of the muscle. When a single copy of the *ote*<sup>DB</sup> mutant allele was placed in a *bocks*<sup>DP01391</sup> homozygous mutant, there was a partial rescue of nuclear positioning with the internuclear distance ratio being 71% of maximal compared to 56% in the *bocks*<sup>DP01391</sup> homozygous mutant rescue controls (Fig 3.9E,F). Nuclear positioning was completely rescued in *ote*<sup>DB</sup>; *bocks*<sup>DP01391</sup> larvae as nuclei formed two parallel lines along the long axis of the muscle (Fig 3.9E) with an internuclear distance ratio of 78% of maximal (Fig 3.9F). Additionally, the positioning relative to the muscle edge was rescued in *ote*<sup>DB/+</sup>; *bocks*<sup>DP01391</sup> and *ote*<sup>DB</sup>; *bocks*<sup>DP01391</sup> (Fig 3.9G). Furthermore, the levels of nuclear localized Klarsicht were rescued to control levels in *ote*<sup>DB</sup>; *bocks*<sup>DP01391</sup> double mutants (Fig 3.9H,I). These data suggest that Bocksbeutel and Otefin have opposing functions in regulating nuclear positioning and balancing these functions is necessary to properly position myonuclei and regulate nuclear Klarsicht levels.

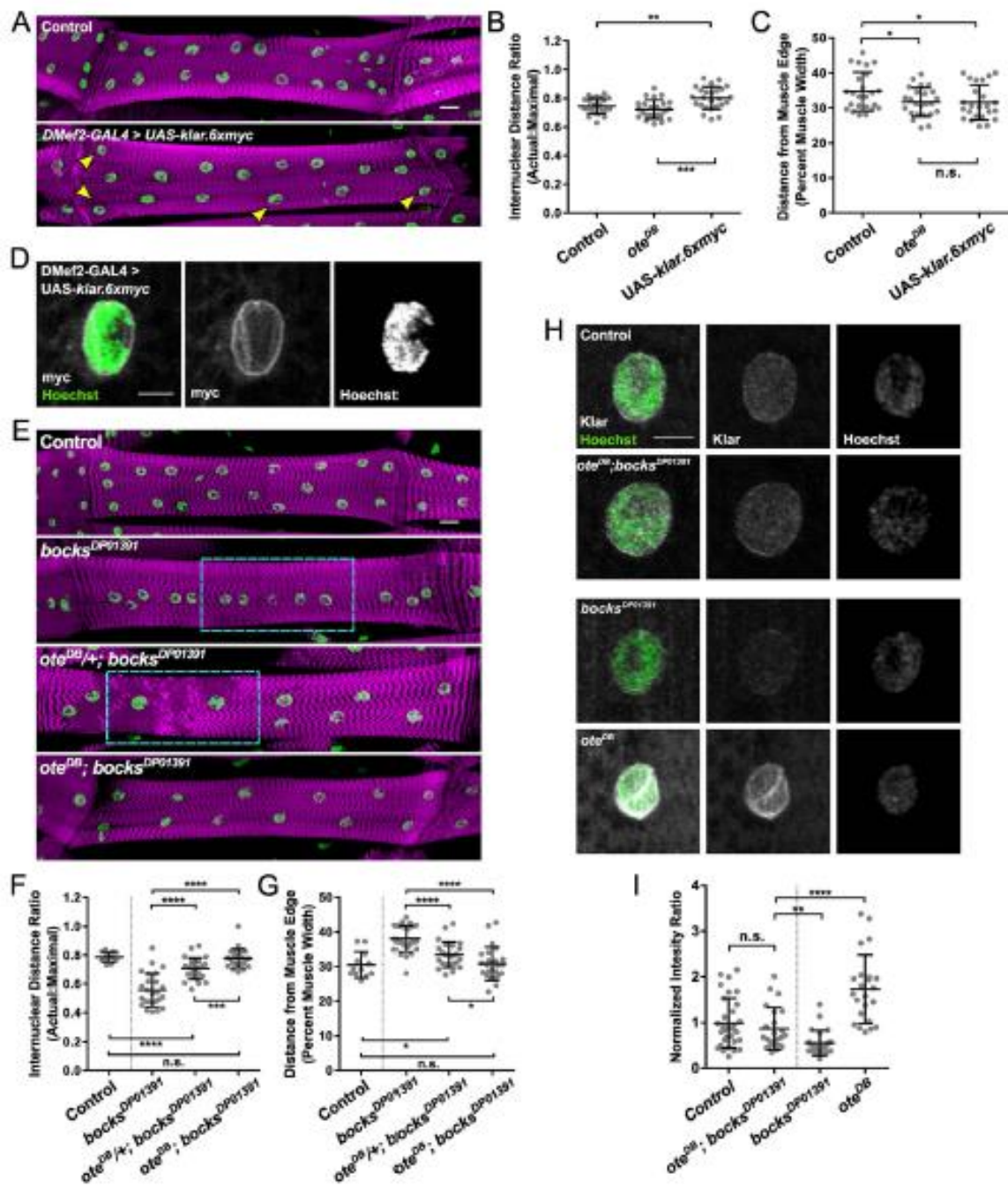


**Figure 3.9** Loss of the *otefin* rescues the nuclear positioning phenotype caused by disruption of *bocksbeutel* and restores nuclear localized Klarsicht to control levels. (A) Immunofluorescence projection images of VL3 muscles from dissected L3 larvae of the indicated genotype. Magenta, Phalloidon/muscles; green, Hoechst/nuclei. Yellow arrowheads indicate nuclei that are closer to the muscle edge. Scale bar, 25  $\mu\text{m}$ . *DMef2-GAL4, apRed* was used as a control. (B) The ratio of actual internuclear distance to maximal internuclear distance in larval muscles from the indicated genotypes. Data points indicate the average value for the internuclear distance ratio for all nuclei within a single VL3 muscle. Error bars indicate the SD from 24 VL3 muscles. (C) The distance between nuclei and the nearest muscle edge in larval muscles from the indicated genotypes. Data points indicate the average distance from the muscle edge for all nuclei within a single VL3 muscle. Error bars indicate the SD from 24 VL3 muscles. (D) (Left) Overlaid immunofluorescence images of nuclei in VL3 muscles from dissected L3 larvae of the indicated genotype. Gray, Myc; Green, Hoechst/nuclei. Scale bar, 10  $\mu\text{m}$ . (Middle, Right) Grayscale, Myc (middle); Grayscale, Hoechst/nuclei (right). (E) Immunofluorescence projection images of VL3 muscles from dissected L3 larvae of the indicated genotype. Magenta, Phalloidon/muscles; green, Hoechst/nuclei. Dashed boxes indicate disrupted nuclear positioning phenotypes; Light Blue, single file nuclei. Scale bar, 25  $\mu\text{m}$ . *Twist-GAL4/apRed; DMef2-GAL4/apRed* was used as a control. (F) The ratio of actual internuclear distance to maximal internuclear distance in larval muscles from the indicated genotypes. Data points indicate the average value for the internuclear distance ratio for all nuclei within a single VL3 muscle. Error bars indicate the SD from 24 VL3 muscles. (G) The distance between nuclei and the nearest muscle edge in larval muscles from the indicated genotypes. Data points indicate the average distance from the muscle edge for all nuclei within a single VL3 muscle. Error bars indicate SD from 24 VL3 muscles. (H) (Left) Overlaid immunofluorescence images of nuclei in VL3 muscles from dissected L3 larvae of the indicated genotype. Gray, Klarsicht; Green, Hoechst/nuclei. Scale bar, 10  $\mu\text{m}$ . (Middle, Right) Grayscale, Klarsicht (middle); Grayscale, Hoechst/nuclei (right). (I) Intensity ratio for average Klarsicht immunofluorescence, with background fluorescence subtracted, normalized to the maximum Hoechst immunofluorescence and nuclear size. Error bars indicate SD from 20 nuclei. Student's *t-test* were used for comparison to controls. n.s.  $p > 0.5$ , \* $p < 0.05$ , \*\* $p < 0.01$ , \*\*\* $p < 0.001$ , \*\*\*\* $p < 0.0001$ .

### 3.4 Discussion

We have used *Drosophila* musculature to elucidate the genetic network and cellular mechanisms that regulate myonuclear position *in vivo*. Consistent with previous work, disruption of EDMD-linked genes caused mispositioned nuclei. Deeper characterization revealed that disruption of *bocksbeutel* (*Drosophila emerlin*), *klarsicht* (*Drosophila KASH-domain protein*), and *klaroid* (*Drosophila SUN*) caused a similar phenotype. However, disruption of *otefin*, the other *Drosophila emerlin* homolog caused a different nuclear positioning phenotype. Furthermore, *bocks*, but not *ote*, genetically interacted with *klar* to

regulate nuclear positioning. The distinct phenotypes and genetic interactions of *bocks* and *ote* suggest a division of emerin functions between the two *Drosophila emerin* homologs.

Mechanistically, the phenotypic differences between *bocks* and *ote* mutants correlate with distinct changes in nuclear localized Klarsicht. Disruption in *bock* leads to a decrease in nuclear localized Klarsicht while disruption in *ote* leads to an increase in nuclear localized Klarsicht. Disruption of *bocks* caused no effect on transcript levels of *klar* suggesting the decrease in nuclear Klarsicht is due to mislocalization of Klarsicht. Conversely, disruption in *ote* caused an increase in transcript levels of *klar* suggesting the increase in nuclear localized Klarsicht is due to an increase in transcription. Although the increase in transcript levels is modest, it is important to note that qPCR was conducted on whole larval lysates. Therefore, if the phenotype is specific to a subset of tissues, or perhaps muscle specific, this would explain the modest change in transcript levels we observe. Together these data suggest that *bocks* and *ote* serve unique functions in *Drosophila* abdominal muscles, but that both functions are critical to the regulation of nuclear positioning.

Nesprins and emerin have previously been shown to interact physically. However, these interactions were demonstrated between shorter nesprin isoforms that localize to the inner nuclear membrane and function independently of the LINC complex (Mislow et al., 2002; Wheeler et al., 2007). In cell culture, emerin interacts with SUN proteins (Haque et al., 2010), but they do not rely on each other for nuclear envelope localization. If Bocksbeutel is not necessary for Klaroid localization, the decrease in nuclear localized Klarsicht may be caused by LINC complex instability, possibly through Lamins, which have been shown to be disrupted in large polytene nuclei that lack Bocksbeutel (Barton et

al., 2014). In support of this, *bocksbeutel* expression was increased in *koi* mutants, perhaps to compensate for the loss of *koi*. Nevertheless, these data suggest that a loss of Klarsicht from the nuclear envelope is a driving factor of mispositioned myonuclei in *bocks*, *klar* and *koi* mutants. In support of this, *klar<sup>l/Df</sup>* mutant (Fig 3.2A-G) and muscle specific knockdown of *klar* by RNAi (Collins et al., 2017) phenocopy *bocks<sup>DP01391</sup>* mutants, *klar<sup>l</sup>* mutants, and *koi<sup>EY03560</sup>* mutants with the clustering phenotype in embryonic muscles and the single file nuclear positioning phenotype in larval muscles. Furthermore, KASH-domain protein levels, such as Klarsicht, at the nucleus being a driving factor of mispositioned nuclei may not be unique to EDMD as Nesprin-1 levels at the nucleus have also been found to be reduced in the MDX mouse model for Duchenne muscular dystrophy (Iyer et al., 2016).

The increased amount of Klar at the nuclear envelope in *ote* mutants, and the associated nuclear positioning phenotype, suggest that any variations in Klarsicht abundance at the nuclear envelope will impact nuclear position in muscle. Consistent with this, overexpression of Klarsicht in a muscle specific manner phenocopied larval nuclear positioning relative to the muscle edge (Fig 3.9A-C). Additionally, as an increase in Klarsicht leads to mispositioned nuclei, an increase in Klaroid has also been demonstrated to disrupt nuclear positioning (Tan et al., 2018). These data suggest that misregulation of LINC-complex components that lead to a change in protein levels at the nucleus may be a common mechanism through which nuclear position is disrupted.

Remarkably, we found that loss of Otefin was sufficient to rescue the nuclear positioning phenotypes present in *bocks<sup>DP01391</sup>* homozygous mutants including both nuclear localized Klarsicht levels and nuclear positioning. Furthermore, even the

introduction of a single *ote*<sup>DB</sup> mutant allele was able to partially rescue nuclear positioning in *bocks*<sup>DP01391</sup> homozygous mutants indicating the distinct emerlin functions divided between the two *Drosophila emerlin* homologs, *bocksbeutel* and *otefin*, must be balanced for proper nuclear positioning.

In all, these data suggest that nuclear positioning can be disrupted not only by the loss of LINC complex components but also increases in LINC complex components. Emerin is a critical regulator of LINC complex levels in the nucleus. Both the expression of Klarsicht and the localization of Klarsicht are regulated by emerlin. However, we found here that in *Drosophila*, these two functions are divided among the two *Drosophila emerlin* homologs, *bocksbeutel* and *otefin*. Thus, the specification of emerlin activity may be the critical determinant of nuclear position and function. Given the functions of emerlin in mechanosignaling (Guilluy and Burrige, 2015), genome organization (Boyle et al., 2001) and autophagy (Deroyer et al., 2014) among other functions the division of different emerlin activities between *bocksbeutel* and *otefin* could serve as a valuable tool to further study emerlin functions.

## 3.5 Materials and Methods

### 3.5.1 *Drosophila* Genetics

All stocks were grown under standard condition at 25°C. Stocks used were *apRed* which expresses *DsRed* fused to a nuclear localization signal downstream of the *apterous* mesodermal enhancer (Richardson et al., 2007), *bocks*<sup>DP01391</sup> (21846; Bloomington *Drosophila* Stock Center), *klar*<sup>l</sup> (3256; Bloomington *Drosophila* Stock Center), *ote*<sup>DB</sup> (5092; Bloomington *Drosophila* Stock Center), *koi*<sup>EY03560</sup> (20000; Bloomington

*Drosophila* Stock Center), *bocks* deficiency Df(3R)Exel6153 (7632; Bloomington *Drosophila* Stock Center), *klar* deficiency Df(3L)BSC247 (9721, Bloomington *Drosophila* Stock Center), *ote* deficiency Df(2R)BSC337 (24361; Bloomington *Drosophila* Stock Center), *koi* deficiency Df(2R)Exel6050 (7532, Bloomington *Drosophila* Stock Center and UAS-*klar.6Xmyc* (derived from stock 25668; Bloomington *Drosophila* Stock Center), *ote*<sup>B279</sup> (16189, Bloomington *Drosophila* Stock Center). Mutants were balanced and identified using *CyO*, *Dfd-GMR-nvYFP* and *TM6b, Dfd-GMR-nvYFP*. UAS-*klar.6Xmyc* was driven specifically in muscle using *DMEf2-GAL4, apRed*. The *twist-GAL4, apRed* and *Dmef2-GAL4, apRed* *Drosophila* lines were both used as controls. 3<sup>rd</sup> chromosome alleles have *twist-GAL4, apRed* on the second chromosome and 2<sup>nd</sup> chromosome alleles have *Dmef2-GAL4, apRed* on the third chromosome to allow visualization of nuclei within the LT muscles during embryonic stages. Because there are slight variations between these two genotypes, each was used as a control. The *twist-GAL4, apRed* and *Dmef2-GAL4, apRed* *Drosophila* lines were made by recombining the *apRed* transgene and the specific *GAL4* driver.

### 3.5.2 Immunohistochemistry

Embryos were collected at 25°C and then dechorionated by submersion in 50% bleach for 4 minutes. Embryos were then washed with water and then fixed in 50% Formalin (HT501128; Sigma-Aldrich) diluted in 1:1 with Heptane and placed on an orbital shaker that rotated at a rate of 250 rpm for 20 min. In all cases, embryos were devitellinized by vortexing in a 1:1 methanol:heptane solution. Embryos were stored in methanol at -20°C until immunostaining.

Larvae were dissected as previously described (Louis et al., 2008; Metzger et al., 2012) with minor modifications. Larvae were dissected in ice-cold 1,4-piperazinediethanesulfonic acid (PIPES) dissection buffer containing 100mM PIPES (P6757; Sigma-Aldrich), 115mM D-sucrose (BP220-1; Fisher Scientific), 5mM trehalose (182550250; Acros Organics), 10 mM sodium bicarbonate (BP328-500; Fisher Scientific), 75 mM potassium chloride (P333-500; Fisher Scientific), 4 mM magnesium chloride (M1028; Sigma-Aldrich) and 1 mM ethylene glycol tetraacetic acid (28-071-G; Fisher Scientific) and then fixed with 10% Formalin (HT501128; Sigma-Aldrich) for 20 minutes.

Antibodies for embryo staining were used at the following final dilutions: rabbit anti-dsRed, 1:400 (632496; Clontech); rat anti-tropomyosin, 1:200 (ab50567; Abcam), and mouse anti-green fluorescent protein, 1:50 (GFP-G1; Developmental Studies Hybridoma Bank). Antibodies for larval staining were used at the following final dilutions: mouse anti-Klar, 1:25 (KLAR-C 9E10; Developmental Studies Hybridoma Bank), mouse anti-LamC, 1:20 (LC28.26, Developmental Studies Hybridoma Bank), mouse anti-MYC, 1:200 (9B11, Cell Signaling). Conjugated fluorescent secondary antibodies used for embryo staining were Alexa Fluor 555 donkey anti-rabbit (1:200), Alexa Fluor 488 donkey anti-rat (1:200) and Alexa Fluor 647 donkey anti-mouse (1:200; all Life Technologies). Alexa Fluor donkey anti-mouse (1:200; Life Technologies), Acti-stain 555 phalloidin (1:400; PHDH1-A; Cytoskeleton) and Hoechst 33342 (1 µg/ml; H3570; Life Technologies) were used for larval staining. Embryos and larvae were mounted in ProLong Gold (P36930; Life Technologies) and imaged with an Apochromat 40X/1.4 numerical aperture (NA) objective with a 1.0X Optical zoom for all embryo images on a Zeiss 700 LSM. Larvae were imaged using the same microscope and objective lens at 0.5X optical zoom for

nuclear positioning analysis and 2.0X optical zoom for Klarsicht localization, Hoechst intensity analysis, and MYC tagged klarsicht localization.

### **3.5.3 Analysis of nuclear position in embryos**

The position on nuclei was measured in stage 16 embryos, which is the latest stage before cuticle development blocks the ability to perform immunofluorescence microscopy. Embryos were staged primarily by gut morphology as previously described (Folker et al., 2012). Images acquired as described above were processed as maximum intensity projections of confocal z-stacks using ImageJ. The positioning of the nuclei was measured using the line function in ImageJ to determine the distance between either the dorsal end of the muscle and the nearest nucleus or the ventral end of the muscle and the nearest nucleus. All four LT muscles were measured in 3-4 hemisegments from each embryo. At least 20 embryos from at least two independent experiments were measured for each genotype, with the exception of experiments investigating mutants crossed to deficiencies, with each data point representing the average for all muscles measured within a single embryo. For experiments investigating mutants crossed to deficiencies at least 7 embryos from at least two independent experiments were measured. Statistical analysis was performed with Prism 4.0. Student's t-test was used to assess the statistical significance of differences in measurements between experimental genotypes and controls.

For qualitative nuclear positioning phenotype analysis, embryos were scored on how nuclei positioned themselves within the first three LT muscles of 3-4 hemisegments in at least 20 embryos from at least two independent experiments, with the exception of experiments investigating mutants crossed to deficiencies. For experiments investigating

mutants crossed to deficiencies at least 7 embryos from at least two independent experiments were measured. LT4 was excluded for this analysis due to its variable muscle morphology. Nuclei were categorized as separated (equal distribution) to indicate that nuclei were properly segregated into two distinct even clusters with a dorsal/ventral cluster area ratio  $>0.6$  and  $<1.4$ , separated (unequal distribution) to indicate that nuclei were separated into two distinct clusters that were uneven in size with a dorsal/ventral cluster area ratio of  $<0.6$  or  $>1.4$ , central to indicate that a nucleus or small cluster of nuclei was located in the middle of the myofiber that is not associated with either the dorsal or ventral cluster, clustered to indicate that nuclei remain in a single cluster toward the ventral end of the myofiber, or spread to indicate that nuclei are distributed along the myofiber with no distinct dorsal or ventral cluster. For the distinction of separated (equal distribution) and separated (unequal distribution) the areas of dorsal and ventral clusters were measured from each LT muscle using ImageJ. The nuclear distribution ratio was calculated by dividing the dorsal areas by the ventral areas. Statistical analysis was performed with Prism 4.0. Student's t-test was used to assess the statistical significance of differences in measurements between experimental genotypes and controls.

#### **3.5.4 Analysis of nuclear position in larvae**

We measured nuclear position in larvae by our previously described method (Auld et al., 2018a; Collins et al., 2017). First, the area and length of the muscle were measured. Next, the position and number of nuclei were calculated using the multipoint tool in ImageJ to place a point in the center of each nucleus. The position of each nucleus was used to calculate the actual internuclear distance. The maximal internuclear distance was then

determined by taking the square root of the muscle area divided by the nuclear number. This value represents the distance between nuclei if their internuclear distance is fully maximized. The ratio between the actual internuclear distance and the maximal internuclear distance was then used to determine how evenly nuclei were distributed. This method normalizes the internuclear distance to both the nuclear count and the muscle area, which leads to a more representative means of comparison between muscles, larvae, and genotypes. In addition, the distance of each nucleus from the lengthwise edge of the muscle was determined by measuring the shortest distance from the center of the nucleus to the nearest lengthwise edge of the muscle. 24 ventral longitudinal (VL3) muscles were measured from at least 6 larvae with at least 3 VL3 muscles measured from each larva from at least 2 independent experiments. Statistical analysis was performed with Prism 4.0. Student's t-test was used to assess the statistical significance of differences in measurements between experimental genotypes and controls. Slope of the linear regression and  $R^2$  values for the distance from muscle edge versus the average muscle width were determined using the linear regression function in Prism 4.0.

### **3.5.5 Analysis of klarsicht localization in larvae**

Nuclear Klarsicht localization was measured in VL3 muscles of L3 larvae. Z-stack maximum projection images that extended through the entire nucleus were analyzed. Fluorescence intensity of Klarsicht and Hoechst were measured for the nucleus and the cytoplasm. The ratio between the background subtracted average nuclear Klarsicht and maximum Hoechst fluorescence intensity was then used to determine Klarsicht localization at the nucleus while normalizing to Hoechst intensity to control for any staining variation

between experiments. Since the EDMD-linked genes tested have an effect on nuclear size the Hoechst normalized average nuclear Klarsicht fluorescence intensity ratio was also normalized to nuclear size. The Hoechst and size normalized intensity ratios were also normalized to intensity ratios of control larvae that were dissected and stained on the same day using the same materials. A total of at least 20 nuclei were measured from at least 6 larvae from at least 2 independent experiments.

### **3.5.6 Analysis of nuclear area, Hoechst integrated density and fluorescence intensities**

Nuclear size, Hoechst integrated density, mean and maximum fluorescence intensities were measured as previously described with minor modifications (Wang et al., 2018; Xiang et al., 2017). Briefly, individual nuclei in VL3 muscles were imaged as Z-stacks with 0.25  $\mu\text{m}$  steps so as to image the entire nucleus. Low laser power was used to avoid saturation of the detectors and imaging settings were kept constant throughout all nuclear size, Hoechst integrated density, mean and maximum fluorescence intensity experiments. The nucleus was identified in ImageJ by converting the Lamin C fluorescence channel to a binary image, applying the fill holes function and using the analyze particle function with a size threshold set at  $>25$  pixels resulting in selected regions of interest (ROI). The area of the ROI was recorded as the nuclear area. All slices from the Hoechst fluorescence channel were summed to create a projection of the nucleus and ROI from Lamin C channel was selected in the Hoechst fluorescence channel using the restore selection function in ImageJ. The ROI in the Hoechst fluorescence channel was then measured for the mean and maximum Hoechst fluorescence intensities as well as the Hoechst integrated density.

### 3.5.7 RT-qPCR

Gene expression was quantified by RT-qPCR. RNA as extracted and isolated from 5 L3 larvae by crushing in an Eppendorf tube in 1 ml of TRIzol according to manufacturer's instructions (15596026, Invitrogen). DNase I (04716728001; Sigma-Aldrich) digest was performed on the isolated RNA at 37°C for 30 min according to manufacturer's instructions. DNase I was inactivated with the addition of EDTA to a final concentration of 8 mM and heat to 75°C for 10 min. RNA integrity and concentrations were determined using the NanoDrop2000 system (Thermo Fisher Scientific). The cDNA library was established by performing reverse transcription using the SuperScript VILO cDNA synthesis kit (11-754-050; Invitrogen), according to manufacturer's protocol. Briefly, purified RNA was incubated with SuperScript III reverse transcriptase at 42°C for 2 h and then reactions were terminated at 85°C for 5 min. The resulting cDNA was used as the template for quantitative PCR using an ABI 7500 Fast real-time PCR system (Applied Biosystems) and Power SYBR green PCR Master Mix (4367659, Applied Biosystems) for detection. For each genotype, biological and technical triplicates were performed. Gene transcript levels were quantified using gene-specific primers designed using FlyPrimerBank (Hu et al., 2013) and primers were validated according to Applied Biosystems' instructions. The primers used were *RP49* forward, 5'-GCCCAAGGGTATCGACAACA-3'; *RP49* reverse, 5'-GCGCTTGTTTCGATCCGTAAC-3'; *GAPDH* forward, 5'-TAAATTCGACTCGACTCACGGT-3'; *GAPDH* reverse, 5'-CTCCACCACATACTCGGCTC-3'; *αTub84b* forward, 5'-

GATCGTGTCCCTCGATTACCGC-3';	<i>αTub84b</i>	reverse,	5'-
GGGAAGTGAATACGTGGGTAGG-3';	<i>bocks</i>	forward,	5'-
AGGACCAGCAGCCTAGACG-3';	<i>bocks</i>	reverse,	5'-
TCAACTTCGCGTGTGTAAGATG-3';	<i>klar</i>	forward,	5'-

GCGTGGGACAACCTACCAAGA-3'; *klar* reverse, 5'-AATTCCAAGAGACGCCGGG-3'; *ote* forward, 5'-GATTCTCTGTCCAATGCTGAGTT-3'; *ote* reverse, 5'-TAGAACCTTCCGGCTGCTATC-3'; *koi* forward, 5'-CTGACCTCGGACTATTCGAGC-3'; *koi* reverse, 5'-GGTGAGAATCGACGTGACTGT-3'. To confirm the effective removal of contaminating DNA and specificity of the primers, experiments were also conducted with reactions lacking reverse transcriptase. The differences in gene expression were calculated using the  $\Delta\Delta C_t$  method. Rp49, GAPDH and  $\alpha$ Tub84b were used as the reference genes for comparison to the gene of interest for  $\Delta C_t$  values for each sample. Fold change were expressed as  $2^{-\Delta\Delta C_t}$  and plotted in  $\text{Log}_2$  for graphical representation. Statistical analysis was performed with Prism 4.0. Student's t-test was used to assess the statistical significance of differences in  $\Delta C_t$  measurements between experimental genotypes and controls.

## **Chapter 4:**

# **An RNAi based screen in *Drosophila* larvae identifies fascin as a regulator of myoblast fusion and myotendinous junction structure**

*The content in this chapter was adapted from:*

**Camuglia, J.M., Mandigo, T.R., Moschella, R., Mark, J., Hudson, C.H., Sheen, D.,  
and Folker, E.S. (2018) An RNAi-based screen in *Drosophila* larvae identifies  
fascin as a regulator of myoblast fusion and myotendinous junction structure.  
*Skeletal Muscle*. **8**: 1-13**

## 4.1 Abstract

A strength of *Drosophila* as a model system is its utility as a tool to screen for novel regulators of various functional and developmental processes. However, the utility of *Drosophila* as a screening tool is dependent on the speed and simplicity of the assay used. Here we use larval locomotion as an assay to identify novel regulators of skeletal muscle function. We combined this assay with muscle specific depletion of 82 genes to identify genes that impact muscle function by their expression in muscle cells. The data from the screen were supported with characterization of the muscle pattern in embryos and larvae that had disrupted expression of the strongest hit from the screen. With this assay, we showed that 12/82 tested genes regulate muscle function. Intriguingly, the disruption of 5 genes caused an increase in muscle function, illustrating that mechanisms that reduce muscle function exist and that the larval locomotion assay is sufficiently quantitative to identify conditions that both increase and decrease muscle function. We extended the data from this screen and tested the mechanism by which the strongest hit, Fascin, impacted muscle function. Compared to controls, animals in which Fascin expression was disrupted with either a mutant allele or muscle specific expression of RNAi, had fewer muscles, smaller muscles, muscles with fewer nuclei, and muscles with disrupted myotendinous junctions. However, expression of RNAi against *fascin* only after the muscle had finished embryonic development did not recapitulate any of these phenotypes. These data suggest that muscle function is reduced due to impaired myoblast fusion, muscle growth, and muscle attachment. Together these data demonstrate the utility of *Drosophila* larval locomotion as an assay for the identification of novel regulators of muscle development and implicate *fascin* as necessary for embryonic muscle development.

## 4.2 Introduction

Skeletal muscle has a distinctive architecture that is generated by a unique set of developmental phases. Making the myofiber syncytium requires the fusion of mononucleated myoblasts. In both *Drosophila* and mammalian systems, individual myoblasts invade growing myotubes and deposit their nucleus into the common cytoplasm to drive myotube growth (Abmayr and Pavlath, 2012; Kim et al., 2015b). Myoblast fusion is an actin dependent process that is reminiscent of a cancer cell invading a tissue during metastasis (Sens et al., 2010). The mononucleated myoblast extends a protrusive invadopodia-like structure that makes possible the penetration of the myotube and the mixing of cytoplasm. Many factors and signaling pathways that regulate myoblast fusion have been identified (Bothe et al., 2014; Kim et al., 2015b; Kim et al., 2015a). However, many of the genes necessary for invadopodia-like structures in other contexts have not yet been implicated in myoblast fusion, suggesting that additional regulators remain to be identified. One glaring omission from the categories of proteins that have been identified as regulators of myoblast fusion is proteins that stabilize filopodia. Invadopodia are filopodia-like structures (Gimona et al., 2008; McNiven, 2013) and they require several factors that are known to stabilize filopodia. Furthermore, although loss-of-function data is lacking, dominant negative mutants of the formin Diaphanous, inhibit myoblast fusion and may suggest that filopodia are essential for myoblast fusion (Deng et al., 2015; Deng et al., 2016). Thus, it is likely that one or more of the proteins that have been identified as capable of stabilizing filopodia for the purpose of protrusion and invasion, in other contexts contribute to myoblast fusion.

Beyond myoblast fusion, there are several features of muscle development that either require, or have been hypothesized to require precise regulation of the actin cytoskeleton including the positioning of nuclei and the development of the myotendinous junction (MTJ). To date, evidence for actin-dependent nuclear movement in muscle is restricted to the squeezing of nuclei to the periphery of the muscle (D'Alessandro et al., 2015; Roman et al., 2017), although it has been proposed that actin may contribute to the movement of nuclei along the length of the muscle (Cadot et al., 2015; Folker and Baylies, 2013). The role of actin in MTJ development is more established. MTJs are integrin-based adhesions that transmit force from the muscle to the skeleton (Brown et al., 2000). The initial formation involves extension of filopodia-like structures from the muscle cell that interact with the tendon cell before forming a stable, and somewhat rigid attachment that enables effective force transmission (Schnorrer et al., 2007; Weitkunat et al., 2014). All of these processes require linear actin-cables. The similarity in the actin-based structures suggests that the same molecular components may contribute to each of these aspects of muscle development. Therefore, it is critical to determine how newly identified genes and proteins contribute to each process.

Because the developmental path and final architecture of muscle cells is conserved from *Drosophila* to humans, flies provide a genetically tractable and inexpensive model for the identification of genes that are necessary for muscle development. Indeed, many screens for regulators of muscle development have been completed. Researchers have used adult locomotion (Schnorrer et al., 2010) and embryonic muscle structure (Metzger et al., 2012) as indicators of muscle development. Although these strategies have proven effective, they each have drawbacks. Analysis of embryonic muscle structure is labor

intensive and requires significant expertise in muscle biology. Analysis of adult locomotion is limited because the disruption of many genes is lethal during pupation. Therefore, we have developed a simple assay for muscle function based on the larval locomotion. We have used this assay to screen for novel regulators of muscle function, and identified Fascin as one such regulator. Subsequent cell biological analysis implicates *fascin* as a regulator of myoblast fusion and MTJ structure.

## 4.3 Results

### 4.3.1 Fascin is necessary for muscle function

Animal movement provides a simple assay for muscle function. Although adult locomotion has been used to perform a full-genome, RNAi-based screen for regulators of muscle function in *Drosophila* adults (Schnorrer et al., 2010), similar screens have not been completed using *Drosophila* larvae. The greatest advantage to evaluating muscle function in larvae rather than adults is that pupation, and the high probability of lethality during pupation, is bypassed. We have therefore modified published larval locomotion assays (Louis et al., 2008; Metzger et al., 2012) to identify regulators of muscle function. To ensure that the identified genes had a muscle-autonomous effect on muscle function, we used the *GAL4/UAS* system (Brand and Perrimon, 1993) to disrupt gene function in a muscle specific manner. Specifically, we used *DMef2-GAL4* to drive the expression of a small library of UAS-RNAi constructs. We measured movement of larvae toward a chemo-attractant as previously described (Louis et al., 2008), with modifications to increase the throughput of the assay. First, we skipped the selection of stage 17 embryos, which previously ensured that the ages of the evaluated larvae were similar. We replaced this step,

which previously took ~60 minutes per genotype per experiment, with a timed-lay. Briefly, virgins that expressed *DMef2-GAL4* and

males that carried the UAS-RNAi were mixed together in a vial for 1 hour. The adults were then moved to another vial. The first vial, which contained all of

the embryos that were laid during the 1 hour period, was then used for the experiment to

ensure that all larvae used in an experiment were of similar age. These vials were aged for 5 days until the animals were third-instar larvae (L3). Second, we measured the movement of many larvae simultaneously rather than measuring locomotion for individual larvae as previously described. The movement of larvae was then tracked using ImageJ (Fig. 4.1A). Measuring larval locomotion of many animals simultaneously provided two benefits. First,

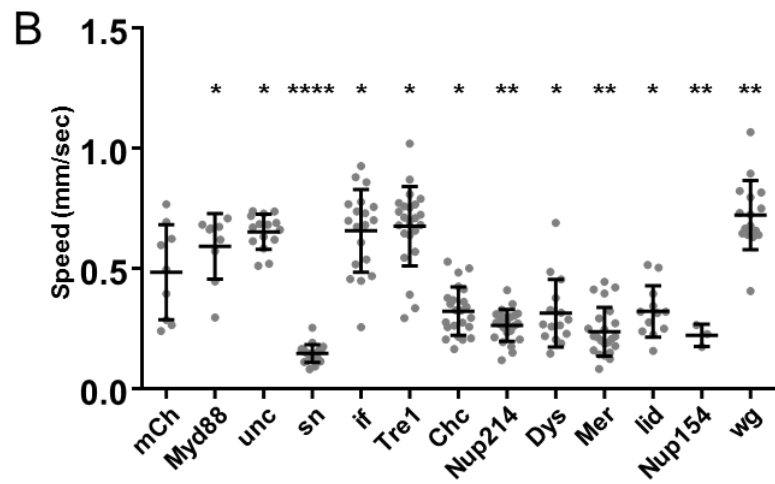
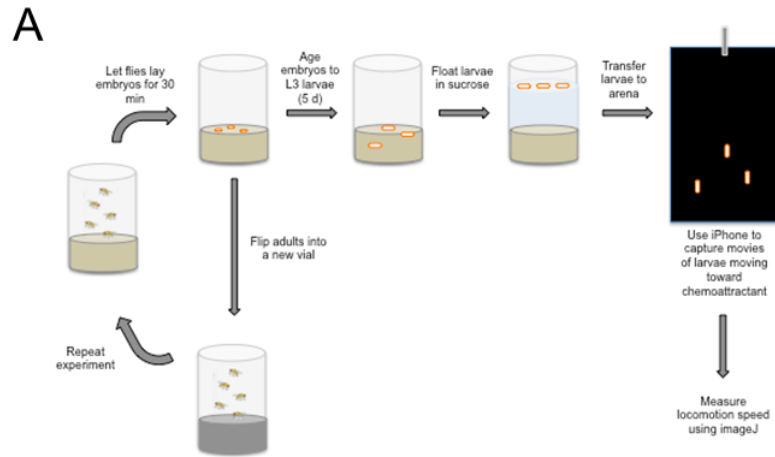


**Figure 4.1** An RNAi screen for larval locomotion identifies fascin as a regulator of muscle function. (A) Cartoon illustrating the locomotion assay that was used to identify RNAi constructs that when expressed specifically in muscle, altered muscle function. (B) Graph indicating the speed of larval locomotion toward a chemoattractant when indicated genes were depleted by expression of RNAi specifically in muscle. All data were compared to their control by Student's t-test. \*,  $p < 0.05$ ; \*\*,  $p < 0.01$ ; \*\*\*\*,  $p < 0.0001$ .

it increased the speed of the assay from ~ 60 minutes/genotype to ~ 10 minutes per genotype. Coincident with the increased speed of the assay, there was less variability in the age of larvae that were tracked in an experiment, thus increasing the precision of the data.

For the proof-of-concept screen, we expressed RNAi against 82 genes (Supplemental Table A1.2). The selected genes included those expected to impact muscle function (e.g. *Dystrophin*, *Msp300*) and many for which we did not have a prediction. The speed of locomotion in larvae that expressed each RNAi was compared to control larvae in which *DMef2-GAL4* drove the expression of mCherry RNAi. The disruption of 12/82 genes significantly altered larval locomotion compared to control larvae, indicating that these 12 genes regulate muscle function. Of these 12 genes, disruption of 5 caused larvae to move faster compared to controls and the disruption of 7 caused the larvae to move more slowly than controls (Fig. 4.1B). RNAi directed against the expression of *singed* (*sn*) which encodes for the actin binding protein Fascin (Bryan et al., 1993; Paterson and O'Hare, 1991) caused the greatest decrease in larval locomotion. Therefore, we investigated the impact that Fascin depletion had on muscle structure to identify the mechanism by which Fascin regulates muscle function.

#### **4.3.2 Fascin is localized to the nucleus in *Drosophila* muscle**

As a first approach to determining how Fascin regulates muscle function, we examined the localization of fascin in *Drosophila* larval muscles and found that Fascin localized to the sarcomeres and to the nuclei. The nuclear localization is similar to the localization of Fascin in nurse cells (Groen et al., 2015) and (Fig. 4.2A).

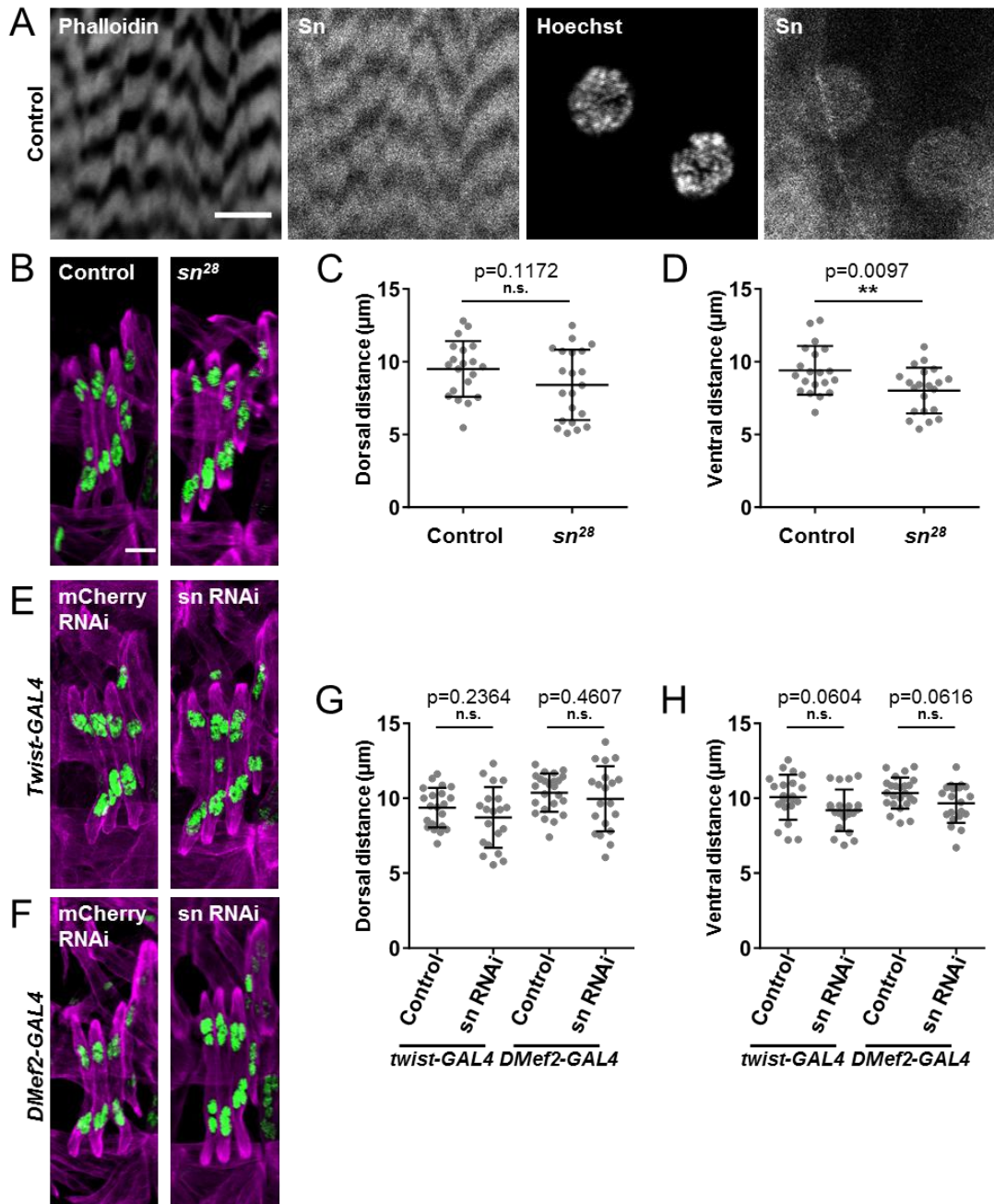


**Figure 4.2** Fascin is localized to actin and the nucleus in muscle. (A) Images from dissected L3 larvae showing that Fascin (*sn*) is colocalized with both phalloidin (F-actin) and Hoechst (nuclei). (B) Immunofluorescence images from stage 16 embryos stained for the muscles (magenta) and the nuclei the LT muscles (green) of control and *sn*<sup>28</sup> mutant embryos. Scale bar, 10μm. (C) Graph indicating the distance between the dorsal end of the muscle and the nearest nucleus in control and *sn*<sup>28</sup> mutant embryos. (D) Graph indicating the distance between the ventral end of the muscle and the nearest nucleus in control and *sn*<sup>28</sup> mutant embryos. (E,F) Immunofluorescence images of the LT muscles (magenta) and the nuclei within the LT muscles (green) in embryos where RNAi against either mCherry (control) or fascin (*sn* RNAi) was driven by *Twist-GAL4* (E) or *Dmef2-GAL4* (F). (G) Graphs indicating the average distance between the dorsal end of the muscle and the nearest nucleus (G) or the ventral end of the muscle and the nearest nucleus (H) in embryos of indicated genotypes. All data (C,D,G,H) were compared to their control by Student's t-test. \*\*,  $p < 0.01$ .

An emergent regulator of muscle function is the position of the many myonuclei within a single cytoplasm (Bruusgaard et al., 2006; Cadot et al., 2015; Folker and Baylies, 2013). Based on the localization of Fascin to the nucleus, we hypothesized that Fascin may regulate nuclear movement during muscle development. Consistent with this hypothesis, fascin interacts with the nuclear envelope protein nesprin-2 and regulates nuclear movement in migrating fibroblasts (Jayo et al., 2016) and is necessary for the positioning of nuclei in developing *Drosophila* oocytes (Groen et al., 2015). To determine whether nuclear position was affected in *Drosophila* muscle, we crossed apRed, a marker for the nuclei in the Lateral Transverse (LT) muscles (Richardson et al., 2007) into the *sn<sup>28</sup>* *Drosophila* and measured the position of nuclei as previously described (Folker et al., 2012). In *sn<sup>28</sup>* mutants, nuclei were closer to the ventral end of the muscle compared to controls (Fig. 4.2B-D). To determine whether the effect on nuclear position was muscle autonomous, we transiently expressed RNAi specifically in the mesoderm during the early stages of muscle development using *Twist-GAL4* or in a more sustained manner using *DMef2-GAL4* and measured the position of the nuclei. Muscle-specific depletion of Fascin had no impact on nuclear position (Fig 4.2E-H). Together these data indicate that although nuclei are closer to the muscle end in *fascin* mutants, this is not regulated by Fascin expressed in muscle during embryonic muscle development in *Drosophila*.

### 4.3.3 Fascin regulates myoblast fusion

Because the loss of Fascin had a limited effect on nuclear position in *Drosophila* embryonic muscles, we looked at the general muscle pattern in the *sn<sup>28</sup>* mutant embryos. At embryonic stage 16 there are 30 well-characterized muscles per hemisegment in the

*Drosophila* embryo (Ruiz-Gómez, 1998). We noted a number of differences between *sn<sup>28</sup>* mutant embryos and controls (Fig. 4.3A). First, there was a reduction in the number of muscles. Although, various muscles were missing in individual hemisegments, we focused on the LT muscles because they are near the embryo surface and are the only muscles that are perfectly aligned on the dorsal-ventral axis of the embryo. These features make the LTs easy to count, image, and analyze.

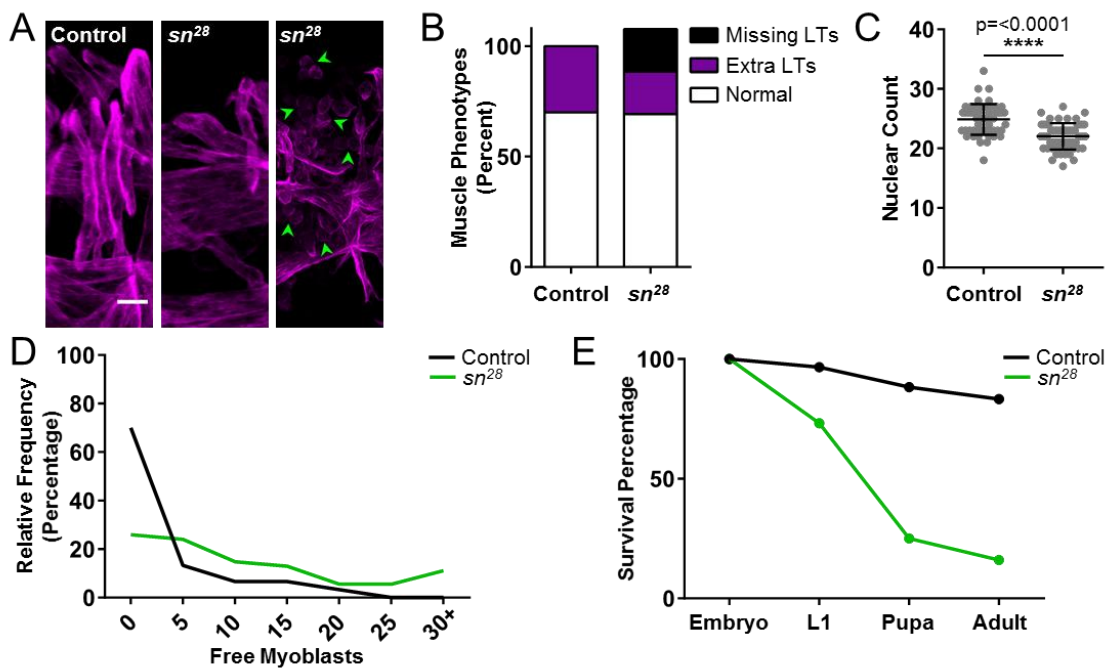


**Figure 4.3 Fascin is necessary for myoblast fusion** (A) Immunofluorescence images showing the pattern of the lateral transverse (LT) muscles in stage 16 embryos. Green arrowheads indicate unfused myoblasts. Scale bar, 10  $\mu$ m. (B) Graph indicating the percentage of embryos that had at least one hemisegment with > 4 LT muscles (Extra LTs) or < 4 LT muscles (missing LTs). Values exceeding 100% indicate the presence of embryos with one hemisegment with > 4 LT muscles (extra muscles) and another hemisegment with < 4 LT muscles (missing muscles). (C) Graph indicating the number of apRed positive nuclei per hemisegment. Student's t-test was used for comparison to controls. \*\*\*\*,  $p < 0.0001$ . (D) Graph indicating how frequently different numbers of unfused myoblasts are seen in control (black) and *sn<sup>28</sup>* mutant embryos (green). (E) Graph indicating the viability of *sn<sup>28</sup>* mutant animals (green) compared to controls (black).

The typical hemisegment from a control embryo has 4 LT muscles. 70% of control embryos had 4 LT muscles per hemisegment and 30% of controls had at least one hemisegment with greater than 4 LT muscles. In *sn<sup>28</sup>* mutants, 70% of embryos had 4 LT muscles and 19% of embryos had at least one hemisegment with greater than 4 LTs. Additionally, 19% of *sn<sup>28</sup>* embryos had at least one hemisegment with fewer than 4 LTs (Fig. 4.3B), and were therefore missing LTs. Because the absence of muscles can indicate a defect in myoblast fusion, we counted the number of nuclei that were incorporated into the LT muscles per hemisegment. This number was reduced from a mean of 26 in controls to a mean of 22 in *sn<sup>28</sup>* mutants (Fig. 4.3C). Consistent with this, there was an increase in unfused myoblasts. In controls, the median number of free myoblasts per embryo was 1, and that number increased to 7.5 in *sn<sup>28</sup>* mutants (Fig. 4.3D). Additionally, 70% of control embryos had two or fewer identifiable unfused myoblasts whereas 75% *sn<sup>28</sup>* mutant embryos had at least three unfused myoblast and 50% of *sn<sup>28</sup>* mutant embryos eight or more unfused myoblasts. Based on the missing muscles and the abundance of unfused myoblasts in mutant embryos, we tested the viability of the *sn<sup>28</sup>* mutants and found that there was significant lethality during both the embryonic and larval stages (Fig. 4.3E). These data suggest that the reduction in muscle number in *sn<sup>28</sup>* mutant embryos may result from impaired myoblast fusion.

To determine whether these phenotypes were muscle autonomous, we used the *GAL4/UAS* system to deplete fascin specifically from the developing mesoderm and muscle of the *Drosophila* embryo. The expression of a UAS-sn RNAi (fascin RNAi) was driven with each of three *GAL4* drivers. *Twist-GAL4* was used to drive RNAi expression in the early mesoderm, *DMef2-Gal4* was used to drive RNAi expression slightly later in

muscle with sustained expression throughout development, and *MHC-GAL4* was used to drive RNAi expression beginning at the final stage of embryonic development and continuing throughout development. We then examined the general muscle structure in stage 16 embryos as we had done for *sn*<sup>28</sup> mutant embryos. There were no defects in muscle morphology when *MHC-GAL4* was used to drive RNAi expression suggesting that Fascin must be depleted early during development to have significant impact (Fig. 4.4).

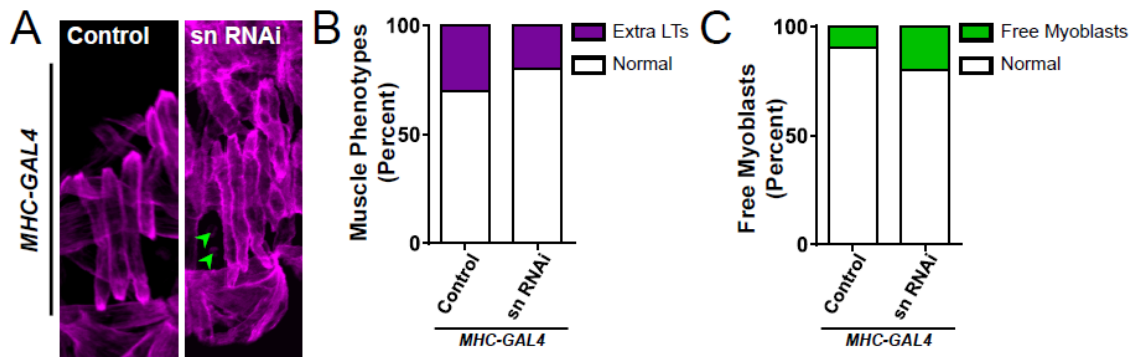


**Figure 4.4** Expression of RNAi against fascin late in embryonic development does not affect muscle development (A) Immunofluorescence images showing the muscle pattern in animals expressing mCherry RNAi (control) and animals expressing fascin RNAi (sn RNAi) under the control of the *MHC-GAL4* driver. (B) Graph comparing the frequency of embryos with extra muscles in each genotype. No embryos with missing muscles were observed in either genotype. (C) Graph comparing the frequency at which embryos were found to have unfused myoblasts in each genotype.

Early mesodermal expression of the RNAi under the control of *Twist-GAL4* and expression of RNAi in muscle under the control of *DMef2-GAL4* both increased the percentage of embryos that were missing LT muscles, but *DMef2-GAL4*-mediated expression resulted in a higher frequency of embryos with missing muscles (Fig. 4.5A,B). Conversely, only *Twist-GAL4*-mediated expression of RNAi against Fascin caused a decrease in the number of nuclei that were incorporated into the LT muscles (Fig 4.5C). This suggested that early expression of Fascin RNAi was necessary to inhibit myoblast fusion. Consistent with this, *Twist-GAL4*-mediated RNAi expression increased both the

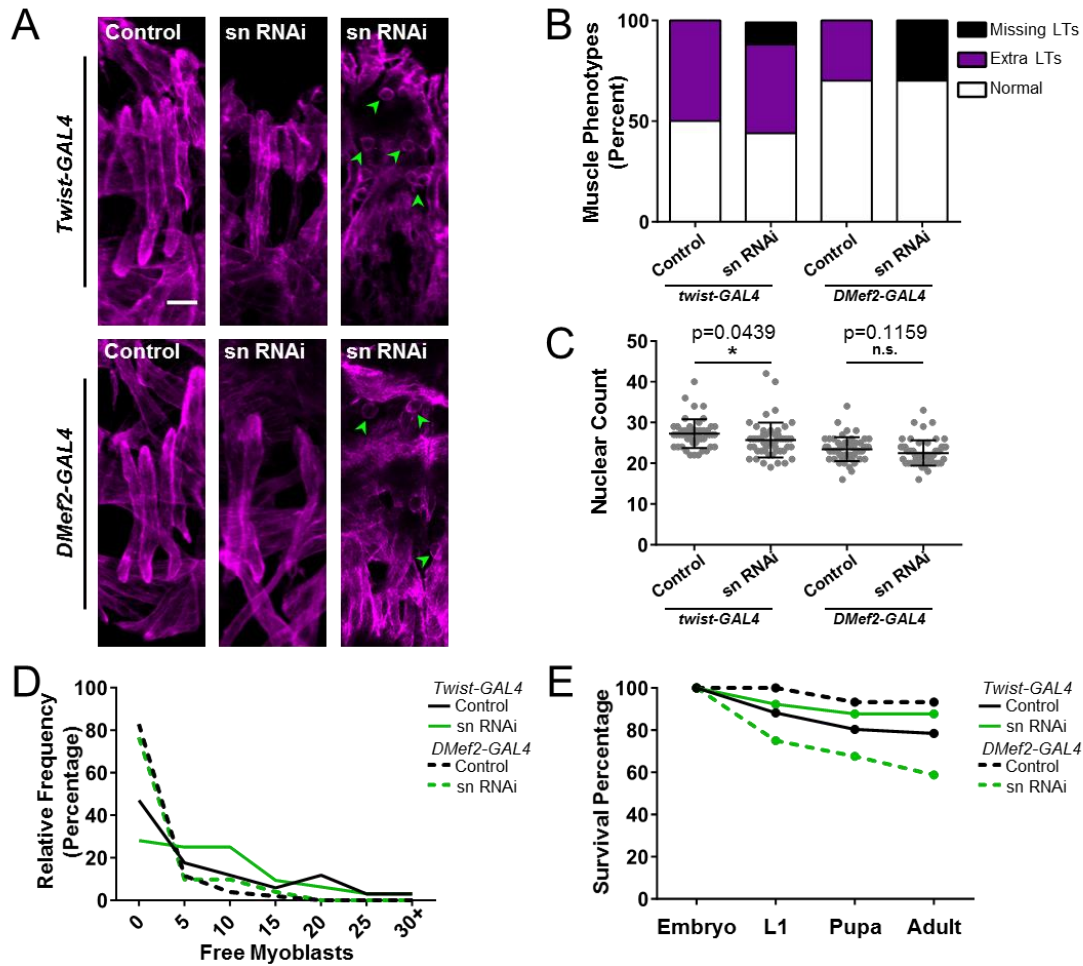


**Figure 4.5** Fascin has muscle autonomous effects on myoblast fusion. (A) Immunofluorescence images of the LT muscles in embryos that expressed RNAi against fascin under the control of *Twist-GAL4* (top) or *Dmef2-GAL4* (bottom). Green arrowheads indicate unfused myoblasts. Scale bar, 10  $\mu$ m. (B) Graph indicating the percentage of embryos of indicated genotypes that have at least one hemisegment with either > 4 LT (extra LTs) muscles or < 4 LT muscles (missing LTs). (C) Graph indicating the number of apRed positive nuclei incorporated into LT muscles per hemisegment in indicated genotypes. Student's t-test was used for comparison to controls. \*,  $p < 0.05$ . (D) Graph indicating how frequently different numbers of unfused myoblasts were seen in indicated genotypes. (E) Graph indicating the viability of animals with indicated genotypes.

percentage of embryos with unfused myoblasts and the number of unfused myoblasts in embryos. *Dmef2-GAL4*-mediated expression of Fascin RNAi affected neither measure of fusion (Fig 4.5D). However, *Dmef2-GAL4*-mediated expression of RNAi had a greater

effect on viability (Fig 4.5E) suggesting that the absence of muscles was more detrimental to animal viability.

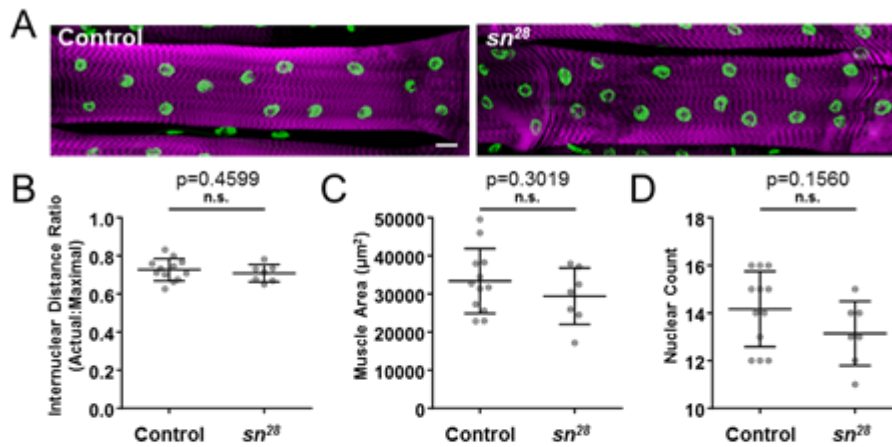


**Figure 4.6** Genetic disruption of fascin did not affect larval muscle structure. (A) Immunofluorescence images of the third ventral longitudinal muscle (VL3) in L3 larvae of indicated genotypes. Sarcomeres (magenta) were used to identify the muscle and Hoechst (green) was used to identify the nuclei. Scale bar, 25 µm. (B) Graph indicating the actual internuclear distance divided by the maximal internuclear distance in indicated genotypes. (C) Graph indicating the area of the muscles as a proxy for muscle size in the indicated genotypes. (D) Graph indicating the number of nuclei in indicated genotypes. All data (B,C) were compared to their control by Student's t-test. All differences were statistically insignificant.

#### 4.3.4 Fascin-dependent fusion effects are evident in larvae

To determine the effects of fascin-depletion later in development, larvae were dissected and stained with Phalloidin to identify the muscles and Hoechst to identify the nuclei (Fig. 4.6). We examined the third ventral longitudinal muscle (VL3) because after dissection this muscle is on the surface and therefore easily imaged. The distribution of myonuclei was similar in controls and *sn*<sup>28</sup> larvae (Fig. 4.6A,B). The size of the muscles (Fig. 4.6A,C) and the number of nuclei in each muscle (Fig. 4.6A,D) were both reduced in *sn*<sup>28</sup> larvae compared to controls, but the reductions were statistically insignificant. We hypothesized that the lack of phenotype may be based on selection of the healthiest animals because they are the animals that survived until the L3 stage. As such, we examined

animals that expressed RNAi specifically in the muscle, which are more viable (Compare Fig. 4.5E to Fig. 4.3E).

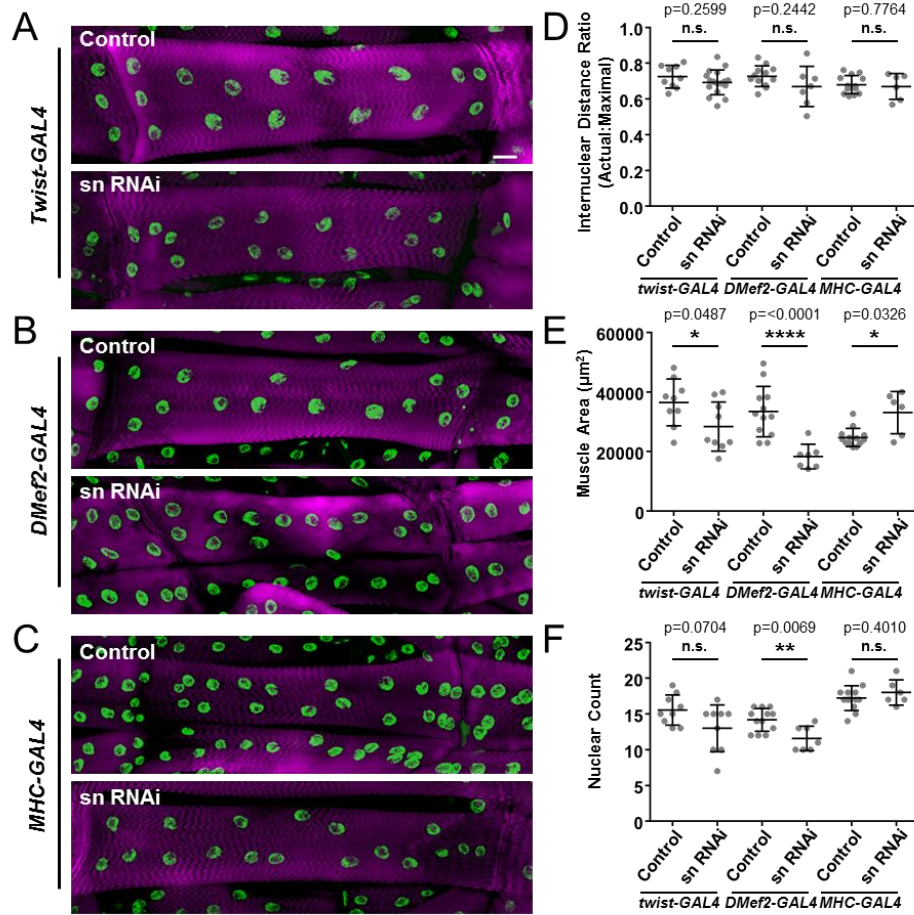


**Figure 4.7** Muscle specific depletion of fascin results in smaller muscles with fewer nuclei. (A,B,C). Immunofluorescence images of the VL3 muscle in L3 larvae that expressed RNAi against either mCherry (control) or fascin (sn RNAi) under the control of *Twist-GAL4* (A), *DMef2-GAL4* (B), or *MHC-GAL4* (C). Sarcomeres were identified by phalloidin (magenta) and nuclei were identified by Hoechst (green). Scale bar, 25 µm. (D) Graph indicating the area of the muscles as a proxy for muscle size in the indicated genotypes. (E) Graph indicating the area of the muscles in larvae of indicated genotypes. (F) Graph indicating the number of nuclei per muscle in larvae of indicated genotypes. All data (D,E,F) were compared to their control by Student's t-test. \*,  $p < 0.05$ ; \*\*,  $p < 0.01$ ; \*\*\*\*,  $p < 0.0001$ .

We expressed RNAi against Fascin under the control of *Twist-GAL4* (early, transient expression), *DMef2-Gal4* (slightly later, sustained expression), or *MHC-Gal4* (late, sustained expression). The distribution of nuclei was the same in each genotype (Fig.

4.7A-D). Muscle size was decreased when either *Twist-GAL4* or *DMef2-GAL4* was used to express Fascin RNAi (Fig. 4.7E) suggesting that early Fascin-dependent processes contribute to Fascin-dependent muscle growth. Finally, the number of nuclei in VL3 muscles were decreased by *DMef2-GAL4*-mediated Fascin depletion. *Twist-GAL4*-mediated depletion did reduce the number of nuclei per muscle, but insignificantly so. *MHC-GAL4* mediated depletion had no impact on the number of nuclei per muscle (Fig. 4.7A-C,F). Thus, the defects in fusion are not transient, but are evident throughout larval development.

### 4.3.5 Fascin regulates muscle attachment

*DMef2-Gal4*-mediated expression of *sn* RNAi did not reduce the number of nuclei incorporated into embryonic LT muscles (Fig. 4.5C), but did reduce the total number of muscles in the embryo (Fig. 4.5B). This could be explained by an effect on the attachments between the muscle and the tendon cell at the myotendinous junction (MTJ). To determine whether fascin affected MTJ integrity, we immunostained embryos for Tropomyosin to identify the muscles and  $\beta$ PS-Integrin to identify the MTJ (Fig. 4.8). We measured the width of the  $\beta$ PS-Integrin signal at the MTJ of dorsal muscle 2. Compared to controls, the signal was wider in *sn*<sup>28</sup> mutants (Fig. 4.8A-C). Similarly, *DMef2-GAL4*-mediated expression of Fascin RNAi, but not *Twist-GAL4*-mediated expression of Fascin RNAi also increased the width of the  $\beta$ PS-Integrin signal (Fig. 4.8D-H). These data suggest that sustained Fascin function is necessary for proper MTJ organization.

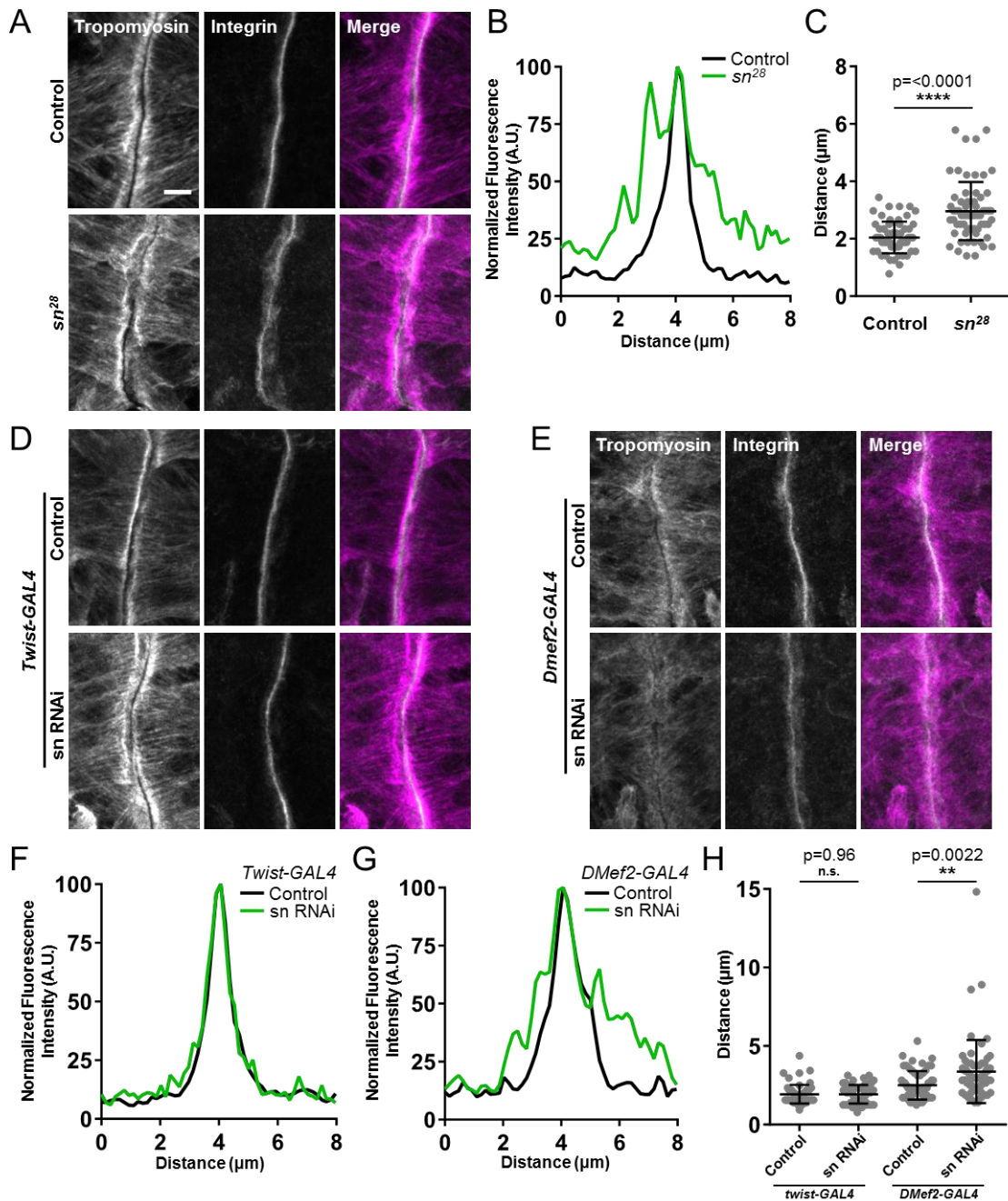


**Figure 4.8** Fascin is necessary for proper myotendinous junction organization (A) Immunofluorescence images of the MTJ of muscle DO2 stained for Tropomyosin and  $\beta$ PS-integrin in control (top) and  $sn^{28}$  mutant embryos (bottom). Scale bar, 10  $\mu$ m. (B) Representative intensity profile of the  $\beta$ PS-integrin signal in control (black) and  $sn^{28}$  mutant embryos (green). (C) Graph indicating the width of the  $\beta$ PS-integrin signal defined by the points at which the signal is 25% of maximal. (D,E) Immunofluorescence images of the MTJ of muscle DO2 stained for Tropomyosin and  $\beta$ PS-integrin in animals in which Twist-GAL4 was used (D) or DMef2-GAL4 was used (E) to express RNAi against either mCherry (control) or fascin (sn RNAi). (F,G) Representative intensity profiles of the  $\beta$ PS-integrin signal in indicated genotypes. (H) Graph indicating the width of the  $\beta$ PS-integrin signal in indicated genotypes as defined by the points at which the signal is 25% of maximal. All data (C,H) were compared to their control by Student's t-test. \*\*,  $p < 0.01$ ; \*\*\*\*  $p < 0.0001$ .

#### 4.4 Discussion

One of the many strengths of *Drosophila* as a model system is its utility as a tool to identify novel regulators of specific biological functions. This ability utilizes the immense genetic tools that are available and requires simple and fast assays to screen many mutants and/or RNAi lines. In this work we adapted a published larval tracking assay (Louis et al., 2008) to perform a proof-of-concept screen for muscle function. We identified 12 genes that regulate muscle function, either positively or negatively. We continued these experiments by examining the mechanism by which *singed*, *Drosophila* Fascin, regulated muscle function because Fascin-depletion had the strongest effect on muscle function.

We used a combination of mutant alleles and tissue specific expression of RNAi against Fascin to demonstrate that fascin regulates both myoblast fusion and the structure of the MTJ. Fascin is well-described as a protein that can bundle F-actin filaments and increase their strength, and the strength of actin based cellular protrusions (Jayo et al., 2016). Furthermore, by this mechanism, fascin contributes to cellular invasions associated with cancer metastasis (Hashimoto et al., 2011; Zanet et al., 2012). Myoblast fusion requires a similar organization of protrusive F-actin structures that invade the growing myotube. The most surprising aspect of the myoblast fusion data is the relatively minor effect that Fascin has compared to other genes necessary for myoblast fusion (Chen and Olson, 2001; Chen et al., 2003; Erickson et al., 1997; Richardson et al., 2007). The reason for this is not clear. One possibility is that maternal loading provides sufficient fascin to facilitate the initial rounds of fusion. Alternatively, perhaps the final fusion events require greater protrusive force and only then does the function of Fascin become critical.

The contribution of fascin to MTJ structure is consistent with previously published data. Fascin contributes to filopodia formation (Zanet et al., 2012) and MTJ development is dependent on filopodia-like extensions. Furthermore, although the MTJ forms as a smooth attachment during pupation (Weitkunat et al., 2014), the MTJ in the embryo is dynamic (Auld et al., 2018b). Thus, perhaps fascin is continually necessary for the turnover and the integrity of the MTJ.

Perhaps most intriguing feature of these data is the temporal separation of Fascin-dependent myoblast fusion and Fascin-dependent MTJ stability. This conclusion is based on our finding that the time and duration of Fascin depletion determines the phenotype that will emerge. Transient depletion of fascin during early stages of muscle development disrupted myoblast fusion but not MTJ structure. Conversely, later, and sustained depletion of Fascin affected MTJ structure, but not myoblast fusion. These data are important because they demonstrate that although both fusion and MTJ structure require Fascin function, they are not codependent features of muscle development.

It is not clear whether either function is more critical than the other. Certainly, sustained depletion of Fascin, which disrupts MTJ integrity has a greater effect on animal survival than does the transient depletion that disrupts fusion. However, this conclusion is limited because the impact that a small reduction in nuclear number has on muscle organization is not clear. Reduced nuclear numbers do correlate with reduced muscle size (Auld et al., 2018b; Bruusgaard et al., 2003), and therefore likely cause reduced muscle function. Data in embryos indicated that *DMef2-GAL4*-mediated expression of Fascin RNAi only affected MTJs and would therefore allow us to isolate the impact of the MTJ versus the impact of myoblast fusion. However, we see that in larvae there is a reduction

in the number of nuclei per muscle. Because there is no repair of embryonic and larval muscles in *Drosophila*, we suspect that this reduction is based in muscle damage that may be linked to improper attachments and poor mechanical stability. However, further work is necessary to understand the mechanism by which nuclei are lost so that the impact that individual Fascin-dependent functions can be determined.

## **4.5 Materials and Methods**

### **4.5.1 *Drosophila* genetics**

All stocks were grown under standard conditions at 25 °C. The *Fascin<sup>sn28</sup>* allele was a generous gift from Tina Tootle (University of Iowa). All UAS-RNAi *Drosophila* lines were purchased from Bloomington Drosophila Stock Center. UAS-RNAi constructs were driven specifically in the mesoderm using *twist-GAL4*, which drives expression in the mesoderm from stage 10 of embryonic development through stage 13 of embryonic development, *DMef2-GAL4* that drives expression in the muscles from stage 12 through adulthood, or *MHC-GAL4* which drives expression in muscle from stage 17 of embryonic development through adulthood.

### **4.5.2 Larval Locomotion Assay**

We performed a modified version of the previously used assay that has been used to measure larval locomotion in individual larvae (Louis et al., 2008). Virgins expressing *DMef2-GAL4* were mixed with males that carried the UAS-RNAi for 1 hour in a vial with standard *Drosophila* food. After 1 hour, adults were moved to a new vial and the embryos laid during the 1 hour period were aged for 5 days until they were L3 larvae. Larvae were

then floated from the food by the addition of 15% sucrose. Using a paintbrush, larvae were moved to a plate with wet yeast. After all of the genotypes had been collected, 10 larvae of each RNAi were moved to an arena that consisted of 3% agarose dyed black with standard food color poured over the top of a 96-well plate cover. Movement of larvae toward a stick dipped in ethyl butyrate was captured using an iPhone mounted above the arena. The speed of each larva was then analyzed using ImageJ.

### **4.5.3 Immunohistochemistry**

#### 4.5.3.1 Preparation of embryos

Embryos were collected at 25 °C and were dechorionated by submersion in 50% bleach for 4 min. Embryos were then fixed in a solution of equal parts heptane and 10% formalin (Sigma, Product # HT501128). Fixation lasted for 20 minutes during which time the embryos were placed on an orbital shaker that rotated at a rate of 250/min. Following fixation, the formalin and heptane were removed and replaced with a solution of equal parts methanol and heptane. The embryos were vortexed for 1 minute to devitellinize the embryos. Embryos were stored in methanol at -20 °C until immunostaining.

#### 4.5.3.2 Preparation of larvae.

Dissection of larvae was carried out as previously described (Metzger et al., 2012) with minor modifications. The primary difference being that the buffer used was modified to increase the preservation of muscle structure. The modified dissection buffer was 100 mM PIPES (Sigma-Aldrich, P6757), 115 mM D-Sucrose (Fisher Scientific, BP220-1), 5 mM Trehalose (Acros Organics, 182550250), 10 mM Sodium Bicarbonate (Fisher Scientific,

BP328-500), 75 mM Potassium Chloride (Fisher Scientific, P333-500), 4 mM Magnesium Chloride (Sigma-Aldrich, M1028) and 1 mM EGTA (Fisher Scientific, 28-071-G). Larvae were then fixed with 10% formalin (Sigma-Aldrich, HT501128) for 20 minutes. Briefly, dissection involved lateral cuts at the anterior and posterior end of the larva that encompassed 70% of larval circumference. These were followed by a longitudinal cut through the dorsal surface of the animal that connected the two lateral cuts. The intestines, other internal tissues, and neurons were then removed and the flaps of tissue composed of epidermis and muscle were pinned down and fixed. For fixation, larvae were incubated in a solution of 10% formalin in PBS for 20 minutes.

#### 4.5.3.3 Immunostaining

Staining of embryos and larvae was identical. Antibodies were used at the following dilutions: rabbit anti-dsRed (1:400, Clontech 632496), rat anti-tropomyosin (1:200, Abcam ab50567), mouse anti-GFP (1:50, Developmental Studies Hybridoma Bank GFP-G1), and mouse anti- $\alpha$ Tubulin (1:200, Sigma-Aldrich T6199). Conjugated fluorescent secondary antibodies used were Alexa Fluor 555 donkey-anti-rabbit (1:200), Alexa Fluor 488 donkey-anti-rat (1:200), and Alexa Fluor 647 donkey-anti-mouse (1:200) (all Life Technologies) and Alexa Fluor 488 donkey-anti-mouse (1:200, Life Technologies). Furthermore, Acti-stain 555 phalloidin (1:400, Cytoskeleton PHDH1-A) and Hoechst 33342 (1  $\mu$ g/ml) were used on larvae. Embryos and larvae were mounted in ProLong Gold (Life Technologies, P36930)

#### 4.5.3.4 Microscopy

All microscopy was performed on a Zeiss LSM700 with an oil-immersion 40X APOCHROMAT, 1.4 NA objective. All images of embryos were acquired with a 1.0-X optical zoom and images of larvae were acquired with a 0.5-X optical zoom. Image tiling was necessary to acquire images of the full larval muscles and was completed using the tiling function in the ZEN software that controls the microscope.

#### 4.5.3.5 Statistics

All statistics were performed using Graphpad Prism. All data sets were compared to appropriate controls by a Student's t-test. \*,  $p < 0.05$ ; \*\*,  $p < 0.01$ ; \*\*\*,  $p < 0.001$ ; \*\*\*\*,  $p < 0.0001$ .

### **4.5.4 Image Analysis**

#### 4.5.4.1 Analysis of nuclear position in larvae

Although the field has traditionally measured the distance between nuclei (Elhanany-Tamir et al., 2012; Folker et al., 2012; Metzger et al., 2012), this measurement does not account for changes in muscle size and nuclear number. We have therefore modified this measurement to determine how evenly nuclei are spaced within a muscle (Collins et al., 2017). First, the area and length of the muscle was measured. Next, the position and number of nuclei is calculated by using the multipoint tool in ImageJ to place a point in the center of each nucleus. The position of each nucleus is used to calculate the actual internuclear distance. The maximal internuclear distance is determined by taking the square root of the

muscle area divided by the nuclear number. This value represents the distance between nuclei, if internuclear distance was fully maximized. The ratio between the actual internuclear distance and the maximal internuclear distance ratio was then used to determine how evenly nuclei were distributed. This method allows us to essentially normalize the internuclear distance to both nuclear count and muscle area which leads to a more representative means of comparison between muscles, larvae and genotypes. All viable (not torn) ventral longitudinal (VL3) muscles were measured from each larva. At least four larvae from one experiment were measured for each genotype. Statistical analysis was performed with Prism 4.0 (GraphPad). Student's t-test was used to assess the statistical significance of differences in measurements between experimental genotypes and controls.

#### 4.5.4.2 Analysis of nuclear position in embryos

The position of nuclei was measured in stage 16 embryos. This is the latest stage before cuticle development blocks the ability to perform immunofluorescence microscopy. Embryos were staged based primarily on gut morphology as previously described (Folker et al., 2012). At stage 16, the nuclei are reliably positioned adjacent to the muscle ends, and disruptions in this positioning can be easily determined as previously described (Folker et al., 2012; Folker et al., 2014; Schulman et al., 2014). Images, acquired as described above, were processed as maximum intensity projections of confocal z-stacks using ImageJ. The position of the nuclei was determined by using the line function in ImageJ to measure the distance between either the dorsal end of the muscle and the nearest nucleus or the ventral end of the muscle and the nearest nucleus. All four LT muscles were

measured in four hemisegments from each embryo. At least 20 embryos from at least two independent experiments were measured for each genotype.

#### 4.5.4.3 Analysis of muscle length in embryos

The length of each of the 4 lateral transverse (LT) muscles was measured from the dorsal tip to the ventral tip using the multipoint tool in ImageJ as previously described (Folker et al., 2012). Data points indicate the average of the 4 LT muscles within a single hemisegment.

#### 4.5.4.4 Analysis of muscle size in larvae

The area of the VL3 muscles were measured using the multipoint tool in ImageJ as previously described (Folker et al., 2012). Data points indicate the size of an individual muscle

### **4.5.5 Analysis of general muscle architecture**

Qualitative muscle phenotype analysis was completed on embryos of each genotype. All analysis was based on the immunofluorescence staining pattern of Tropomyosin in stage 16 embryos. The frequency of the following phenotypes were scored: the number of free myoblasts in an embryo that indicated a defect indicating a defect in myoblast fusion (small, unfused circles stained by tropomyosin), and the number of muscles in each hemisegment (>4 defined as extra muscles, <4 defined as missing muscles) indicating gross abnormalities in the specification of muscle tissue. For analysis of unfused myoblasts, embryos were grouped into bins with a width of 5 and the first bin centered on zero.

## **Chapter 5:**

### **Discussion**

#### **5.1 Summary and Significance**

The aim of this thesis was to understand the mechanisms that regulate myonuclear positioning within the context of muscle disease. Data presented in this thesis provide a better understanding of how nuclei become mispositioned in distinct muscle diseases and demonstrates advantages of using *Drosophila* skeletal muscle as an *in vivo* model to understand muscle development and the impact of disease-linked genes to muscle disease pathologies.

##### **5.1.1 Nuclear positioning is regulated by distinct mechanisms in different muscle diseases**

Chapter 2 investigated the different mechanisms by which nuclear positioning is disrupted in the muscle diseases Emery-Dreifuss Muscular Dystrophy and Centronuclear Myopathy. First, we showed that genes linked to EDMD and CNM impacted *Drosophila* skeletal muscle function when disrupted. Furthermore, these defects in muscle function correlated with mispositioning of nuclei in larval muscles. Nuclear positioning defects were most severe when either the EDMD-linked genes, *bocksbeutel* or *klarsicht*, or the CNM-linked gene, *amphiphysin*, were disrupted. Nuclei were strictly single-file within the center of the muscle in larvae where *bocks* or *klar* were disrupted. However, nuclei were clustered in some regions while in other regions nuclei were single-file in larval muscles

in which *amph* was disrupted. From this data, we proposed that nuclear positioning is disrupted by distinct mechanisms in EDMD and CNM.

Our hypothesis was supported by genetic interactions and microtubule imaging, which clearly demonstrate that EDMD- and CNM-linked genes have distinct genetic interactions and distinct impacts on microtubule organization. Genetic interactions were carried out between the EDMD- and CNM-linked genes and the microtubule motors, Dynein and Kinesin. While genetic interactions regulating nuclear positioning were detected between *bocks* and the microtubule motors, no genetic interactions were detected between *amph* and the microtubule motors. Furthermore, microtubule imaging showed that microtubules become polarized in muscles where *bocks* or *klar* were disrupted, while some nuclei lacked microtubules emanating from them in muscles where *amph* was disrupted. Taken together, this study is the first to demonstrate that mispositioned nuclei arise from distinct mechanisms in disparate muscle diseases.

### **5.1.2 *Drosophila* Emerin homologs regulate nuclear positioning by distinct mechanisms and impact nuclear positioning in contrasting manners**

Expanding upon our initial study, Chapter 3 investigated the mechanisms through which EDMD-linked genes regulate nuclear movement and positioning throughout *Drosophila* muscle development. First, we showed that disruption of the EDMD-linked gene *koi* recapitulated the larval nuclear positioning defects caused by *bocks* and *klar*. Furthermore, disruption of the EDMD-linked gene *ote* also led to larval nuclear positioning defects. However, the nuclear positioning phenotypes were distinct, with nuclei being too close to the edge of the muscle when Otefin was disrupted and nuclei aligning in the center

of the muscle when *bocks*, *klar* or *koi* were disrupted. Differences in nuclear positioning phenotypes also manifested during embryonic muscle development. When *bocks*, *klar* or *koi* were disrupted nuclei failed to separate into two clusters. While in embryos where *ote* was disrupted nuclei dissociated from their clusters more readily, leading to central nuclei that were not associated with either nuclear cluster. Furthermore, we demonstrated that the two *emerin* homologs, *bock* and *ote*, have opposing effects on nuclear levels of Klarsicht, indicating nuclear positioning can be disrupted not only by the loss of LINC complex components but also increases in LINC complex components. This led to the hypothesis that the two *emerin* homologs were working through independent mechanisms to regulate myonuclear positioning.

Our hypothesis was supported by genetic interactions and qPCR experiments, which demonstrated that *ote* works by regulating Klarsicht at the transcriptional level while *bocks* regulated Klarsicht localization. Furthermore, disruption of *ote* could rescue the nuclear positioning phenotypes caused by a disruption in *bocks*. Together, these data demonstrated, for the first time, that although the expression and localization of Klarsicht are regulated by Emerin, in *Drosophila* the two functions are divided among the two *Drosophila emerin* homologs, *bocksbeutel* and *otefin*.

### **5.1.3 *Drosophila* larval mobility phenotypes are effective in screening for novel regulators of muscle development and function.**

Chapter 4 presented adaptations to an existing assay to increase the throughput of the assay and make it a more efficient screening tool for novel regulators of muscle function and development. Utilizing this adapted assay and muscle-specific depletion of 82 genes,

we identified 12 genes that impacted muscle function. Furthermore, of the 12 genes identified, we found that the disruption of five genes decreased muscle function while the disruption of seven genes increased muscle function. The strongest screen hit, Fascin, caused a significant decrease in larval locomotion when disrupted by RNAi. Functional characterization of *fascin* in muscle development showed a decrease in the number of muscles present, a decrease in the number of nuclei within muscles and muscles with disrupted myotendinous junctions. Together, these data demonstrated the strength of *Drosophila* larval locomotion as a tool for identifying novel regulators of muscle development and function. Furthermore, the data in this chapter implicates Fascin, for the first time, in embryonic muscle development.

## **5.2 Broader Impact and Future Directions**

### **5.2.1 Distinct mechanisms underlie the nuclear positioning phenotypes present in EDMD and CNM**

In Chapter 2, we demonstrated that although mispositioned nuclei are present in models of both EDMD and CNM, nuclear positioning is regulated by distinct mechanisms that are disrupted in each disease. This distinction is important for the understanding of the effects of nuclear positioning on muscle health, as patients with EDMD and CNM can experience disease-associated muscle phenotypes that are unique to each disease. Therefore, these data suggest that nuclear positioning phenotypes, and the mechanisms underlying them, should not be treated similarly. Instead, further identification of the molecular mechanisms impacted by each disease should be investigated individually.

The LINC complex-dependent mechanism that is proposed in this chapter is dependent on Dynein and Kinesin, as evident by the positive genetic interactions. However, Dynein and Kinesin have been implicated in multiple nuclear movement and positioning mechanisms. Therefore, further investigation is needed to pinpoint which established mechanisms are LINC complex-dependent. Additionally, for the CNM-linked gene *amphiphysin*, the impact on microtubule organization and nucleation is of particular interest. In *amph* mutant larva, some nuclei fail to nucleate microtubules. These same nuclei are often elongated and reside deeper in the muscle between myofibrils rather than being positioned at the periphery and above the sarcomere. The unique characteristics of these nuclei suggest that nuclei are not able to position out at the periphery of the muscle and instead remain within the muscle center or nuclei that are unable to nucleate microtubules are unable to maintain their peripheral localization and sink back into the myofibrils. Nonetheless, why these nuclei are unable to nucleate microtubules and whether centrosomal proteins that normally get relocated to the nucleus during muscle development are affected in muscles with disrupted CNM-linked genes is unclear. However, further investigation into the differences between nuclei that are able to nucleate microtubules and those that are unable could inform us more about the mechanisms leading to mispositioned nuclei in CNM.

### **5.2.2 Distinct Emerin function's impact on disease-relevant phenotypes**

In Chapter 3, we demonstrated that although *bocksbeutel* and *otefin* are both *Drosophila* homologs of *emerin*, they each have distinct impacts on the levels of nuclear localized Klarsicht. Upon further investigation, the mechanical and transcriptional

regulatory functions of emerin are divided between Bocksbeutel and Otefin. This isolation of emerin functions makes *Drosophila* a unique model system to further investigate the impacts of emerin's transcriptional regulatory role independent of its mechanical role and vice versa.

With regards to the opposing roles of Bocksbeutel and Otefin in the regulation of nuclear movement and positioning in skeletal muscle, the mechanisms underlying the impacts on nuclear levels of Klarsicht are only beginning to be understood. Although *bocks* genetically interacted with *klar* to regulate nuclear positioning, no genetic interaction was detected between *bocks* and *koi*. However, disruption of *bocks*, *klar* and *koi* all share similar nuclear positioning phenotypes. It is possible that the interaction between *bocks* and *koi* is indirect, previous studies have noted an impact on lamin organization in *bocks* mutants and *koi* binds directly to lamins. This highlights the need for further investigation into the mechanism by which Bocksbeutel regulates Klarsicht localization, possibly through impacts on lamin organization, are necessary. Additionally, although we demonstrated that Otefin regulates nuclear levels of Klarsicht at the transcriptional level, the direct mechanism remains unclear. Further investigation into the localization of the *klar* locus as well as the binding of transcription factors in the presence and absence of Otefin could provide valuable insight into Otefin's role in transcriptional regulation of the LINC complex.

These data demonstrating that both increases and decreases in LINC complex components lead to disruptions in nuclear positioning suggest a high level of regulation governs proper nuclear positioning in skeletal muscle. It is important to realize that two KASH-domain containing proteins exist in *Drosophila* and although both have been

implicated in nuclear positioning, the exact contribution toward nuclear positioning for each is not fully defined. It is possible that an increase or decrease in one of these LINC complex components could shift the balance of contributions from each KASH-domain containing protein. Alternatively, it is possible that a decrease in LINC complex components disrupts the ability to transduce force onto the nucleus. While an increase in LINC complex components may saturate binding sites of partner LINC complex components causing excess LINC complex components to be localized to other compartments that are contiguous to the nuclear envelope, such as the ER and Golgi. This mispositioning of LINC complex components could lead to an imbalance in forces upon the nucleus, leading to the premature dissociation of nuclei from the cluster or mispositioning relative to the muscle edge as seen in embryos and larvae, respectively.

### **5.2.3 A sensitive screening assay for novel regulators of muscle development and function**

In Chapter 4, we developed high-throughput screening assay to screen for novel regulators of muscle development and function. Although previous screens for regulators of muscle development have been completed using adult locomotion and embryonic muscle structure, these methods have their drawbacks. While testing adult locomotion is fairly easy, genes that are lethal during pupation are untestable. Furthermore, testing embryonic musculature is rather labor intensive but is able to test genes that are not viable as adults. By adapting a larval tracking protocol, we have developed a simple assay that combines the ease in labor of adult locomotion assays with the ability to screen many genes that are lethal in later stages of development. In the future, this assay could be easily utilized

to identify genetic modifiers of larval locomotion phenotypes, such as those in larva with disruptions in EDMD- and CNM-linked genes.

### 5.3 Concluding Remarks

Although the phenomena of nuclear movement and positioning have been observed and noted in various cell types for many decades, recent scientific advancements have facilitated our understanding of mechanisms governing the process. In this thesis we provide a framework to further our understanding of the mechanisms regulating nuclear movement and positioning as well as muscle development as a whole. This thesis demonstrates a time-efficient high-throughput screening assay to identify novel regulators of muscle development and function, we provide robust and quantitative novel cellular analysis techniques to characterize the impact of disrupting these novel regulators and we utilize molecular analysis techniques to determine the mechanisms underlying these cellular disruptions. These functional, cellular and molecular techniques could be utilized to further our understanding of the molecular mechanisms impacted by distinct muscular disease. Genetic modifiers of disease-specific phenotypes could be identified using the groundwork laid out in this thesis to further incorporate novel contributors to existing mechanisms or identify proteins that multiple genetic pathways regulating nuclear movement and positioning converge upon. Nonetheless, this thesis helps to establish *Drosophila* as a powerful *in vivo* model for the correlation between mispositioned nuclei and muscle function, while providing novel insight into the mechanisms regulating nuclear movement and positioning and highlighting the importance of studying the impact of disease-linked genes on myonuclear positioning, muscle development and muscle health.

## Appendix:

### A1: Chapter 4 – Supplemental Table

**Supplemental Table A1.1:** Muscle disease-linked mutants utilized.

Gene	Mutant	Allele Class	Molecular Defect
<i>amph</i>	<i>amph</i> <sup>26</sup>	Hypomorph	Deletion removing the entire first exon of Amph (Razzaq et al., 2001)
<i>bocks</i>	<i>bocks</i> <sup>DP01391</sup>	Unreported	P-element insertion (Staudt et al., 2005)
<i>klar</i>	<i>klar</i> <sup>1</sup>	Loss of Function	Nonsense point mutation (Welte et al., 1998)
<i>ote</i>	<i>ote</i> <sup>DB</sup>	Amorphic	Nonsense point mutation (Barton et al., 2013)
	<i>ote</i> <sup>B279</sup>	Unreported	P-element insertion (Jiang et al., 2008)
<i>koi</i>	<i>koi</i> <sup>EY03560</sup>	Unreported	P-element insertion (Technau and Roth, 2008)

**Supplemental Table A1.2:** All of the data acquired during the limited RNAi-based screen for regulators of muscle function.

Drivers	TRiP	Data Count	Minute 3 Speed	Minute 3 St.Dev	t-test
DMef2Gal4	mCh	9	0.484318519	0.197186589	
DMef2Gal4	Alk	11	0.330749311	0.070968181	0.05135355
DMef2Gal4	eyg	10	0.449525	0.093293016	0.63848877
DMef2Gal4	not	18	0.389675	0.223676971	0.27603277
DMef2Gal4	Nup75	16	0.606995833	0.143446012	0.12554894
DMef2Gal4	slou	10	0.467798333	0.145316198	0.83963965
DMef2Gal4	tin	19	0.486021053	0.151405086	0.98208623
DMef2Gal4	jar	18	0.444092593	0.126288438	0.58797649
DMef2Gal4	N	10	0.603808333	0.126876691	0.14400199
DMef2Gal4	nwk	14	0.451880952	0.134326988	0.67215023
DMef2Gal4	Tollo	19	0.583319298	0.135580375	0.19896387
DMef2Gal4	Shot	14	0.462590476	0.123988125	0.77285928
DMef2Gal4	bnl	1	0.629933333		
DMef2Gal4	Myd88	9	0.780703623	0.237116199	0.00209739
DMef2Gal4	shu	23	0.572036232	0.102891172	0.23399634
DMef2Gal4	unc	15	0.652436667	0.07272363	0.0353297
DMef2Gal4	Cac	23	0.557966667	0.120771273	0.31903586

DMef2Gal4	wupA	22	0.708602273	0.128675018	0.00935297
DMef2Gal4	Nup98-96	21	0.650319841	0.220300923	0.05744977
DMef2Gal4	Tre1	23	0.675723913	0.165144242	0.02329149
DMef2Gal4	Rac1	18	0.52365	0.113874947	0.59092904
DMef2Gal4	Vang	20	0.531365833	0.132941847	0.52720872
DMef2Gal4	wg	16	0.722467708	0.143763863	0.0073269
DMef2Gal4	sn	21	0.146266667	0.036393413	0.00084398
DMef2Gal4	if	19	0.656307895	0.171997361	0.04156853
DMef2Gal4	Him	20	0.4544925	0.138091105	0.68871839
DMef2Gal4	Apc	23	0.561425362	0.134842061	0.30373954
DMef2Gal4	Egfr	15	0.500688889	0.200547194	0.84718063
DMef2Gal4	mael	23	0.356563043	0.110694421	0.09644317
DMef2Gal4	smo	22	0.500797727	0.080826131	0.81374364
DMef2Gal4	vvl	23	0.429733333	0.123181669	0.45622448
DMef2Gal4	Insc	4	0.463504167	0.141333184	0.83454401
DMef2Gal4	Chc	23	0.3222	0.100393582	0.041446468
DMef2Gal4	Nup214	23	0.262912319	0.066661251	0.009695968
DMef2Gal4	mus	23	0.428624638	0.118652987	0.44556685
DMef2Gal4	mbl	23	0.429234783	0.120445489	0.45113419
DMef2Gal4	Rbf	23	0.511402899	0.131314596	0.71097455
DMef2Gal4	Dys	15	0.313902222	0.140440293	0.040962822
DMef2Gal4	Akt1	14	0.479138095	0.084186984	0.94204412
DMef2Gal4	lac	20	0.369674167	0.121764046	0.1357798
DMef2Gal4	Max	10	0.398453333	0.132995847	0.28995135
DMef2Gal4	tsr	21	0.60314127	0.192961358	0.14888353
DMef2Gal4	Imp	6	0.418377778	0.115305357	0.42953098
DMef2Gal4	raps	6	0.357316667	0.078412133	0.1096662
DMef2Gal4	Mer	23	0.237402899	0.101337394	0.005290206
DMef2Gal4	phl	22	0.334489394	0.158406138	0.06456794
DMef2Gal4	foxB25997	10	0.409451667	0.11495148	0.3376516
DMef2Gal4	lid	12	0.321336111	0.107364126	0.045408071
DMef2Gal4	hh	13	0.546273077	0.125833648	0.42076512
DMef2Gal4	Cg25C	22	0.534558333	0.176463681	0.5182251
DMef2Gal4	SoxN	1	0.246083333		
DMef2Gal4	Nup154	3	0.221783333	0.046176666	0.004250752
DMef2Gal4	lms	23	0.508844928	0.107727273	0.73139874
DMef2Gal4	Nup133	21	0.491593651	0.153817524	0.92305429
DMef2Gal4	E2F	8	0.595639583	0.172774985	0.23380661

DMef2Gal4	Mad	23	0.493397101	0.133237569	0.90106191
DMef2Gal4	Scaf	23	0.55526087	0.151029677	0.34979557
DMef2Gal4	ea	22	0.512959091	0.153990532	0.70339249
DMef2Gal4	beat-la	22	0.430246212	0.185709234	0.49244434
DMef2Gal4	nmo	23	0.52343913	0.127320692	0.59235881
DMef2Gal4	p53	23	0.603881159	0.111936406	0.11700875
DMef2Gal4	mtm	23	0.630017391	0.151591664	0.06914109
DMef2Gal4	Dsor1	23	0.539943478	0.126565183	0.44931508
DMef2Gal4	Tsc1	23	0.636095652	0.159494709	0.06111673
DMef2Gal4	Myo3DF	19	0.592053509	0.12566915	0.16102503
DMef2Gal4	Nos	9	0.545481481	0.11753778	0.4384215
DMef2Gal4	foxB23	23	0.579510145	0.105786192	0.20017617
DMef2Gal4	rhea	15	0.626348889	0.130691324	0.07805901
DMef2Gal4	nau	15	0.592858889	0.111738888	0.15834268
DMef2Gal4	Nup50	21	0.425521429	0.13026535	0.42887561
DMef2Gal4	betaTub56D	20	0.524993333	0.139955583	0.5868077
DMef2Gal4	Ote	23	0.44444058	0.151559329	0.59463405
DMef2Gal4	Koi	11	0.428819697	0.15752762	0.50402665
DMef2Gal4	Klar	23	0.581669565	0.191922776	0.22605245
DMef2Gal4	LamC	10	0.562736667	0.117337754	0.31812136
DMef2Gal4	Act5C	Lethal			
DMef2Gal4	Vrp1	Lethal			
DMef2Gal4	Twi	Lethal			
DMef2Gal4	Imp	Lethal			
DMef2Gal4	Nup153	Lethal			
DMef2Gal4	Nup160	Lethal			
DMef2Gal4	Wit	Lethal			
DMef2Gal4	Wts	Lethal			
DMef2Gal4	Vkg	Lethal			

## A2: Additional Experiments

**A2.1 *Bocksbeutel* and *klarsicht* genetically interacts with components of the cortical pathway to regulate larval nuclear positioning.**

Microtubules have been implicated in many mechanisms of nuclear movement. In Chapter 2, we found that *bocks* genetically interacted with *dynein* and *kinesin* and was necessary for proper microtubule organization. In Chapter 3, we found that *bocks* and *klar* genetically interacted to regulate nuclear positioning in both embryonic and larval muscles, while *ote* regulated nuclear positioning through an alternate genetic pathway. Therefore, we hypothesized that *bocks* and *klar* would genetically interact with components of the cortical pathway to regulate nuclear positioning while *ote* would not. To evaluate genetic interactions and nuclear positioning in larvae, larvae were dissected, fixed, stained, mounted and imaged as described in Section 2.5.3 and 2.5.4. All stocks were grown under standard condition at 25°C. Stocks used were *bocks*<sup>DP01391</sup> (21846; Bloomington *Drosophila* Stock Center), *klar*<sup>l</sup> (3256; Bloomington *Drosophila* Stock Center), *ote*<sup>DB</sup> (5092; Bloomington *Drosophila* Stock Center), *clip190*<sup>KG06490</sup> (14493; Bloomington *Drosophila* Stock Center) and *raps*<sup>193</sup> (6491; Bloomington *Drosophila* Stock Center)

In *clip190*<sup>KG06490/+</sup>; *bocks*<sup>DP01391/+</sup> doubly heterozygous larvae, nuclei formed a single-line positioned in the center of the muscle, parallel to the long axis of the muscle. This phenotype was absent from each of the individual heterozygotes, although some regions of *bocks*<sup>DP01391/+</sup> single heterozygote larval muscles contained single-file nuclei (Fig. A2.1A). Quantitatively, the internuclear distance ratio was significantly reduced in *clip190*<sup>KG06490/+</sup>; *bocks*<sup>DP01391/+</sup> doubly heterozygous larval muscles compared to either individual heterozygote (Fig. A2.1B). Similar phenotypes were seen in *clip190*<sup>KG06490/+</sup>; *klar*<sup>l/+</sup> doubly heterozygous larvae, with a more nuclei positioned within the center of the muscle in a single-file line than in either of the individual heterozygotes (Fig. A2.1C). Quantitatively, the internuclear distance ratio was significantly reduced in *clip190*<sup>KG06490/+</sup>;

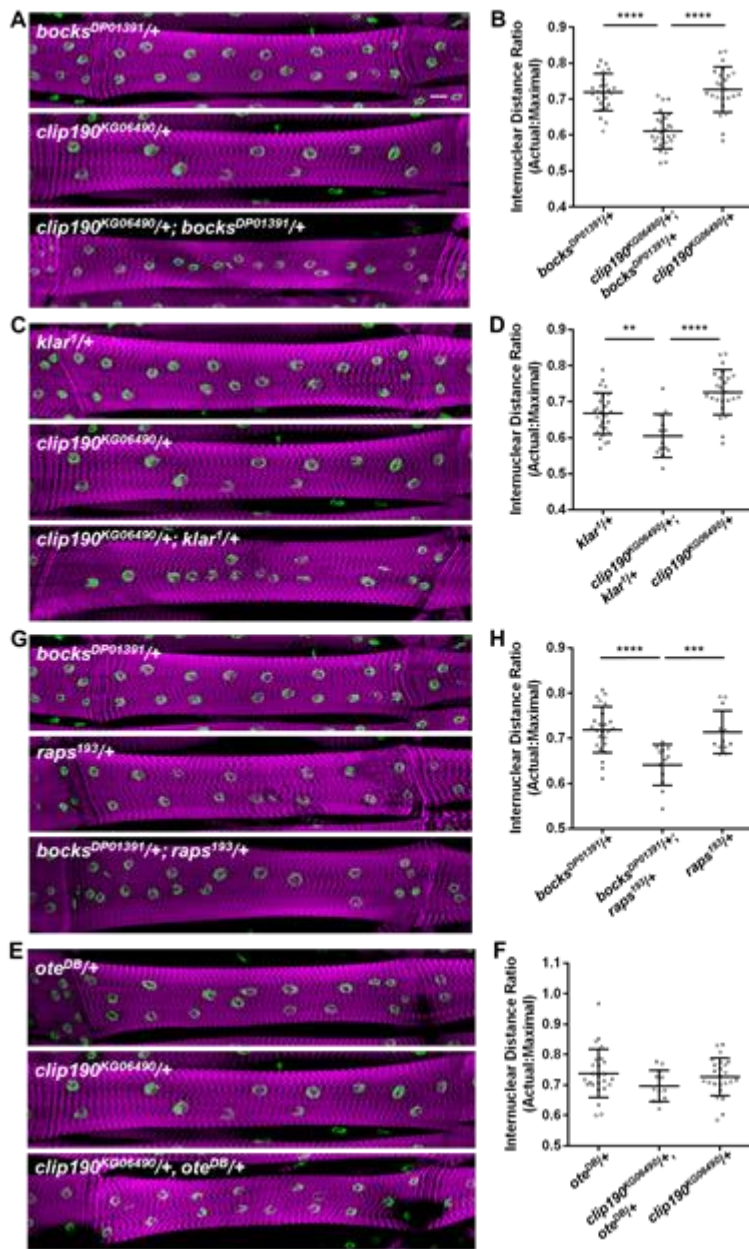


**Figure A2.1** *Bocksbeutel* and *klarsicht* genetically interacts with components of the cortical pathway to regulate larval nuclear positioning. (A,C,E,G) Immunofluorescence projection images of VL3 muscles from dissected L3 larvae of the indicated genotype. Magenta, Phalloidin/muscles; green, Hoechst/nuclei. Scale bar, 25  $\mu$ m. (B,D,F,G) The ratio of actual internuclear distance to maximal internuclear distance in larval muscles from the indicated genotypes. Data points indicate the average value for the internuclear distance ratio for all nuclei within a single VL3 muscle. Error bars indicate the SD from at least 12 VL3 muscles. Student's t-test were used for comparison to controls. \*\*p < 0.01, \*\*\*p < 0.001, \*\*\*\*p < 0.0001.

*klar<sup>1/+</sup>* doubly heterozygous larval muscles compared to either individual heterozygote (Fig. A2.1D). No genetic interaction was found between *ote<sup>DB</sup>* and *clip190<sup>KG06490</sup>* in larval muscles (Fig. A2.1E,F).

A genetic interaction was also found between *bocks* and *raps*. In *bocks<sup>DP01391/+</sup>*, *raps<sup>193/+</sup>* doubly heterozygous larvae, nuclei formed a single-line positioned in the center of the muscle, parallel to the long axis of the muscle in some regions of the muscle.

Although some regions of *bocks*<sup>DP01391/+</sup> single heterozygote larval muscles contained single-file nuclei, the occurrence of this phenotype was increased in *bocks*<sup>DP01391/+</sup>, *raps*<sup>193/+</sup> doubly heterozygous larvae (Fig. A2.1G). Quantitatively, the internuclear distance ratio was significantly reduced in *bocks*<sup>DP01391/+</sup>, *raps*<sup>193/+</sup> doubly heterozygous larval muscles compared to either individual heterozygote (Fig. A2.1H).

## A2.2 Disruption of the cis-Golgi matrix protein gene, *GM130*, impacts nuclear positioning in *Drosophila* larvae.

Recently, the Golgi complex has been implicated in the regulation of nuclear positioning in muscle in mouse cells. However, little evidence exists in other model organisms. We hypothesize that the Golgi complex is also a regulator of nuclear positioning in *Drosophila* skeletal muscle. To evaluate the Golgi complex as a regulator of nuclear positioning, we disrupted *GM130* in larvae. Larvae were dissected, fixed,

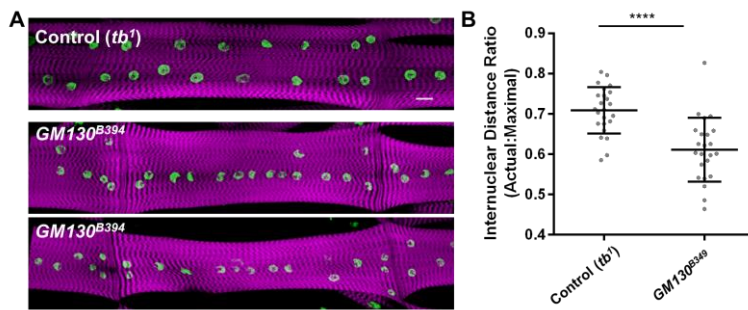


**Figure A2.2** *GM130* is necessary for proper myonuclear positioning in *Drosophila* larvae. (A) Immunofluorescence projection images of VL3 muscles from dissected L3 larvae of the indicated genotype. Magenta, Phalloidin/muscles; green, Hoechst/nuclei. Scale bar, 25  $\mu$ m. (B) The ratio of actual internuclear distance to maximal internuclear distance in larval muscles from the indicated genotypes. Data points indicate the average value for the internuclear distance ratio for all nuclei within a single VL3 muscle. Error bars indicate the SD from at least 12 VL3 muscles. Student's t-test were used for comparison to controls. \*\*\*\* $p < 0.0001$ .

stained, mounted and imaged as described in Section 2.5.3 and 2.5.4. All stocks were grown under standard condition at 25°C. Stocks used were *tb*<sup>1</sup> (120; Bloomington *Drosophila* Stock Center), *GM130*<sup>B394</sup> (16211; Bloomington *Drosophila* Stock Center).

In *tb<sup>1</sup>* controls, nuclei were typically positioned in two parallel lines on the long axis of the muscle of the muscle (Fig. A2.2A) with an internuclear ratio of 70% of maximal (Fig. A2.2B). In *GMI30<sup>B394</sup>* larvae, nuclei formed a single-file line in the center of the muscle similar to the phenotypes seen in *bocks<sup>DP01391</sup>*, *klar<sup>1</sup>* and *koi<sup>EY03560</sup>* mutants (Fig. A2.2A). In *GMI30<sup>B394</sup>* mutants, this leads to significant reduction in the internuclear distance ratio to 65% of maximal (Fig. A2.2B).

## REFERENCES

- Abmayr, S. M. and Pavlath, G. K.** (2012). Myoblast fusion: Lessons from flies and mice. *Development* **139**, 641–656.
- Al-Qusairi, L., Weiss, N., Toussaint, A., Berbey, C., Messaddeq, N., Kretz, C., Sanoudou, D., Beggs, A. H., Allard, B., Mandel, J. L., et al.** (2009). T-tubule disorganization and defective excitation-contraction coupling in muscle fibers lacking myotubularin lipid phosphatase. *Proc. Natl. Acad. Sci. U. S. A.* **106**, 18763–18768.
- Almonacid, M. and Paoletti, A.** (2010). Mechanisms controlling division-plane positioning. *Semin. Cell Dev. Biol.* **21**, 874–880.
- Amoasii, L., Hnia, K. and Laporte, J.** (2012). Myotubularin phosphoinositide phosphatases in human diseases. In *Phosphoinositides and Disease*, pp. 209–233.
- Artero, R. D., Castanon, I. and Baylies, M. K.** (2001). The immunoglobulin-like protein hibris functions as a dose-dependent regulator of myoblast fusion and is differentially controlled by Ras and Notch signaling. *Development* **128**, 4251–4264.
- Ashery-Padan, R., Weiss, A. M., Femstein, N. and Gruenbaum, Y.** (1997). Distinct regions specify the targeting of otefin to the nucleoplasmic side of the nuclear envelope. *J. Biol. Chem.* **272**, 2493–2499.
- Ashery-Padan, R., Ulitzur, N., Arbel, A., Goldberg, M., Weiss, A. M., Maus, Na., Fisher, P. A. and Gruenbaum, Y.** (2015). Localization and posttranslational modifications of otefin, a protein required for vesicle attachment to chromatin, during *Drosophila melanogaster* development. *Mol. Cell. Biol.* **17**, 4114–4123.
- Auld, A. L. and Folker, E. S.** (2016). Nucleus-dependent sarcomere assembly is mediated by the LINC complex. *Mol. Biol. Cell* **27**, 2351–2359.
- Auld, A. L., Collins, M. A., Mandigo, T. R. and Folker, E. S.** (2018a). High-Resolution Imaging Methods to Analyze LINC Complex Function During *Drosophila* Muscle Development. *Methods Mol. Biol.* **1840**, 181–203.
- Auld, A. L., Roberts, S. A., Murphy, C. B., Camuglia, J. M. and Folker, E. S.** (2018b). Aplip1, the *Drosophila* homolog of JIP1, regulates myonuclear positioning and muscle stability. *J. Cell Sci.* **131**,.
- Aumailley, M. and Smyth, N.** (1998). The role of laminins in basement membrane function. *J. Anat.* **193**, 1–21.
- Bao, Z. Z., Lakonishok, M., Kaufman, S. and Horwitz, A. F.** (1993). A7B1 Integrin Is a Component of the Myotendinous Junction on Skeletal Muscle. *J. Cell Sci.* **106**, 579–589.
- Barton, L. J., Pinto, B. S., Wallrath, L. L. and Geyer, P. K.** (2013). The *drosophila* nuclear lamina protein otefin is required for germline stem cell survival. *Dev. Cell* **25**, 645–654.
- Barton, L. J., Wilmington, S. R., Martin, M. J., Skopec, H. M., Lovander, K. E., Pinto, B. S. and Geyer, P. K.** (2014). Unique and shared functions of nuclear lamina LEM domain proteins in *Drosophila*. *Genetics* **197**, 653–665.
- Barton, L. J., Duan, T., Ke, W., Luttinger, A., Lovander, K. E., Soshnev, A. A. and Geyer, P. K.** (2018). Nuclear lamina dysfunction triggers a germline stem cell checkpoint. *Nat. Commun.* **9**,.
- Baye, L. M. and Link, B. A.** (2008). Nuclear migration during retinal development. *Brain*

*Res.* **1192**, 29–36.

- Beckett, K. and Baylies, M. K.** (2007). 3D analysis of founder cell and fusion competent myoblast arrangements outlines a new model of myoblast fusion. *Dev. Biol.* **309**, 113–125.
- Bione, S., Maestrini, E., Rivella, S., Mancini, M., Regis, S., Romeo, G. and Toniolo, D.** (1994). Identification of a novel X-linked gene responsible for Emery- Dreifuss muscular dystrophy Silvia. *Nat. Genet.* **8**, 323–327.
- Bitoun, M., Maugenre, S., Jeannet, P. Y., Lacène, E., Ferrer, X., Laforêt, P., Martin, J. J., Laporte, J., Lochmüller, H., Beggs, A. H., et al.** (2005). Mutations in dynamin 2 cause dominant centronuclear myopathy. *Nat. Genet.* **37**, 1207–1209.
- Blondeau, F., Laporte, J., Bodin, S., Superti-furga, G., Payrastre, B., Mandel, J., Génétique, I. De, Biologie, D., Ulp, C. I., Fries, L., et al.** (2000). Myotubularin , a phosphatase deficient in myotubular myopathy , acts on phosphatidylinositol 3-kinase and phosphatidylinositol 3-phosphate pathway. **9**, 2223–2230.
- Boissy, P., Saltel, F., Bouniol, C., Jurdic, P. and Machuca-gayet, I.** (2002). Transcriptional Activity of Nuclei in Multinucleated Osteoclasts and Its Modulation by Calcitonin. **143**, 1913–1921.
- Bonne, G., Di Barletta, M. R., Varnous, S., Bécane, H. M., Hammouda, E. H., Merlini, L., Muntoni, F., Greenberg, C. R., Gary, F., Urtizbera, J. A., et al.** (1999). Mutations in the gene encoding lamin A/C cause autosomal dominant Emery-Dreifuss muscular dystrophy. *Nat. Genet.* **21**, 285–288.
- Bonne, G., Yaou, R. Ben, Beroud, C., Boriani, G., Brown, S., Visser, M. De, Duboc, D., Ellis, J., Hausmanowa-petrusewicz, I., Lattanzi, G., et al.** (2003). 108th ENMC International Workshop , 3rd Workshop of the MYO-CLUSTER project : EUROMEN , 7th International Emery-Dreifuss Muscular Dystrophy ( EDMD ) Workshop. *Neuromuscul. Disord.* **13**, 508–515.
- Bothe, I., Deng, S. and Baylies, M.** (2014). PI(4,5)P2 regulates myoblast fusion through Arp2/3 regulator localization at the fusion site. *Dev.* **141**, 2289–2301.
- Bour, B. A., Chakravarti, M., West, J. M. and Abmayr, S. M.** (2000). Drosophila SNS, a member of the immunoglobulin superfamily that is essential for myoblast fusion. *Genes Dev.* **14**, 1498–1511.
- Boyle, S., Gilchrist, S., Bridger, J. M., Mahy, N. L., Ellis, J. A. and Bickmore, W. A.** (2001). The spatial organization of human chromosomes within the nuclei of normal and emerin-mutant cells. *Hum. Mol. Genet.* **10**, 211–219.
- Brand, A. H. and Perrimon, N.** (1993). Targeted gene expression as a means of altering cell fates and generating dominant phenotypes. *Development* **118**, 401–15.
- Brendza, K. M., Rese, D. J., Gilbert, S. P. and Saxton, W. M.** (1999). Lethal kinesin mutations reveal amino acids important for ATPase activation and structural coupling. *J. Biol. Chem.* **274**, 31506–31514.
- Brown, N. H.** (2000). Cell-cell adhesion via the ECM: Integrin genetics in fly and worm. *Matrix Biol.* **19**, 191–201.
- Brown, N. H., Gregory, S. L. and Martin-Bermudo, M. D.** (2000). Integrins as mediators of morphogenesis in Drosophila. *Dev. Biol.* **223**, 1–16.
- Bruusgaard, J. C., Liestøl, K., Ekmark, M., Kollstad, K. and Gundersen, K.** (2003). Number and spatial distribution of nuclei in the muscle fibres of normal mice studied

in vivo. *J. Physiol.* **551**, 467–478.

- Bruusgaard, J. C., Liestø, K. and Gundersen, K.** (2006). Distribution of myonuclei and microtubules in live muscle fibers of young, middle-aged, and old mice. *J. Appl. Physiol.* **100**, 2024–2030.
- Bryan, J., Edwards, R., Matsudaira, P., Otto, J. and Wulfschlegel, J.** (1993). Fascin, an echinoid actin-bundling protein, is a homolog of the *Drosophila* singed gene product. *Proc. Natl. Acad. Sci. U. S. A.* **90**, 9115–9119.
- Cadot, B., Gache, V., Vasyutina, E., Falcone, S., Birchmeier, C. and Gomes, E. R.** (2012). Nuclear movement during myotube formation is microtubule and dynein dependent and is regulated by Cdc42, Par6 and Par3. *Nat. Publ. Gr.* **13**, 741–74989.
- Cadot, B., Gache, V. and Gomes, E. R.** (2015). Moving and positioning the nucleus in skeletal muscle—one step at a time. *Nucleus* **6**, 373–381.
- Cai, M., Huang, Y., Ghirlando, R., Wilson, K. L., Craigie, R. and Clore, G. M.** (2001). Solution structure of the constant region of nuclear envelope protein LAP2 reveals two LEM-domain structures: One binds BAF and the other binds DNA. *EMBO J.* **20**, 4399–4407.
- Capers, C. R.** (1960). Multinucleation of skeletal muscle in vitro. *J. Biophys. Biochem. Cytol.* **7**, 559–66.
- Chang, W., Folker, E. S., Worman, H. J. and Gundersen, G. G.** (2013). Emerin organizes actin flow for nuclear movement and centrosome orientation in migrating fibroblasts. *Mol. Biol. Cell* **24**, 3869–80.
- Chapman, M. a, Zhang, J., Banerjee, I., Guo, L. T., Zhang, Z., Shelton, G. D., Ouyang, K., Lieber, R. L. and Chen, J.** (2014). Disruption of both nesprin 1 and desmin results in nuclear anchorage defects and fibrosis in skeletal muscle. *Hum. Mol. Genet.* **23**, 1–14.
- Chen, E. H. and Olson, E. N.** (2001). Antisocial, an Intracellular Adaptor Protein, Is Required for Myoblast Fusion in *Drosophila*. *Dev. Cell* **1**, 705–715.
- Chen, E. H., Pryce, B. A., Tzeng, J. A., Gonzalez, G. A. and Olson, E. N.** (2003). Control of myoblast fusion by a guanine nucleotide exchange factor, loner, and its effector ARF6. *Cell* **114**, 751–762.
- Cheresh, D. A. and Mecham, R. P.** (1994). *Integrins: molecular and biological responses to the extracellular matrix.*
- Chin, Y. H., Lee, A., Kan, H. W., Laiman, J., Chuang, M. C., Hsieh, S. T. and Liu, Y. W.** (2015). Dynamin-2 mutations associated with centronuclear myopathy are hypermorphic and lead to T-tubule fragmentation. *Hum. Mol. Genet.* **24**, 5542–5554.
- Chiquet, M. and Fambrough, D. M.** (1984). Chick myotendinous antigen. I. A monoclonal antibody as a marker for tendon and muscle morphogenesis. *J. Cell Biol.* **98**, 1926–1936.
- Collins, M. A., Mandigo, T. R., Camuglia, J. M., Vazquez, G. A., Anderson, A. J., Hudson, C. H., Hanron, J. L. and Folker, E. S.** (2017). Emery–Dreifuss muscular dystrophy–linked genes and centronuclear myopathy–linked genes regulate myonuclear movement by distinct mechanisms. *Mol. Biol. Cell* **28**, 2303–2317.
- Cowling, B. S., Toussaint, A., Amoasii, L., Koebel, P., Ferry, A., Davignon, L., Nishino, I., Mandel, J. L. and Laporte, J.** (2011). Increased expression of wild-type or a centronuclear myopathy mutant of dynamin 2 in skeletal muscle of adult mice

- leads to structural defects and muscle weakness. *Am. J. Pathol.* **178**, 2224–2235.
- Crisp, M., Liu, Q., Roux, K., Rattner, J. B., Shanahan, C., Burke, B., Stahl, P. D. and Hodzic, D.** (2006). Coupling of the nucleus and cytoplasm: Role of the LINC complex. *J. Cell Biol.* **172**, 41–53.
- D’Alessandro, M., Hnia, K., Gache, V., Koch, C., Gavriilidis, C., Rodriguez, D., Nicot, A., Romero, N. B., Schwab, Y., Gomes, E., et al.** (2015). Amphiphysin 2 Orchestrates Nucleus Positioning and Shape by Linking the Nuclear Envelope to the Actin and Microtubule Cytoskeleton. *Dev. Cell* **35**, 186–198.
- Del Bene, F.** (2011). Interkinetic nuclear migration: Cell cycle on the move. *EMBO J.* **30**, 1676–1677.
- Demmerle, J., Koch, A. J. and Holaska, J. M.** (2012). The nuclear envelope protein emerin binds directly to histone deacetylase 3 (HDAC3) and activates HDAC3 activity. *J. Biol. Chem.* **287**, 22080–22088.
- Deng, S., Bothe, I. and Baylies, M. K.** (2015). The Formin Diaphanous Regulates Myoblast Fusion through Actin Polymerization and Arp2/3 Regulation. *PLoS Genet.* **11**, 1–29.
- Deng, S., Bothe, I. and Baylies, M.** (2016). Diaphanous regulates SCAR complex localization during *Drosophila* myoblast fusion. *Fly (Austin)*. **10**, 178–186.
- Deroyer, C., Réner, A., Merville, M., Deroyer, C., Réner, A., Merville, M. and Fillet, M.** (2014). New role for the EMD (emerin), a key inner nuclear membrane protein, as an enhancer of autophagosome formation in the C16-ceramide autophagy pathway. *Autophagy* **8627**,.
- Dialynas, G., Speese, S., Budnik, V., Geyer, P. K. and Wallrath, L. L.** (2010). The role of *Drosophila* Lamin C in muscle function and gene expression. *Development* **137**, 3067–3077.
- Ding, Z. Y., Wang, Y. H., Huang, Y. C., Lee, M. C., Tseng, M. J. and Chi, Y. H.** (2017). Outer nuclear membrane protein Kuduk modulates the LINC complex and nuclear envelope architecture. **216**,.
- Dobi, K. C., Schulman, V. K. and Baylies, M. K.** (2015). Specification of the somatic musculature in *Drosophila*. *Wiley Interdiscip. Rev. Dev. Biol.* **4**, 357–375.
- Dubowitz, V., Sewry, C. A., Oldfors, A. and Lane, R.** (2007a). *Muscle biopsy: a practical approach*. Elsevier Health Sciences.
- Dubowitz, V., Sewry, C. A. and Lane, R.** (2007b). Definition of pathological changes seen in muscle biopsies. In *Muscle Biopsy: A Practical Approach*, pp. 231–358. Philadelphia, PA: Elsevier Limited.
- Dundon, S. E. R., Chang, S. S., Kumar, A., Occhipinti, P., Shroff, H., Roper, M. and Gladfelter, A. S.** (2016). Clustered nuclei maintain autonomy and nucleocytoplasmic ratio control in a syncytium. *Mol. Biol. Cell* **27**, 2000–2007.
- Elhanany-Tamir, H., Yu, Y. V., Shnyder, M., Jain, A., Welte, M. and Volk, T.** (2012). Organelle positioning in muscles requires cooperation between two KASH proteins and microtubules. *J. Cell Biol.* **198**, 833–846.
- Emery, A. E. H.** (2000). Emery ± Dreifuss muscular dystrophy ± a 40 year retrospective. **10**, 228–232.
- Emery, A. E. and Dreifuss, F. E.** (1966). Unusual type of benign x-linked muscular dystrophy. *J. Neurol. Neurosurg. Psychiatry* **29**, 338–342.

- Erickson, M. R. S., Galletta, B. J. and Abmayr, S. M.** (1997). *Drosophila* myoblast city Encodes a Conserved Protein That Is Essential for Myoblast Fusion, Dorsal Closure, and Cytoskeletal Organization. *Cell* **138**, 589–603.
- Espigat-Georger, A., Dyachuk, V., Chemin, C., Emorine, L. and Merdes, A.** (2016). Nuclear alignment in myotubes requires centrosome proteins recruited by nesprin-1. *J. Cell Sci.* **129**, 4227–4237.
- Falcone, S., Roman, W., Hnia, K., Gache, V., Didier, N., Auradé, F., Marty, I., Nishino, I., Charlet-berguerand, N., Romero, B., et al.** (2014). N-WASP is required for Amphiphysin-2/BIN1-dependent nuclear positioning and triad organization in skeletal muscle and is involved in the pathophysiology of centronuclear myopathy. *Embo Mol.* **6**, 1455–1475.
- Ferguson, S. M. and Camilli, P. De** (2012). Dynamin, a membrane-remodelling GTPase. *Nat. Rev. Mol. Cell Biol.* **13**, 75–88.
- Finlan, L. E., Sproul, D., Thomson, I., Boyle, S., Kerr, E., Perry, P., Ylstra, B., Chubb, J. R. and Bickmore, W. A.** (2008). Recruitment to the nuclear periphery can alter expression of genes in human cells. *PLoS Genet.* **4**,.
- Flucher, B. E., Takekura, H. and Franzini-Armstrong, C.** (1993). Development of the Excitation-Contraction Coupling Apparatus in Skeletal Muscle: Association of Sarcoplasmic Reticulum and Transverse Tubules with Myofibrils. *Dev. Biol.* **160**, 135–147.
- Folker, E. S. and Baylies, M. K.** (2013). Nuclear positioning in muscle development and disease. *Front. Physiol.* **4** DEC.,.
- Folker, E. S., Schulman, V. K. and Baylies, M. K.** (2012). Muscle length and myonuclear position are independently regulated by distinct Dynein pathways. *Development* **139**, 3827–3837.
- Folker, E. S., Schulman, V. K. and Baylies, M. K.** (2014). Translocating myonuclei have distinct leading and lagging edges that require Kinesin and Dynein. *Development* **141**, 355–366.
- Furukawa, K., Sugiyama, S., Osouda, S., Goto, H., Inagaki, M., Horigome, T., Omata, S., McConnell, M., Fisher, P. A. and Nishida, Y.** (2003). Barrier-to-autointegration factor plays crucial roles in cell cycle progression and nuclear organization in *Drosophila*. *J. Cell Sci.* **116**, 3811–3823.
- Gache, V., Gomes, E. R. and Cadot, B.** (2017). Microtubule motors involved in nuclear movement during skeletal muscle differentiation. *Mol. Biol. Cell* **28**, 865–874.
- Gepner, J., Li, M. G., Ludmann, S., Kortas, C., Boylan, K., Iyadurai, S. J. P., McGrail, M. and Hays, T. S.** (1996). Cytoplasmic dynein function is essential in *Drosophila melanogaster*. *Genetics* **142**, 865–878.
- Gibbs, E. M., Davidson, A. E., Telfer, W. R., Feldman, E. L. and Dowling, J. J.** (2014). The myopathy-causing mutation DNM2-S619L leads to defective tubulation in vitro and in developing zebrafish. *DMM Dis. Model. Mech.* **7**, 157–161.
- Gibeaux, R., Politi, A. Z., Philippsen, P. and Nédélec, F.** (2017). Mechanism of nuclear movements in a multinucleated cell. *Mol. Biol. Cell* **28**, 645–660.
- Gimona, M., Buccione, R., Courtneidge, S. A. and Linder, S.** (2008). Assembly and biological role of podosomes and invadopodia. *Curr. Opin. Cell Biol.* **20**, 235–241.
- Gimpel, P., Lee, Y. L., Sobota, R. M., Burke, B., Cadot, B., Gomes, E. R., Gimpel, P.,**

- Lee, Y. L., Sobota, R. M., Calvi, A., et al. (2017). Nesprin-1  $\alpha$ -Dependent Microtubule Nucleation from the Nuclear Envelope via Akap450 Is Necessary for Nuclear Positioning in Muscle Cells Report Nesprin-1  $\alpha$ -Dependent Microtubule Nucleation from the Nuclear Envelope via Akap450 Is Necessary for Nuclear Po. 1–11.
- Gomes, E. R., Jani, S. and Gundersen, G. G. (2005). Nuclear movement regulated by Cdc42, MRCK, myosin, and actin flow establishes MTOC polarization in migrating cells. *Cell* **121**, 451–463.
- Grady, R. M., Starr, D. a, Ackerman, G. L., Sanes, J. R. and Han, M. (2005). Syne proteins anchor muscle nuclei at the neuromuscular junction. *Proc. Natl. Acad. Sci. U. S. A.* **102**, 4359–4364.
- Groen, C. M., Jayo, A., Parsons, M. and Tootle, T. L. (2015). Prostaglandins regulate nuclear localization of Fascin and its function in nucleolar architecture. *Mol. Biol. Cell* **26**, 1901–1917.
- Guelen, L., Pagie, L., Brassat, E., Meuleman, W., Faza, M. B., Talhout, W., Eussen, B. H., de Klein, A., Wessels, L., de Laat, W., et al. (2008). Domain organization of human chromosomes revealed by mapping of nuclear lamina interactions. *Nature* **453**, 948–51.
- Guilluy, C. and Burridge, K. (2015). Nuclear mechanotransduction: Forcing the nucleus to respond. *Nucleus* **6**, 19–22.
- Gundersen, G. G. and Worman, H. J. (2013). Nuclear positioning. *Cell* **152**, 1376–1389.
- Haque, F., Lloyd, D. J., Smallwood, D. T., Dent, C. L., Shanahan, C. M., Fry, A. M., Trembath, R. C. and Shackleton, S. (2006). SUN1 Interacts with Nuclear Lamin A and Cytoplasmic Nesprins To Provide a Physical Connection between the Nuclear Lamina and the Cytoskeleton. *Mol. Cell. Biol.* **26**, 3738–3751.
- Haque, F., Mazzeo, D., Patel, J. T., Smallwood, D. T., Ellis, J. a., Shanahan, C. M. and Shackleton, S. (2010). Mammalian SUN protein interaction networks at the inner nuclear membrane and their role in laminopathy disease processes. *J. Biol. Chem.* **285**, 3487–3498.
- Harris, A. J., Duxson, M. J., Fitzsimons, R. B. and Rieger, F. (1989). Myonuclear birthdates distinguish the origins of primary and secondary myotubes in embryonic mammalian skeletal muscles. *Development* **107**, 771–784.
- Hashimoto, Y., Kim, D. J. and Adams, J. C. (2011). The Roles of the Proprotein Convertases in Health and Disease”. *Clin. Res.* 4574–4574.
- Holaska, J. M. and Wilson, K. L. (2007). An emerin “Proteome”: Purification of distinct emerin-containing complexes from HeLa cells suggests molecular basis for diverse roles including gene regulation, mRNA splicing, signaling, mechanosensing, and nuclear architecture. *Biochemistry* **46**, 8897–8908.
- Holaska, J. M., Lee, K. K., Kowalski, A. K. and Wilson, K. L. (2003). Transcriptional repressor germ cell-less (GCL) and barrier to autointegration factor (BAF) compete for binding to emerin in vitro. *J. Biol. Chem.* **278**, 6969–6975.
- Holaska, J. M., Rais-Bahrami, S. and Wilson, K. L. (2006). Lmo7 is an emerin-binding protein that regulates the transcription of emerin and many other muscle-relevant genes. *Hum. Mol. Genet.* **15**, 3459–3472.
- Hu, Y., Sopko, R., Foos, M., Kelley, C., Flockhart, I., Ammeux, N., Wang, X., Perkins,

- L., Perrimon, N. and Mohr, S. E.** (2013). FlyPrimerBank: An Online Database for *Drosophila melanogaster* Gene Expression Analysis and Knockdown Evaluation of RNAi Reagents. *Genes|Genomes|Genetics* **3**, 1607–1616.
- Iyer, S. R., Shah, S. B., Valencia, A. P., Schneider, M. F., Hernandez-Ochoa, E. O., Stains, J. P., Blemker, S. S. and Lovering, R. M.** (2016). Altered nuclear dynamics in MDX myofibers. *J. Appl. Physiol.* jap.00857.2016.
- James, N. G., Digman, M. A., Ross, J. A., Barylko, B., Wang, L., Li, J., Chen, Y., Mueller, J. D., Gratton, E., Albanesi, J. P., et al.** (2014). A mutation associated with centronuclear myopathy enhances the size and stability of dynamin 2 complexes in cells. *Biochim. Biophys. Acta* **1840**, 315–321.
- Jayo, A., Malboubi, M., Antoku, S., Chang, W., Ortiz-Zapater, E., Groen, C., Pfisterer, K., Tootle, T., Charras, G., Gundersen, G. G., et al.** (2016). Fascin Regulates Nuclear Movement and Deformation in Migrating Cells. *Dev. Cell* **38**, 371–383.
- Jiang, X., Xia, L., Chen, D., Yang, Y., Huang, H., Yang, L., Zhao, Q., Shen, L., Wang, J. and Chen, D.** (2008). Otefin, a Nuclear Membrane Protein, Determines the Fate of Germline Stem Cells in *Drosophila* via Interaction with Smad Complexes. *Dev. Cell* **14**, 494–506.
- Jungbluth, H., Zhou, H., Sewry, C. A., Robb, S., Treves, S., Bitoun, M., Guicheney, P., Buj-Bello, A., Bönnemann, C. and Muntoni, F.** (2007). Centronuclear myopathy due to a de novo dominant mutation in the skeletal muscle ryanodine receptor (RYR1) gene. *Neuromuscul. Disord.* **17**, 338–345.
- Kelly, A. M. and Zacks, S. I.** (1969). The histogenesis of rat intercostal muscle. *J. Cell Biol.* **42**, 135–153.
- Kenniston, J. A. and Lemmon, M. A.** (2010). Dynamin GTPase regulation is altered by PH domain mutations found in centronuclear myopathy patients. *EMBO J.* **29**, 3054–3067.
- Kim, J. H., Ren, Y., Ng, W. P., Li, S., Son, S., Kee, Y. S., Zhang, S., Zhang, G., Fletcher, D. A., Robinson, D. N., et al.** (2015a). Mechanical Tension Drives Cell Membrane Fusion. *Dev. Cell* **32**, 561–573.
- Kim, J. H., Jin, P., Duan, R. and Chen, E. H.** (2015b). Mechanisms of myoblast fusion during muscle development. *Curr. Opin. Genet. Dev.* **32**, 162–170.
- Kojima, H., Sakuma, E., Mabuchi, Y., Mizutani, J., Horiuchi, O., Wada, I., Horiba, M., Yamashita, Y., Herbert, D. C., Soji, T., et al.** (2008). Ultrastructural changes at the myotendinous junction induced by exercise. *J. Orthop. Sci.* **13**, 233–239.
- Kotak, S. and Gönczy, P.** (2013). Mechanisms of spindle positioning: Cortical force generators in the limelight. *Curr. Opin. Cell Biol.* **25**, 741–748.
- Kramer, S. G., Kidd, T., Simpson, J. H. and Goodman, C. S.** (2001). Switching repulsion to attraction: Changing responses to slit during transition in mesoderm migration. *Science (80-)*. **292**, 737–740.
- Laguri, C., Gilquin, B., Wolff, N., Romi-Lebrun, R., Courchay, K., Callebaut, I., Worman, H. J. and Zinn-Justin, S.** (2001). Structural characterization of the LEM motif common to three human inner nuclear membrane proteins. *Structure* **9**, 503–511.
- Laporte, J., Hu, L. J., Kretz, C., Mandel, J., Kioschis, P., Coy, J. F., Klauck, S. M.,**

- Poustka, A. and Dahl, N.** (1996). A gene mutated in X-linked myotubular myopathy defines a new putative tyrosine phosphatase family conserved in yeast. *Nat. Genet.* **13**, 175–182.
- Lee, K. K., Haraguchi, T., Lee, R. S., Koujin, T., Hiraoka, Y. and Wilson, K. L.** (2001). Distinct functional domains in emerin bind lamin A and DNA-bridging protein BAF. *J. Cell Sci.* **114**, 4567–4573.
- Lei, K., Zhang, X., Ding, X., Guo, X., Chen, M., Zhu, B., Xu, T., Zhuang, Y., Xu, R. and Han, M.** (2009). SUN1 and SUN2 play critical but partially redundant roles in anchoring nuclei in skeletal muscle cells in mice. *Proc. Natl. Acad. Sci. U. S. A.* **106**, 10207–10212.
- Liechti-Gallati, S., Müller, B., Grimm, T., Kress, W., Müller, C., Boltshauser, E., Moser, H. and Braga, S.** (1991). X-linked centronuclear myopathy: Mapping the gene to Xq28. *Neuromuscul. Disord.* **1**, 239–245.
- Lin, F., Blake, D. L., Callebaut, I., Skerjanc, I. S., Holmer, L., McBurney, M. W., Paulin-Levasseur, M. and Worman, H. J.** (2000). MAN1, an inner nuclear membrane protein that shares the LEM domain with lamina-associated polypeptide 2 and emerin. *J. Biol. Chem.* **275**, 4840–4847.
- Liu, J., Tom, †, Ben-Shahar, R., Riemer, D., Treinin, M., Spann, P., Weber, K., Fire, A. and Gruenbaum, Y.** (2000). Essential Roles for *Caenorhabditis elegans* Lamin Gene in Nuclear Organization, Cell Cycle Progression, and Spatial Organization of Nuclear Pore Complexes. *Mol. Biol. Cell* **11**, 3937–3947.
- Liu, J., Lee, K. K., Segura-Totten, M., Neufeld, E., Wilson, K. L. and Gruenbaum, Y.** (2003). MAN1 and emerin have overlapping function(s) essential for chromosome segregation and cell division in *Caenorhabditis elegans*. *Proc. Natl. Acad. Sci. U. S. A.* **100**, 4598–4603.
- Lombardi, M. L., Jaalouk, D. E., Shanahan, C. M., Burke, B., Roux, K. J. and Lammerding, J.** (2011). The interaction between nesprins and sun proteins at the nuclear envelope is critical for force transmission between the nucleus and cytoskeleton. *J. Biol. Chem.* **286**, 26743–26753.
- Louis, M., Huber, T., Benton, R., Sakmar, T. P. and Vossahl, L. B.** (2008). Bilateral olfactory sensory input enhances chemotaxis behavior. *Nat. Neurosci.* **11**, 187–199.
- Maeda, K., Nakata, T., Noda, Y., Sato-Yoshitake, R. and Hirokawa, N.** (1992). Interaction of dynamin with microtubules: Its structure and GTPase activity investigated by using highly purified dynamin. *Mol. Biol. Cell* **3**, 1181–1194.
- Manilal, S., Man, N., Sewry, C. A. and Morris, G. E.** (1996). The Emery – Dreifuss muscular dystrophy protein, emerin, is a nuclear membrane protein. **5**, 801–808.
- Mansharamani, M. and Wilson, K. L.** (2005). Direct binding of nuclear membrane protein MAN1 to emerin in vitro and two modes of binding to barrier-to-autointegration factor. *J. Biol. Chem.* **280**, 13863–13870.
- Margalit, A., Segura-Totten, M., Gruenbaum, Y. and Wilson, K. L.** (2005). Barrier-to-autointegration factor is required to segregate and enclose chromosomes within the nuclear envelope and assemble the nuclear lamina. *Proc. Natl. Acad. Sci. U. S. A.* **102**, 3290–3295.
- Markiewicz, E., Tilgner, K., Barker, N., Wetering, M. Van De, Clevers, H., Dorobek, M., Hausmanowa-petrusewicz, I., Ramaekers, F. C. S., Broers, J. L. V,**

- Blankesteyn, W. M., et al.** (2006). The inner nuclear membrane protein Emerin regulates  $\beta$ -catenin activity by restricting its accumulation in the nucleus. 3275–3285.
- McNiven, M. A.** (2013). Breaking away: Matrix remodeling from the leading edge. *Trends Cell Biol.* **23**, 16–21.
- Meinke, P., Nguyen, T. D. and Wehnert, M. S.** (2011). The LINC complex and human disease. *Biochem. Soc. Trans.* **39**, 1693–1697.
- Meinke, P., Mattioli, E., Haque, F., Antoku, S., Columbaro, M., Wehnert, M. and Shackleton, S.** (2014). Muscular Dystrophy-Associated SUN1 and SUN2 Variants Disrupt Nuclear-Cytoskeletal Connections and Myonuclear Organization. **10**,.
- Metzger, T., Gache, V., Xu, M., Cadot, B., Folker, E. S., Richardson, B. E., Gomes, E. R. and Baylies, M. K.** (2012). MAP and kinesin-dependent nuclear positioning is required for skeletal muscle function. *Nature* **484**, 120–124.
- Minc, N., Burgess, D. and Chang, F.** (2011). Influence of cell geometry on division-plane positioning. *Cell* **144**, 414–426.
- Mislow, J. M. K., Holaska, J. M., Kim, M. S., Lee, K. K., Segura-totten, M., Wilson, K. L. and McNally, E. M.** (2002). Nesprin-1a self-associates and binds directly to emerin and lamin A in vitro. *FEBS J.* **525**, 135–140.
- Montes De Oca, R., Lee, K. K. and Wilson, K. L.** (2005). Binding of barrier to autointegration factor (BAF) to histone H3 and selected linker histones including H1.1. *J. Biol. Chem.* **280**, 42252–42262.
- Nagano, A., Koga, R., Ogawa, M., Kurano, Y., Kawada, J., Okadas, R., Hayashi, Y. K., Tsukahara, T. and Arahata, K.** (1996). Emerin deficiency at the nuclear membrane in patients with Emery-Dreifuss muscular dystrophy. *Nat. Genet.* **12**, 254–259.
- Navarro, A. P., Collins, M. A. and Folker, E. S.** (2016). The nucleus is a conserved mechanosensation and mechanoresponse organelle. *Cytoskeleton* **73**, 59–67.
- Nicot, A. S. and Laporte, J.** (2008). Endosomal phosphoinositides and human diseases. *Traffic* **9**, 1240–1249.
- Nicot, A. S., Toussaint, A., Tosch, V., Kretz, C., Wallgren-Pettersson, C., Iwarsson, E., Kingston, H., Garnier, J. M., Biancalana, V., Oldfors, A., et al.** (2007). Mutations in amphiphysin 2 (BIN1) disrupt interaction with dynamin 2 and cause autosomal recessive centronuclear myopathy. *Nat. Genet.* **39**, 1134–1139.
- Ordan, E. and Volk, T.** (2015). A non-signaling role of robo2 in tendons is essential for slit processing and muscle patterning. *Dev.* **142**, 3512–3518.
- Paterson, J. and O’Hare, K.** (1991). Structure and transcription of the singed locus of *Drosophila melanogaster*. *Genetics* **129**, 1073–1084.
- Patterson, K., Molofsky, A. B., Robinson, C., Acosta, S., Cater, C. and Fischer, J. A.** (2004). The functions of klarsicht and nucleolar lamin in developmentally regulated nuclear migrations of photoreceptor cells in *Drosophila* eye. *Mol. Biol. Cell* **15**, 600–610.
- Peric-Hupkes, D., Meuleman, W., Pagie, L., Bruggeman, S. W. M., Solovei, I., Brugman, W., Gräf, S., Flicek, P., Kerkhoven, R. M., van Lohuizen, M., et al.** (2010). Molecular Maps of the Reorganization of Genome-Nuclear Lamina Interactions during Differentiation. *Mol. Cell* **38**, 603–613.
- Pfaff, J., Rivera Monroy, J., Jamieson, C., Rajanala, K., Vilardi, F., Schwappach, B.,**

- Kehlenbach, R. H., Abell, B. M., Pool, M. R., Schlenker, O., et al.** (2016). Emery-Dreifuss muscular dystrophy mutations impair TRC40-mediated targeting of emerin to the inner nuclear membrane. *J. Cell Sci.* **129**, 502–16.
- Pickersgill, H., Kalverda, B., De Wit, E., Talhout, W., Fornerod, M. and Van Steensel, B.** (2006). Characterization of the *Drosophila melanogaster* genome at the nuclear lamina. *Nat. Genet.* **38**, 1005–1014.
- Pinto, B. S., Wilmington, S. R., Hornick, E. E. L., Wallrath, L. L. and Geyer, P. K.** (2008). Tissue-specific defects are caused by loss of the *drosophila* MAN1 LEM domain protein. *Genetics* **180**, 133–145.
- Prokop, A., Martín-Bermudo, M. D., Bate, M. and Brown, N. H.** (1998). Absence of PS integrins or laminin affects extracellular adhesion, but not intracellular assembly, of hemiadherens and neuromuscular junctions in *Drosophila* embryos. *Dev. Biol.* **196**, 58–76.
- Ralston, E., Ploug, T., Kalhovde, J. and Lomo, T.** (2001). Golgi complex, endoplasmic reticulum exit sites, and microtubules in skeletal muscle fibers are organized by patterned activity. *J. Neurosci.* **21**, 875–883.
- Ramsey, R. W. and Street, S. F.** (1940). The isometric length-tension diagram of isolated skeletal muscle fibers of the frog. *J. Cell. and Comp. Physiol.* **15**, 11–34.
- Razzaq, A., Robinson, I. M., McMahon, H. T., Skepper, J. N., Su, Y., Zelfhof, A. C., Jackson, A. P., Gay, N. J. and Kane, C. J. O.** (2001). Amphiphysins 1 and 2 are enriched in the mammalian brain and are proposed to recruit dynamin to sites of endocytosis. Shorter amphiphysin 2 splice variants are also found ubiquitously, with an enrichment in skeletal muscle. *Genes Dev.* 2967–2979.
- Reddy, K. L., Zullo, J. M., Bertolino, E. and Singh, H.** (2008). Transcriptional repression mediated by repositioning of genes to the nuclear lamina. *Nature* **452**, 243–7.
- Richardson, B. E., Beckett, K., Nowak, S. J. and Baylies, M. K.** (2007). SCAR/WAVE and Arp2/3 are crucial for cytoskeletal remodeling at the site of myoblast fusion. *Development* **134**, 4357–67.
- Richardson, B., Beckett, K. and Baylies, M.** (2008). Visualizing new dimensions in *Drosophila* myoblast fusion. *BioEssays* **30**, 423–431.
- Roman, W. and Gomes, E. R.** (2018). Nuclear positioning in skeletal muscle. *Semin. Cell Dev. Biol.* **82**, 51–56.
- Roman, W., Martins, J. P., Carvalho, F. A., Voituriez, R., Abella, J. V. G., Santos, N. C., Cadot, B., Way, M. and Gomes, E. R.** (2017). Myofibril contraction and crosslinking drive nuclear movement to the periphery of skeletal muscle. *Nat. Cell Biol.* **19**, 1189–1201.
- Romero, N. B.** (2010). Neuromuscular Disorders Centronuclear myopathies : A widening concept. *Neuromuscul. Disord.* **20**, 223–228.
- Rossi, S. G., Vazquez, A. E. and Rotundo, R. L.** (2000). Local Control of Acetylcholinesterase Gene Expression in Multinucleated Skeletal Muscle Fibers : Individual Nuclei Respond to Signals from the Overlying Plasma Membrane. **20**, 919–928.
- Rowat, A. C., Lammerding, J. and Ipsen, J. H.** (2006). Mechanical Properties of the Cell Nucleus and the Effect of Emerin Deficiency. *Biophys. J.* **91**, 4649–4664.

- Ruiz-Gómez, M.** (1998). Muscle patterning and specification in *Drosophila*. *Int. J. Dev. Biol.* **42**, 283–290.
- Ruiz-Gómez, M., Coutts, N., Price, A., Taylor, M. V. and Bate, M.** (2000). *Drosophila* dumbfounded: A myoblast attractant essential for fusion. *Cell* **102**, 189–198.
- Salpingidou, G., Smertenko, A., Hausmanowa-Petrucewicz, I., Hussey, P. J. and Hutchison, C. J.** (2007). A novel role for the nuclear membrane protein emerlin in association of the centrosome to the outer nuclear membrane. *J. Cell Biol.* **178**, 897–904.
- Schnorrer, F., Kalchauer, I. and Dickson, B. J.** (2007). The Transmembrane Protein Kon-tiki Couples to Dgrip to Mediate Myotube Targeting in *Drosophila*. *Dev. Cell* **12**, 751–766.
- Schnorrer, F., Schönbauer, C., Langer, C. C. H., Dietzl, G., Novatchkova, M., Schernhuber, K., Fellner, M., Azaryan, A., Radolf, M., Stark, A., et al.** (2010). Systematic genetic analysis of muscle morphogenesis and function in *Drosophila*. *Nature* **464**, 287–291.
- Schulman, V. K., Folker, E. S., Rosen, J. N. and Baylies, M. K.** (2014). Syd/JIP3 and JNK Signaling Are Required for Myonuclear Positioning and Muscle Function. *PLoS Genet.* **10**, e1004880.
- Schweitzer, R., Zelzer, E. and Volk, T.** (2010). Connecting muscles to tendons: Tendons and musculoskeletal development in flies and vertebrates (*Development* **137** (2807–2817)). *Development* **137**, 3347.
- Sens, K. L., Zhang, S., Jin, P., Duan, R., Zhang, G., Luo, F., Parachini, L. and Chen, E. H.** (2010). An invasive podosome-like structure promotes fusion pore formation during myoblast fusion. *J. Cell Biol.* **191**, 1013–1027.
- Sewry, C. A., Brown, S. C., Mercuri, E., Bonne, G., Feng, L., Camici, G., Morris, G. E. and Muntoni, F.** (2001). Skeletal muscle pathology in autosomal dominant Emery-Dreifuss muscular dystrophy with lamin A/C mutations. *Neuropathol. Appl. Neurobiol.* **27**, 281–290.
- Shaw, S. L., Maddox, P., Skibbens, R. V., Yeh, E., Salmon, E. D. and Bloom, K.** (1998). Nuclear and spindle dynamics in budding yeast. *Mol. Biol. Cell* **9**, 1627–1631.
- Sher, J. H., Rimalovski, A. B., Athanassiades, T. J. and Aronson, S. M.** (1967). Familial centronuclear myopathy. *Neurology* **17**, 727 LP – 727.
- Shpetner, H. S. and Vallee, R. b.** (1989). Identification of Dynamin, a Novel Mechanochemical Enzyme that mediates interactions between microtubules. *Cell* **59**, 421–432.
- Sosa, B. A., Rothballer, A., Kutay, U. and Schwartz, T. U.** (2012). LINC Complexes Form by Binding of Three KASH Peptides to Domain Interfaces of Trimeric SUN Proteins. *Cell* **149**, 1035–1047.
- Spiro, A., Shy, G. and Gonatas, N.** (1966). Myotubular myopathy: Persistence of fetal muscle in an adolescent boy. *Arch. Neurol.* **14**, 1–14.
- Starr, D. A. and Fischer, J. A.** (2005). KASH 'n Karry: The KASH domain family of cargo-specific cytoskeletal adaptor proteins. *BioEssays* **27**, 1136–1146.
- Starr, D. a and Han, M.** (2002). Role of ANC-1 in tethering nuclei to the actin cytoskeleton. *Science* **298**, 406–409.
- Staudt, N., Molitor, A., Somogyi, K., Mata, J., Curado, S., Eulenberg, K., Meise, M.,**

- Siegmund, T., Häder, T., Hilfiker, A., et al.** (2005). Gain-of-function screen for genes that affect *Drosophila* muscle pattern formation. *PLoS Genet.* **1**, 0499–0506.
- Strünkelnberg, M., Bonengel, B., Moda, L. M., Hertenstein, A., Gert de Couet, H., Ramos, R. G. P. and Fischbach, K. F.** (2001). Rst and its paralogue kirre act redundantly during embryonic muscle development in *Drosophila*. *Development* **128**, 4229–4239.
- Sung, H. H., Telley, I. A., Papadaki, P., Ephrussi, A., Surrey, T. and Rørth, P.** (2008). *Drosophila* Enscosin Promotes Productive Recruitment of Kinesin-1 to Microtubules. *Dev. Cell* **15**, 866–876.
- Tan, K. L., Haelterman, N. A., Kwartler, C. S., Lin, G., Milewicz, D. M., Bellen, H. J., Tan, K. L., Haelterman, N. A., Kwartler, C. S., Regalado, E. S., et al.** (2018). Ari-1 Regulates Myonuclear Organization Together with Parkin and Is Associated with Aortic Aneurysms Article Ari-1 Regulates Myonuclear Organization Together with Parkin and Is Associated with Aortic Aneurysms. *Dev. Cell* **45**, 226-244.e8.
- Tanabe, K. and Takei, K.** (2009). Dynamic instability of microtubules requires dynamin 2 and is impaired in a Charcot-Marie-Tooth mutant. **185**, 939–948.
- Tapley, E. C. and Starr, D. A.** (2013). Connecting the nucleus to the cytoskeleton by SUN–KASH bridges across the nuclear envelope. *Curr. Opin. Cell Biol.* **25**, 57–62.
- Tassin, A. M., Maro, B. and Bornens, M.** (1985). Fate of microtubule-organizing centers during myogenesis in vitro. *J. Cell Biol.* **100**, 35–46.
- Taylor, G. S., Maehama, T. and Dixon, J. E.** (2000). Myotubularin, a protein tyrosine phosphatase mutated in myotubular myopathy, dephosphorylates the lipid second messenger, phosphatidylinositol 3-phosphate. *Proc. Natl. Acad. Sci. U. S. A.* **97**, 8910–8915.
- Technau, M. and Roth, S.** (2008). The *Drosophila* KASH domain proteins Msp-300 and Klarsicht and the SUN domain protein klaroid have no essential function during oogenesis. *Fly (Austin)*. **2**, 82–91.
- Ten Hoopen, R., Cepeda-García, C., Fernández-Arruti, R., Juanes, M. A., Delgehr, N. and Segal, M.** (2012). Mechanism for astral microtubule capture by cortical Bud6p priming spindle Polarity in *S. cerevisiae*. *Curr. Biol.* **22**, 1075–1083.
- Tidball, J. G. and Lin, C.** (1989). Structural changes at the myoneic cell surface during the formation of myotendinous junctions. *Cell Tissue Res.* **257**, 77–84.
- Tilgner, K., Wojciechowicz, K., Jahoda, C., Hutchison, C. and Markiewicz, E.** (2009). Dynamic complexes of A-type lamins and emerin influence adipogenic capacity of the cell via nucleocytoplasmic distribution of  $\beta$ -catenin. *J. Cell Sci.* **122**, 401–413.
- Tran, P. T., Marsh, L., Doye, V., Inoué, S. and Chang, F.** (2001). A mechanism for nuclear positioning in fission yeast based on microtubule pushing. *J. Cell Biol.* **153**, 397–411.
- Valdivia, M., Vega-Macaya, F. and Olguín, P.** (2017). Mechanical control of myotendinous junction formation and tendon differentiation during development. *Front. Cell Dev. Biol.* **5**, 1–8.
- Vallee, R. B., Seale, G. E. and Tsai, J. W.** (2009). Emerging roles for myosin II and cytoplasmic dynein in migrating neurons and growth cones. *Trends Cell Biol.* **19**, 347–355.
- Wagner, N. and Krohne, G.** (2007). LEM-Domain Proteins: New Insights into Lamin-

- Interacting Proteins. *Int. Rev. Cytol.* **261**, 1–46.
- Wagner, N., Schmitt, J. and Krohne, G.** (2004). Two novel LEM-domain proteins are splice products of the annotated *Drosophila melanogaster* gene CG9424 (Bocksbeutel). *Eur. J. Cell Biol.* **82**, 605–616.
- Wagner, N., Kagermeier, B., Loserth, S. and Krohne, G.** (2006). The *Drosophila melanogaster* LEM-domain protein MAN1. *Eur. J. Cell Biol.* **85**, 91–105.
- Wang, L., Barylko, B., Byers, C., Ross, J. A., Jameson, D. M. and Albanesi, J. P.** (2010). Dynamin 2 mutants linked to centronuclear myopathies form abnormally stable polymers. *J. Biol. Chem.* **285**, 22753–22757.
- Wang, W., Shi, Z., Jiao, S., Chen, C., Wang, H., Liu, G., Wang, Q., Zhao, Y., Greene, M. I. and Zhou, Z.** (2012). Structural insights into SUN-KASH complexes across the nuclear envelope. *Cell Res.* **22**, 1440–1452.
- Wang, S., Stoops, E., Cp, U., Markus, B., Reuveny, A., Ordan, E. and Volk, T.** (2018). Mechanotransduction via the LINC complex regulates DNA replication in myonuclei. *J. Cell Biol.* **217**, jcb.201708137.
- Warnock, D. E., Baba, T. and Schmid, S. L.** (1997). Ubiquitously expressed dynamin-II has a higher intrinsic GTPase activity and a greater propensity for self-assembly than neuronal dynamin-i. *Mol. Biol. Cell* **8**, 2553–2562.
- Weitkunat, M., Kaya-Çopur, A., Grill, S. W. and Schnorrer, F.** (2014). Tension and force-resistant attachment are essential for myofibrillogenesis in *drosophila* flight muscle. *Curr. Biol.* **24**, 705–716.
- Welte, M. A., Gross, S. P., Postner, M., Block, S. M. and Wieschaus, E. F.** (1998). Developmental regulation of vesicle transport in *Drosophila* embryos: Forces and kinetics. *Cell* **92**, 547–557.
- Wheeler, M. A., Davies, J. D., Zhang, Q., Emerson, L. J., Hunt, J., Shanahan, C. M. and Ellis, J. A.** (2007). Distinct functional domains in nesprin-1 $\alpha$  and nesprin-2 $\beta$  bind directly to emerin and both interactions are disrupted in X-linked Emery-Dreifuss muscular dystrophy. *Exp. Cell Res.* **313**, 2845–2857.
- Wilkinson, F. L., Holaska, J. M., Zhang, Z., Sharma, A., Manilal, S., Holt, I., Stamm, S., Wilson, K. L. and Morris, G. E.** (2003). Emerin interacts in vitro with the splicing-associated factor, YT521-B. *Eur. J. Biochem.* **270**, 2459–2466.
- Wilson, K. L. and Foisner, R.** (2010). Lamin-binding Proteins. *Cold Spring Harb. Perspect. Biol.* **2**, 1–18.
- Wilson, M. H. and Holzbaur, E. L. F.** (2012). Opposing microtubule motors drive robust nuclear dynamics in developing muscle cells. *J. Cell Sci.* **125**, 4158–4169.
- Wilson, M. H. and Holzbaur, E. L. F.** (2015). Nesprins anchor kinesin-1 motors to the nucleus to drive nuclear distribution in muscle cells. *Development* **142**, 218–228.
- Windner, S. E., Manhart, A., Brown, A., Mogilner, A. and Baylies, M. K.** (2019). Nuclear Scaling Is Coordinated among Individual Nuclei in Multinucleated Muscle Fibers. *Dev. Cell* 1–15.
- Wolff, N., Gilquin, B., Courchay, K., Callebaut, I., Worman, H. J. and Zinn-Justin, S.** (2001). Structural analysis of emerin, an inner nuclear membrane protein mutated in X-linked Emery-Dreifuss muscular dystrophy. *FEBS Lett.* **501**, 171–176.
- Xiang, J., Bandura, J., Zhang, P., Jin, Y., Reuter, H. and Edgar, B. A.** (2017). EGFR-dependent TOR-independent endocycles support *Drosophila* gut epithelial

- regeneration. *Nat. Commun.* **8**, 1–13.
- Yeh, E., Skibbens, R. V., Cheng, J. W., Salmon, E. D. and Bloom, K.** (1995). Spindle dynamics and cell cycle regulation of dynein in the budding yeast, *Saccharomyces cerevisiae*. *J. Cell Biol.* **130**, 687–700.
- Zaal, K. J. M., Reid, E., Mousavi, K., Zhang, T., Mehta, A., Bugnard, E., Sartorelli, V. and Ralston, E.** (2011). Who needs microtubules? myogenic reorganization of MTOC, golgi complex and er exit sites persists despite lack of normal microtubule tracks. *PLoS One* **6**,.
- Zanet, J., Jayo, A., Plaza, S., Millard, T., Parsons, M. and Stramer, B.** (2012). Fascin promotes filopodia formation independent of its role in actin bundling. *J. Cell Biol.* **197**, 477–486.
- Zhang, Q., Skepper, J. N., Yang, F., Davies, J. D., Hegyi, L., Roberts, R. G., Weissberg, P. L., Ellis, J. a and Shanahan, C. M.** (2001). Nesprins: a novel family of spectrin-repeat-containing proteins that localize to the nuclear membrane in multiple tissues. *J. Cell Sci.* **114**, 4485–4498.
- Zhang, Q., Ragnauth, C. D., Skepper, J. N., Worth, N. F., Warren, D. T., Roberts, R. G., Weissberg, P. L., Ellis, J. A. and Shanahan, C. M.** (2005). Nesprin-2 is a multi-isomeric protein that binds lamin and emerin at the nuclear envelope and forms a subcellular network in skeletal muscle. **1**,.
- Zhang, Q., Bethmann, C., Worth, N. F., Davies, J. D., Wasner, C., Feuer, A., Ragnauth, C. D., Yi, Q., Mellad, J. A., Warren, D. T., et al.** (2007). Nesprin-1 and -2 are involved in the pathogenesis of Emery - Dreifuss muscular dystrophy and are critical for nuclear envelope integrity. *Hum. Mol. Genet.* **16**, 2816–2833.
- Zhang, J., Felder, A., Liu, Y., Guo, L. T., Lange, S., Dalton, N. D., Gu, Y., Peterson, K. L., Mizisin, A. P., Shelton, G. D., et al.** (2009). Nesprin 1 is critical for nuclear positioning and anchorage. *Hum. Mol. Genet.* **19**, 329–341.
- Zheng, R., Ghirlando, R., Lee, M. S., Craigie, R., Mizuuchi, K. and Krause, M.** (2002). Barrier-to-autointegration factor (BAF) bridges DNA in a discrete, higher-order nucleoprotein complex. *Proc. Natl. Acad. Sci.* **97**, 8997–9002.